U.S. Industry Opportunities for Advanced Nuclear Technology Development
Advanced Reactor Development Projects Pathway

Final Report on

Integrated Fire Probabilistic Risk Assessment (PRA) Modeling in Support of Operational Efficiency

Report Number: DOE-UIUC-0008856
Project ID: DE-NE0008856

Prepared by:

Kristin Kaspar (Principal Investigator), Brian Ratté, Mary Anne Billings
South Texas Project Nuclear Operating Company

Zahra Mohaghegh (Co-Principal Investigator), Tatsuya Sakurahara, Seyed Reihani, Ernie Kee, Sari Alkhatib, Mohammad Albati
Socio-Technical Risk Analysis (SoTeRiA) Research Laboratory
Department of Nuclear, Plasma, and Radiological Engineering
Grainger College of Engineering, University of Illinois at Urbana-Champaign

Terry L. von Thaden, Richard Kesler, Farzaneh Masoud
Illinois Fire Service Institute

Prepared for

U.S. Department of Energy
Office of Nuclear Energy

Urbana, Illinois

March 2022

Page intentionally left blank

ACKNOWLEDGEMENT

This material is based upon work supported by the Department of Energy under Award Number DE-NE0008856.

DISCLAIMER

Page intentionally left blank

EXECUTIVE SUMMARY

A literature review identified five areas of the "current Fire PRA methodology" (based on NUREG/CR-6850 and subsequent NUREGs) where realism could be improved: (1) fire ignition frequency, (2) fire progression and damage modeling, (3) interaction between fire progression and manual suppression, (4) circuit failure analysis, and (5) post-fire Human Reliability Analysis (HRA).

To improve the realism of Fire PRA associated with areas #2 and #3, previous research by the Socio-Technical Risk Analysis (SoTeRiA) Research Laboratory at the University of Illinois at Urbana-Champaign focused on the development of an Integrated PRA (I-PRA) methodological framework for fire risk analysis in NPPs. This I-PRA framework, when compared with the current Fire PRA methodology, is advanced in *three aspects*:

i. *The coupling between a fire model and a fire crew performance model is advanced.* The current Fire PRA methodology uses a data-driven model for human performance in manual suppression and utilizes an implicit time-based coupling between fire propagation and human performance, where the time-to-damage and the time-to-suppression are computed by separate models without consideration of their interactions. Fire I-PRA has improved the coupling between fire progression and manual suppression in three steps. The first step created the explicit unidirectional coupling between the data-driven fire crew performance model and a Computational Fluid Dynamics (CFD)-based fire model (Fire Dynamics Simulator [FDS]) by modifying the Heat Release Rate (HRR) curve based on the key timings of manual suppression activities. The second step developed an HRA-based approach, where an explicit coupling between the HRA model for the fire crew and the FDS model was created. In the third step, a spatiotemporal fire crew performance model was developed using Agent-Based Modeling (ABM). The ABM model is coupled with a fire model utilizing a Geographic Information System (GIS)-based spatial environment. This new spatiotemporal coupling can be useful for both (a) fully dynamic PRA and (b) the integration of plant classical PRA with the simulation approaches under the I-PRA framework.

ii. *The probabilistic connection between plant PRA and the fire-human coupled model is advanced.* The I-PRA methodology integrates the underlying simulation models with the existing PRAs of NPPs by generating a probabilistic interface equipped with advanced uncertainty analysis,

dependency treatment, and Bayesian updating. In the current Fire PRA methodology, however, the connection between a fire model and the plant PRA is "passive," i.e., the equipment damage probabilities are computed as outputs from a fire model and then used as inputs to the PRA software. In contrast, in I-PRA, the existing plant PRA model is integrated with underlying simulations in a "unified" computational platform. The spatial and temporal information on input-output relationships between the plant PRA scenarios and the underlying simulation (i.e., the coupling of the fire model and the human performance model) are recorded and analyzed in a unified platform. This unified connection allows advanced importance measure analysis to be conducted to generate the risk-importance ranking based on the impact of the fire protection parameters on the plant risk metrics.

iii. *The Fire I-PRA framework is equipped with advanced uncertainty quantification techniques.* The current Fire PRA methodology adopts the severity factor method, which can be considered as a "simplified" uncertainty quantification as it only accounts for one uncertain input variable with predefined bins discretizing the quantile space. Meanwhile, Fire I-PRA performs full uncertainty quantification, accounting for multiple uncertain input parameters using sampling-based uncertainty propagation techniques. This advancement contributes to a more accurate estimation of the fire-induced failure probabilities and dependency treatment. In previous research by Co-PI Mohaghegh and her team, the Fire I-PRA methodological framework was applied to a critical fire-induced scenario. With this framework, the realism of PRA was improved, and a 50% reduction in core damage frequency was obtained.

In order to enhance the methodological and practical values of Fire I-PRA, this Department of Energy (DOE)-funded academic-industry project, in collaboration with South Texas Project Nuclear Operating Company (STPNOC), started in 2019. This project has been conducted in three phases:

- In Phase I, the Fire Risk-informed over Deterministic (RoverD) Screening Methodology is developed to improve the Degree of Realism (DoR) gradually and efficiently during the screening process. The RoverD methodology is based on utilizing a blend of deterministically and risk-based elements to demonstrate compliance with the regulatory requirements. In Fire RoverD, some of the bounding assumptions used in Task 7.b of NUREG/CR-6850 (e.g., no credit for fire protection systems) are still utilized, while some aspects of the fire modeling are made more realistic than those in Task 7.b (e.g., the use of a zone model instead of engineering correlations, explicit modeling of cable heat conduction, consideration of the full distribution of the peak HRR value). The Fire-RoverD approach is mapped to the NUREG/CR-6850 procedure to demonstrate that Fire-

RoverD can be seamlessly combined with the current Fire PRA procedure. The Fire-RoverD approach is applied to two fire zones at the STPEGS plant to demonstrate its feasibility.

- Phase II is focused on the enhancement of the Multi-Compartment Analysis (MCA) for the Plant Analysis Units (PAUs) containing transient ignition sources. A methodological and computational platform called, "SoTeRiA-Fire," is developed to automate the "Fire Scenario Selection and Analysis (FSS)" supporting MCA in the Fire PRA of NPPs. While reflecting the guidelines of NUREG/CR-6850 and ASME/ANS RA-Sa-2009, SoTeRiA-Fire can help NPPs reduce resources required for Fire PRA implementation by (a) automating the pre-processing of input data, execution of a fire model, and post-processing of outputs for various tasks in the FSS and (b) providing a mechanism to gradually increase the realism of FSS while screening out insignificant scenarios. SoTeRiA-Fire assembles the input parameters, conducts required input data processing, and constructs the input files for the Consolidated Model of Fire and Smoke Transport (CFAST) fire simulation program. It then analyzes various combinations or ranges of key input parameters based on the fire propagation event tree logic and prepares the outputs to be post-processed for FSS. SoTeRiA-Fire is applied in a plant and the results are reported; however, the code is applicable for various fire compartments in NPPs and can automate resource-efficient screening for single- or multi-compartment fire scenarios.
    - Additionally, as part of Phase II, the applicability, challenges, gaps, and considerations when applying the current Fire PRA methodology to advanced nuclear power reactors are analyzed. The potential challenges identified in the literature review are mapped to the corresponding task(s) in the NUREG/CR-6850 procedure. As a result, recommendations for future work are provided to extend the applicability of the current Fire PRA and I-PRA methodologies to advanced reactors.
- In Phase III, experimental validation is conducted for the ABM-based fire crew model developed by Co-PI Mohaghegh and her team in their previous work. The fire crew performance tests are conducted by leveraging the existing fire testing capabilities at the Illinois Fire Service Institute (IFSI). The validation scope focuses on the fire search phase of the fire crew response. This study is the first-of-its-kind research effort to validate the probabilistic simulation of the fire crew performance at NPPs using the test data and to connect the fire-human experimental data to the system-level PRA scenarios. As the validation methodology, this study adopts the uncertainty quantification-based approach recommended by the U.S. Nuclear Regulatory Commission (NRC) for the validation of fire models in support of Fire PRA.

Page intentionally left blank

CONTENTS

FIGURES

TABLES

Page intentionally left blank

ABBREVIATIONS

ABM	Agent-Based Modeling
ARIS	Advanced Reactor Information System
ASP	Auxiliary Shutdown Panel
CCDP	Conditional Core Damage Probability
CDF	Core Damage Frequency
CEFR	China Experimental Fast Reactor
CFAST	Consolidated Model of Fire and Smoke Transport
CFD	Computational Fluid Dynamics
DOE	Department of Energy
DoR	Degree of Realism
EPRI	Electric Power Research Institute
FDS	Fire Dynamics Simulator
FIVE	Fire-Induced Vulnerability Evaluation
FLASH-CAT	Flame Spread over Horizontal Cable Trays
FSS	Fire Scenario Selection and Analysis
GAIN	Gateway for Accelerated Innovation in Nuclear
GFR	Gas-cooled Fast Reactor
GIS	Geographic Information System
GSI	Generic Safety Issue
HEP	Human Error Probability
HGL	Hot Gas Layer
HRR	Heat Release Rate

HTGR	High Temperature Gas-cooled Reactor
HTR-PM	High Temperature GCR Pebble-Bed Module
I-PRA	Integrated Probabilistic Risk Assessment
IAEA	International Atomic Energy Agency
IFSI	Illinois Fire Service Institute
IPRO-ZONE	Interface Program for Constructing a Zone Effect Table
JAEA	Japan Atomic Energy Agency
KAERI	Korea Atomic Energy Research Institute
KPM	Key Performance Measure
LERF	Large Early Release Frequency
LFR	Lead-cooled Fast Reactor
LHS	Latin Hypercube Sampling
LOCA	Loss of Coolant Accident
LWR	Light Water Reactor
MCA	Multi-Compartment Analysis
MCR	Main Control Room
MSO	Multiple Spurious Operation
MSR	Molten Salt Reactor
NPM	NuScale Power Module
NPP	Nuclear Power Plant
NRC	Nuclear Regulatory Commission
PAU	Physical Analysis Unit
PGSFR	Prototype Gen-IV Sodium-cooled Fast Reactor
PIRT	Phenomena Identification and Ranking Table

PRA	Probabilistic Risk Assessment
PRISM	Power Reactor Innovative Small Module
QDPS	Qualified Display Processing System
RI-PB	Risk-Informed, Performance-Based
RoverD	Risk-informed over Deterministic
SCWR	Supercritical Water-cooled Reactors
SFR	Sodium-cooled Fast Reactor
SMART	System-integrated Modular Advanced Reactor
SMR	Small Modular Reactor
SoTeRiA	Socio-Technical Risk Analysis
SSC	Structures, Systems, and Components
STPNOC	South Texas Project Nuclear Operating Company
TP	Thermoplastic
TS	Thermoset
V&V	Validation and Verification
VHTR	Very High Temperature Reactor
ZOI	Zone of Influence

Page intentionally left blank

1. Introduction

Fire Probabilistic Risk Assessment (PRA) has been a challenging area for risk-informed applications and regulation of Nuclear Power Plants (NPPs) due to the complex and dynamic progression of underlying physical failure mechanisms and their interaction with human interventions. Since the introduction of Risk-Informed, Performance-Based (RI-PB) fire protection approaches in 2005, the U.S. Nuclear Regulatory Commission (NRC) and the nuclear industry have made significant efforts to increase the realism of Fire PRA. Industry experience shows that the NFPA-805 transition can be resource-intensive and that the advantages of the RI-PB approach have not yet been fully realized due to excessive conservatism in the current Fire PRA methodology. A literature review identified five areas of the "current Fire PRA methodology" (based on NUREG/CR-6850 [1] and subsequent NUREGs) where realism could be improved: (1) fire ignition frequency, (2) fire progression and damage modeling, (3) interaction between fire progression and manual suppression, (4) circuit failure analysis, and (5) post-fire Human Reliability Analysis (HRA).

To improve the realism of Fire PRA associated with areas #2 and #3, previous research by the Socio-Technical Risk Analysis (SoTeRiA) Research Laboratory at the University of Illinois at Urbana-Champaign focused on the development of an Integrated PRA (I-PRA) methodological framework for fire risk analysis in NPPs [2, 3]. When compared with the current Fire PRA methodology, Fire I-PRA is advanced in three aspects: (i) probabilistic connection between plant PRA and the fire physics model, (ii) uncertainty propagation and computation of fire-induced cable damage probability, and (iii) fire detection and suppression analysis focusing on treatment of manual suppression [4].

The current Fire PRA methodology uses a data-driven approach for modeling human performance in manual suppression and utilizes an implicit time-based coupling between fire propagation and human performance, where the time-to-damage and the time-to-suppression are computed by separate models without consideration of their interactions. Fire I-PRA has improved the coupling between fire progression and manual suppression in three steps [5]. In the first step, the explicit unidirectional coupling between the data-driven fire crew performance model and a Computational Fluid Dynamics (CFD)-based fire model (Fire Dynamics Simulator [FDS]) was created by modifying the Heat Release Rate (HRR) curve based on the key timings of manual suppression activities [2]. In the second step, an HRA-based approach was developed by generating an explicit coupling between an HRA model for the onsite fire crew and the FDS model [6]. In the third step, a spatiotemporal fire crew performance model was developed using an Agent-Based Modeling (ABM) technique and by bidirectionally coupling it with a fire propagation model utilizing a Geographic Information System (GIS)-based spatial environment [7].

Although this new spatiotemporal coupling can be useful for fully dynamic PRAs, the widespread use of classical PRA logic by the nuclear industry and regulatory agency means that a transition to a fully dynamic PRA would require a significant investment of resources. To avoid this, the I-PRA methodology [2, 3] integrates the underlying simulation models with the existing static PRAs of NPPs by generating a probabilistic interface equipped with advanced uncertainty analysis, dependency treatment, and Bayesian updating. Uncertainty propagation in Fire I-PRA is performed by conducting Monte Carlo simulation for the FDS coupled with the agent-based fire crew performance model using the Latin Hypercube Sampling (LHS) method. In I-PRA, the existing plant PRA model is integrated with underlying simulations in a "unified" computational platform. In the current Fire PRA methodology, the connection between a fire model and the plant PRA is "passive," i.e., the cable damage probabilities are computed as outputs from the fire model, which are then used as inputs to the PRA software. In contrast, in Fire I-PRA, the spatial and temporal information on input-output relationships between the plant PRA model and the underlying simulation (i.e., the coupling of the fire model and the human performance model) are recorded and analyzed in a unified platform. This unified connection allows the advanced importance measure analysis to be conducted to generate the risk-importance ranking based on the impact of the fire protection parameters on the plant risk metrics [8-10]. The Fire I-PRA methodological framework was applied to a critical fire-induced scenario. With this framework, the realism of PRA was improved, and a 50% reduction in core damage frequency was obtained [4].

In order to enhance the methodological and practical values of Fire I-PRA, this Department of Energy (DOE)-funded academic-industry project, in collaboration with South Texas Project Nuclear Operating Company (STPNOC), started in 2019. This project has been conducted in three phases:

- **Phase I: Development of a streamlined approach to performing more efficient screening of fire zones and ignition sources (Chapter 2 of this report).**

  The Fire Risk-informed over Deterministic (RoverD) Screening Methodology is developed to improve the Degree of Realism (DoR) gradually and efficiently during the screening process. The RoverD methodology is based on utilizing a blend of deterministically and risk-based elements to demonstrate compliance with the regulatory requirements. In Task 7 of NUREG/CR-6850, four types of quantitative screening methods (Tasks 7.a to 7.d) with different levels of realism are recommended. Task 7.a uses the most conservative assumptions: all fire-induced component failures occur with certainty. Task 7.d considers realistic fire ignition frequencies, detailed fire modeling, circuit failure analysis, and detailed Fire HRA. Tasks 7.b and 7.c are between Tasks 7.a and 7.d with respect to the level of detail and realism of the analysis. The efficiency of the screening

analysis in Fire PRA can be enhanced by adding a step-by-step consideration of the relationship among the ignition frequency, the fire intensity (i.e., maximum HRR), and different types of fire models. In the current methodology, Task 7.b only considers the "upper bound" of maximum HRR value and relies on correlation-based fire models (e.g., Electric Power Research Institute [EPRI] Fire-Induced Vulnerability Evaluation [FIVE] tool). Then, in Task 7.c, a detailed fire modeling is conducted with full consideration of uncertainty of the maximum HRR and by using a more sophisticated fire model (either a zone model or a CFD-based model).

Phase I of this project consists of one task (Task 1) and three associated subtasks (1.1 to 1.3). In Subtask 1.1 of this project, a RoverD approach for Fire PRA (Fire-RoverD) is developed, including a theoretical foundation and an algorithm for the practical implementation. In Fire-RoverD, some of the bounding assumptions in Task 7.b (e.g., no credit for fire protection systems) are still used, while some aspects of the fire modeling are made more realistic than those in Task 7.b (e.g., the use of a zone model instead of engineering correlations, explicit modeling of cable heat conduction, consideration of the full distribution of the peak HRR value). In Subtask 1.2 of this project, the Fire-RoverD approach is mapped to the NUREG/CR-6850 procedure to demonstrate that Fire-RoverD can be combined with the current Fire PRA methodology smoothly. In Subtask 1.3 of this project, the Fire-RoverD approach is applied to a selected set of fire zones at STPEGS to demonstrate its feasibility.

- **Phase II: Advancing and Implementing an Integrated Fire PRA Approach (Chapters 3 and 5 of this report).**

The purpose of Phase II is to develop advanced methodologies for improving realism in Fire PRA. As a computational platform, the Fire I-PRA methodological framework developed by Co-PI Mohaghegh and her team is utilized [2, 3]. Phase II consists of two tasks. Task 2 advances the Fire I-PRA methodological framework by focusing on the area identified as the most critical. Task 3 analyzes the applicability of the advanced Fire I-PRA methodology developed in this phase to advanced reactors in support of risk-informed design and licensing.

Phase II is focused on the enhancement of the Multi-Compartment Analysis (MCA) for the Plant Analysis Units (PAUs) containing transient ignition sources. A methodological and computational platform called, "SoTeRiA-Fire," is developed to automate the "Fire Scenario Selection and Analysis (FSS)" supporting MCA in the Fire PRA of NPPs (Chapter 3 of this report). While reflecting the guidelines of NUREG/CR-6850 and ASME/ANS RA-Sa-2009, SoTeRiA-Fire

can help NPPs reduce resources required for Fire PRA implementation by (a) automating the pre-processing of input data, execution of a fire model, and post-processing of outputs for various tasks in the FSS and (b) providing a mechanism to gradually increase the realism of FSS while screening out insignificant scenarios. The fire hazard propagation event tree in SoTeRiA Fire includes multiple pivotal events: (1) initial fire ignition, (2) ignition of secondary combustibles and fire spread, (3) formation of damaging conditions for target equipment and cables, (4) failure of detection and suppression systems in the exposing compartment containing the initial fire source, (5) failure of fire barriers, and (6) failure of a suppression system in the exposed compartment. The SoTeRiA-Fire assembles the input parameters, conducts required input data processing, and constructs the input files for the Consolidated Model of Fire and Smoke Transport (CFAST) fire simulation program. It then analyzes various combinations or ranges of key input parameters based on the fire propagation event tree logic and prepares the outputs to be post-processed for FSS. SoTeRiA-Fire is applied to two fire zones at a plant and the results are reported; however, the code is applicable for various fire compartments in NPPs and can automate resource-efficient screening for single- or multi-compartment fire scenarios.

Task 3 analyzes the applicability, challenges, gaps, and special considerations when applying the existing Fire PRA methodologies, developed for light-water reactors, to advanced nuclear power reactors (Chapter 5 of this report). A systematic literature review on Fire PRA for advanced reactors is performed. The methodology and setup of the literature review, including the databases used, selection and combinations of keywords, and statistical insights of the search results, are described. A detailed review of all relevant references is then performed to compile a list of the features of advanced reactors that could generate challenges when applying the current Fire PRA methodologies. The potential challenges identified in the literature review are mapped with the corresponding task(s) of the NUREG/CR-6850 procedure. This part of the report is concluded by providing recommendations for future work to extend the applicability of the current Fire PRA and I-PRA methodologies to advanced reactors.

- **Phase III: Experimental Validation of the Fire Crew Performance Model (Chapter 4 of this report).**

For the regulatory acceptance of advanced simulation modeling used in PRA, validation is a crucial step. In Phase III, the agent-based human performance model for manual suppression, developed by Co-PI Mohaghegh and her team in their previous work [7], undergoes experimental validation using limited-scope fire testing. While the agent-based fire crew model can improve the resolution

and realism of the manual suppression analysis in Fire PRA, it was not validated in the previous research. This research leverages the fire testing capabilities at the Illinois Fire Service Institute (IFSI). The validation scope focuses on the fire search phase of the fire crew response. In the nuclear power domain, the historical fire tests (e.g., Sandia National Laboratory, National Institute of Standards and Technology) have focused on physical fire models, while no existing fire test has investigated the validation of human performance models considering fire-human interactions. This study is the first-of-its-kind research effort to validate the probabilistic simulation of fire-human interactions using the fire-human test data and to connect the fire-human test data to the system-level PRA scenarios. As the validation methodology, this study adopts the uncertainty quantification-based approach recommended by the U.S. NRC for the validation of fire models in support of Fire PRA.

Page intentionally left blank

2. Fire RoverD Methodology and Application for Efficient Quantitative Screening in Fire PRA

Phase I of the project focuses on the development of a streamlined approach to perform quantitative screening of fire zones and ignition sources more efficiently. Phase I consists of the following tasks:

- Task 1: Develop and Implement an Efficient Fire Scenario Screening Method
    - Subtask 1.1: Develop a Fire Risk-informed over Deterministic (RoverD) Screening Methodology and Algorithm.
    - Subtask 1.2: Incorporate the Fire-RoverD Screening Methodology into the Current Fire PRA Methodology.
    - Subtask 1.3: Implement the Fire-RoverD Screening Analysis for South Texas Project Nuclear Operating Company (STPNOC).

Section 2.1 describes the Fire-RoverD screening methodology developed in this project (Subtasks 1.1). Section 2.2 summarizes the relationships of the Fire-RoverD methodology to the existing Fire PRA tasks, recommended in NUREG/CR-6850, Vol. 2 [11] (Subtask 1.2). Section 2.3 shows the implementation of the Fire-RoverD methodology for Physical Analysis Units (PAUs) at the STPNOC plant (Subtask 1.3). Section 2.4 summarizes the outcomes of Phase I and the potential future work.

2.1 Fire-RoverD Methodology

In Phase I of the project, a new quantitative screening approach for Fire Probabilistic Risk Assessment (PRA) is developed by leveraging the RoverD methodology. The RoverD approach was proposed by Co-PI Mohaghegh and her research team and applied to two areas: Generic Safety Issue 191 (GSI-191) [12] and seismic re-evaluation of nuclear power plants (NPPs) [13]. In this section, the extension of RoverD to the context of Fire PRA is described.

RoverD utilizes a blend of deterministically and risk-based elements to demonstrate compliance with the regulatory requirements. RoverD provides the possibility to efficiently quantify, using simplistic but conservative approaches, the extent of safety margin and defense-in-depth in the current design of protective systems, which can help identify Structures, Systems, and Components (SSC) modifications that can be avoided or addressed at a lower cost.

The premise of RoverD is that protective system equipment installed in NPPs has been successfully tested against a performance requirement or is designed based on the known standards of performance and, when challenged within the design requirement, are very likely to succeed. The concept underlying this assumption is that an equipment design is effectively 'guaranteed' against failure up to a tested, qualified level (i.e., designed equipment strength or reliability), denoted by M_o, and, beyond that level, failure is conditionally certain, even though in reality, failure is uncertain with a specific probability between 0 and 1. The 'hazard level' on the equipment induced by a particular hazard scenario is represented by a physical Key Performance Measure (KPM), denoted by m, e.g., the debris mass on each containment sump strainer for GSI-191 [12] and the peak ground acceleration for seismic damage [13].

The "underlying hazard scenarios" are defined as a set of consequential conditions or events associated with hazard initiation and progression that could lead to different levels of m. The hazard scenario 'space', denoted by $\boldsymbol{S}$, is characterized by the magnitude and location of the hazards and their progression. If the 'hazard level' induced by the hazard scenario s, denoted by $m_s; s \in \boldsymbol{S}$, is below M_o, the system protection against that hazard scenario is ensured by the current design; hence, the corresponding hazard scenario is categorized as a "deterministic" scenario and is not considered in the subsequent detailed risk-informed analysis. If $m_s > M_o$, the corresponding hazard scenario is categorized as a "risk-informed" scenario and would require further detailed analyses.

The total frequency of the "risk-informed" scenarios is obtained by a bounding risk assessment with conservative assumptions and is used as a conservative estimate of the system-level risk, e.g., Core Damage Frequency (CDF) and Large Early Release Frequency (LERF). Those bounding risk estimates are compared with the risk-informed acceptance criteria. If the conservative estimates of the plant risk metrics, computed by RoverD for a specific area of concern, fall within the acceptable region, safety is ensured as long as defense-in-depth and adequate safety margins are satisfied. In this case, the use of RoverD could result in significant cost savings on operating plants as plant modifications or design changes would not be required. If the bounding risk metrics estimated by RoverD are beyond the acceptable region, detailed PRA modeling would need to be performed to obtain more accurate risk estimations.

Figure 1 shows a generic formalization of the RoverD methodology suggested for the screening processes in PRA [14]. Although Figure 1 is generic for the screening process in diverse risk-informed applications, this section explains the RoverD process in the context of Fire PRA.

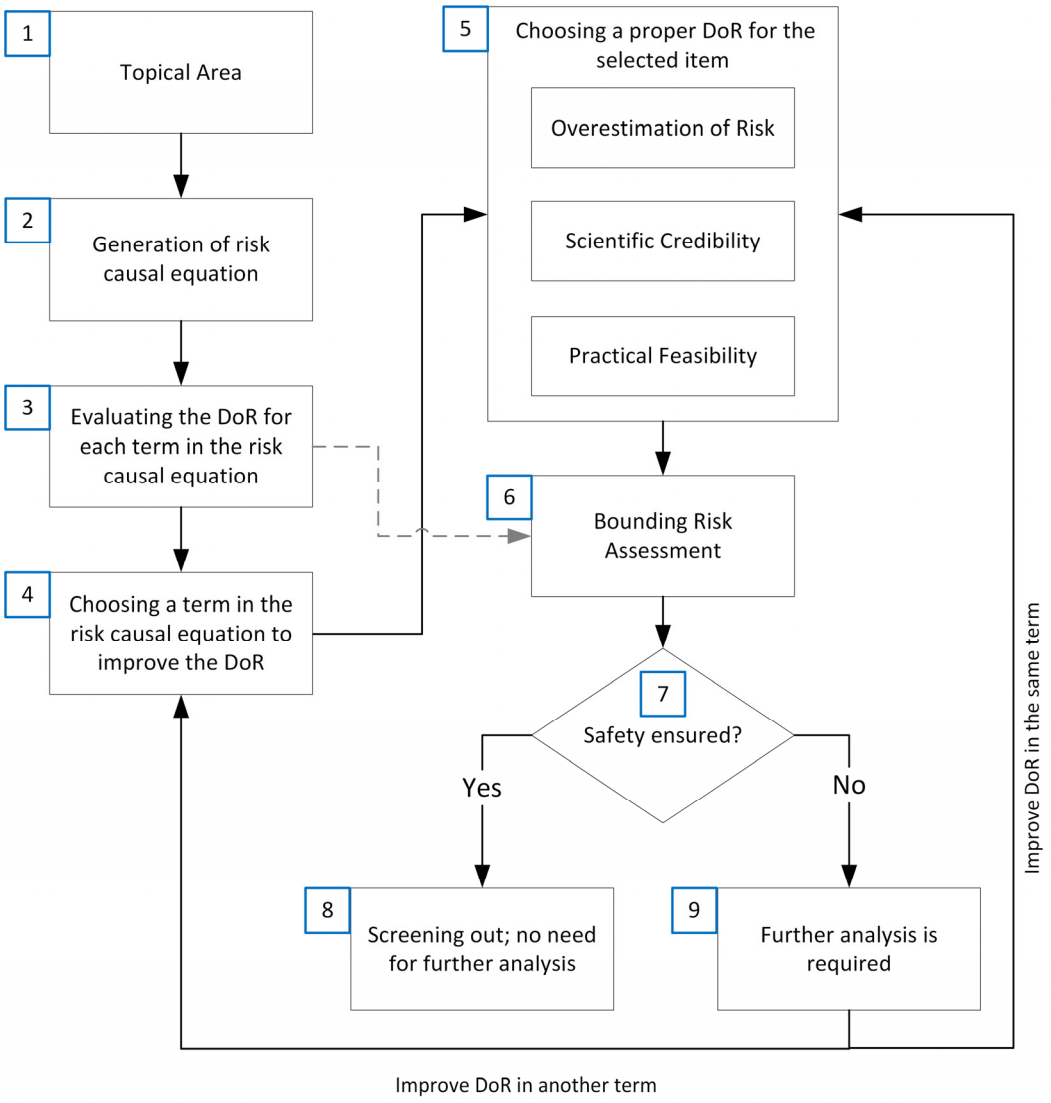

Figure 1: RoverD Methodology for Screening Processes in Diverse Risk-Informed Applications.

For a given topical area (#1 in Figure 1) in PRA, the hazard progression scenarios can be represented through logical causality, which can be quantified by the multiplication of conditional probabilities using the chain rule for joint events. Usually, this can be done by utilizing a mathematical representation called the risk causal equation (#2 in Figure 1). For example, to develop the risk causal equation (# 2 in Figure 1) for fire PRA of NPPs, there is a need to consider sequences of stochastic events that could occur due to a fire. After a specific ignition source starts to burn, the fire can grow and propagate until safety-related components are impacted, leading to functional failure modes such as spurious actuation that might affect the safety of the reactor core. Therefore, elements of fire-induced damage scenarios can be formalized as highlighted below:

- Fire occurrence,
- Fire-induced damage to a set of damage targets. The damage target can be either cable trays that can further propagate fire or safety-related components (e.g., PRA equipment),
- Fire-induced functional failure of safety component(s) due to failure of damage targets, and
- Core damage due to the functional failure (e.g., spurious action) of safety component(s).

For example, for single compartment fire scenarios, Equation (1) expresses the risk causal equation (#2 in Figure 1), representing the CDF associated with a fire compartment (i):

$$CDF_i = \sum_j f\left(FR_{i,j}\right) \times Pr\left(\boldsymbol{CB}_{i,j} | FR_{i,j}\right) \times Pr\left(\boldsymbol{PE}_{i,j} | FR_{i,j}, \boldsymbol{CB}_{i,j}\right) \times Pr\left(CD | \boldsymbol{PE}_{i,j}\right), \quad (1)$$

where:

CDF_i: The CDF [per year] associated with a fire in fire compartment $i \in \{1,2,\dots,I\}$,

$f\left(FR_{i,j}\right)$: Ignition frequency [per year] for ignition source $j \in \{1,2,\dots,J\}$ in fire compartment i,

$\boldsymbol{CB}_{i,j}$: Fire-induced damage to a set of cable trays due to ignition source j in fire compartment i,

$\boldsymbol{PE}_{i,j}$: Fire-induced functional failure of PRA equipment due to $\boldsymbol{CB}_{i,j}$, and

CD: Core damage state.

After establishing the risk causal equation, preliminary evaluation of the Degree of Realism (DoR) is conducted for each term in the causal equation (#3 in Figure 1). The DoR expresses "the degree to which an analysis represents the technical and organizational system relevant to the decision problem" [15, 16]. The issue of realism has been highlighted in Fire PRA [17]; however, in this section, a more general approach is utilized to formalize the methodology. The next step is to choose a term in the risk causal equation to improve the DoR (#4 in Figure 1) and the next relates to choosing a *proper* DoR for the selected term (#5 in Figure 1). The estimated risk in the screening process depends on the DoR. In this research, a *proper* DoR for the screening processes is defined as a set of assumptions that are:

(1) Scientifically credible such that they do not violate the limits or the scientific basis of the existing theories or physics that are accepted by the community,

(2) Practically feasible (e.g., compatible with the availability of required computational resources), and

(3) Overestimating risk (i.e., leading to the estimation of risk that is equal or greater than the true risk; or a conservative risk estimation).

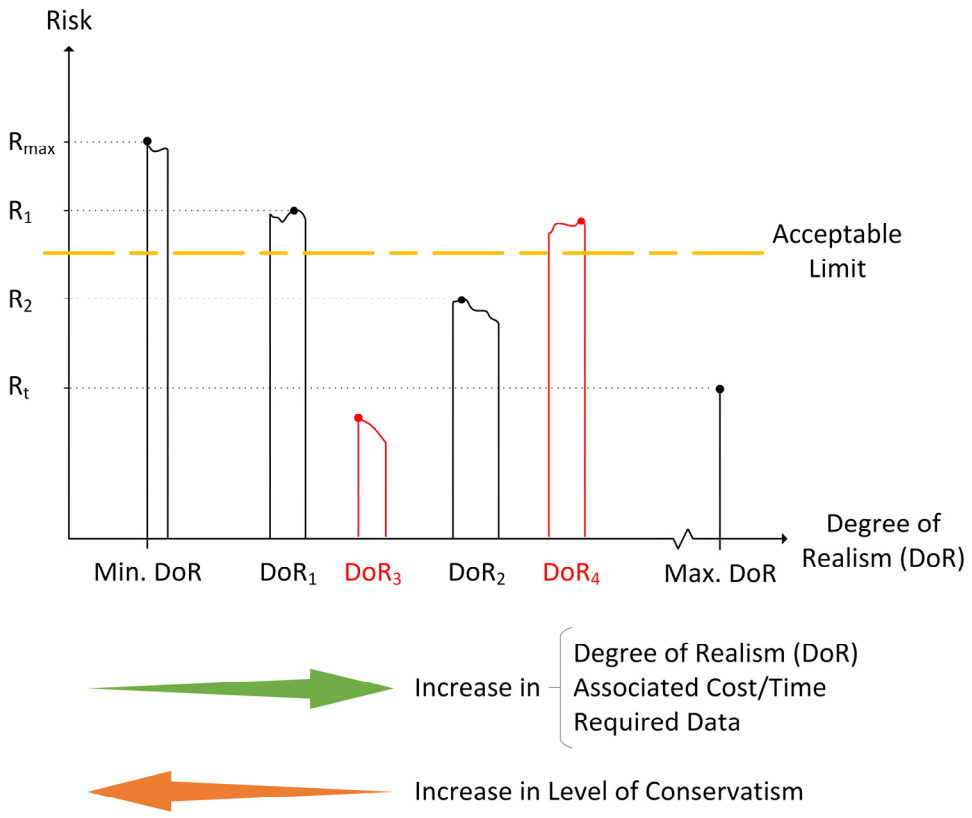

Figure 2: Degree of Realism (DoR) & the estimated risk.

Such *proper* DoRs are represented by the black bars in Figure 2, e.g., DoR_1 and DoR_2. The arrows below the plot indicate how different aspects, such as the associated cost and time, required data, and the level of conservatism, can be affected by the DoR. Ideally, the true risk of the system, R_t, can be achieved when the maximum DoR is considered. The maximum DoR is considered to be an expression, in the most realistic and comprehensive way, of the full and most detailed analysis of all the underlying contributing physical and organizational parameters. In Figure 2, minimum DoR represents the lowest DoR, whereas when compared to DoR_1 and DoR_2 - or any other DoR, it is associated with less realistic data and more conservative assumptions.

Some parts of the DoR axis in Figure 2 could be *improper* DoRs. That is, they are either not scientifically credible or practically feasible, and they are not guaranteed to lead to conservative risk estimates. For instance, both DoR_3 and DoR_4 represent cases for which the risk estimation is not appropriate for risk-informed decision-making. Using such cases in the screening process will produce erroneous and unreliable results and can mislead the risk-informed decision-making process.

Once a proper DoR has been determined, a bounding risk assessment (# 6 in Figure 1) should be conducted using the bounding values in the risk causal equation. The bounding risk assessment in RoverD is based on the requirement that the protective system equipment installed in NPPs has been successfully tested against a performance requirement or is designed based on the known standards of performance and, when challenged within the design requirement, that equipment is very likely to succeed. The concept underlying this assumption is that an equipment design is effectively 'guaranteed' against failure up to a tested, qualified level (i.e., designed equipment strength, denoted by M_o), and beyond that level, failure is conditionally certain, even though in reality, failure is uncertain with a specific probability between 0 and 1. The stress level on the equipment induced by a particular hazard scenario is represented by a physical KPM, denoted by $\boldsymbol{m}$, e.g., the target temperature and heat flux in Fire PRA or the debris mass on each containment sump strainer in RoverD for GSI-191 [12] or the peak ground acceleration in RoverD for Seismic PRA [13]. The hazard scenario space, denoted by $\boldsymbol{S}$, is typically characterized by the magnitude and location of the hazards. If the stress induced by the hazard scenario $\boldsymbol{s}$, denoted by $\boldsymbol{m_s}; \boldsymbol{s} \in \boldsymbol{S}$, is below M_o, the system protection against that hazard scenario is ensured by the current design; hence, the corresponding hazard scenario is classified in the "deterministic" category and is not considered in the subsequent risk-informed analysis. If $\boldsymbol{m_s} > M_o$, the corresponding hazard scenario is categorized as "risk-informed." The total frequency of "risk-informed" scenarios is obtained by implementing a bounding risk assessment with the appropriate assumptions, as explained, that correspond to a proper DoR for the system response, and they are used as conservative estimates of the system-level risk, e.g., CDF and LERF. Those bounding risk estimates are compared with the risk-informed acceptance criteria.

If the estimated bounding risk is proven to be within the acceptance safety criteria (#7 in Figure 1), the safety of the system is ensured; thus, there is no need for further improvement (#8 in Figure 1) in the DoR of the scenario. If not, the analysis will require further improvement (#9 in Figure 1) in the DoR. Improving the DoR would then be directed either to increase the DoR in the same term of the risk causal equation or to choose another term in the risk causal equation.

2.2 Incorporation of Fire-RoverD Screening Methodology into NUREG/CR-6850 Methodology

This section reports the outcome of Subtask 1.2 under Phase I of the project. The purpose of Subtask 1.2 was to identify how the Fire-RoverD methodology can be incorporated into the existing Fire PRA procedure recommended in NUREG/CR-6850 [11]. In the current Fire PRA flowchart (Figure 1 of NUREG/CR-6850 [11]), Fire-RoverD can be added as an optional additional task between Task 7B and Tasks 9 and 11. In

this report, the corresponding quantitative screening task is referred to as "Task 7B-RoverD," while the Scoping Fire Modeling (Task 8) conducted under the Fire-RoverD methodology (as part of #6 in Figure 1) is referred to as "Task 8-RoverD." Tasks 7B-RoverD and 8-RoverD aim to further screen out the ISs, covering the same scope of the fixed ISs as Table 8-1 of NUREG/CR-6850 [11].

To map Task 7B-RoverD and Task 8-RoverD into the existing Fire PRA procedure, the following modifications should be made to the Task 7 description in NUREG/CR-6850 [11]:

1) Section 7.1 (Purpose): "Task 7B-RoverD (Optional)" is added between Task 7B (Quantitative Screening II) and Task 7C (Quantitative Screening III [Optional]).

2) Section 7.2 (Scope): Four subtasks of quantitative screening are categorized into two groups: the fire compartment level screening (Tasks 7A and 7B) and the fire scenario level screening (Tasks 7C and 7D). Task 7B-RoverD is considered as an additional subtask under the fire compartment level screening.

3) Section 7.3 (Background Information): Task 7B-RoverD is performed by using the same principles as those for the compartment-level subtasks (Tasks 7A and 7B). The same screening criteria should be used, i.e., the single compartment risk criteria (1.0E-7/year for CDF and 1.0E-8/year for LERF) and the cumulative plant risk criteria (the cumulative CDF and LERF of screened compartments is less than 10% of the total internal events risk). The bases for the quantitative screening criteria, provided in Appendix D of NUREG/CR-6850 [11], should remain applicable for Task 7B-RoverD.

4) Section 7.4 (Task Interfaces): The inputs from other tasks for Task 7B-RoverD include (i) the list of retained fire compartments and ignition sources from Task 7B and (ii) the plant information collected in Tasks 7B and 8. The outputs of Task 7B-RoverD are: (a) revised compartment fire frequencies considering the updated screening of the fixed ISs and severity factors obtained by the Fire-RoverD; and (b) for each fire compartment, an updated list of unscreened fixed ISs with their associated severity factors. These outputs will be used as a starting point of the detailed fire modeling in Task 11 of NUREG/CR-6850 [11].

5) Section 7.5 (Procedure): The statement that "With the exception of the inputs and outputs, the implementation of the quantitative screening procedure is the same for all quantitative screening tasks" is also valid for Task 7B-RoverD. Table 7-1 of NUREG/CR-6850 [11] summarizes the inputs and outputs of each subtask (7A to 7D). To this table, the row corresponding to Task 7B-RoverD, shown below, should be added between Tasks 7B and 7C:

Task	Inputs	Outputs
Task 7B-RoverD (Fire RoverD)	Insights from Task 8-RoverD (Advanced Scoping Fire Modeling) are incorporated into the Fire PRA Model using Task 5. Updates, if appropriate, to the fire scenario frequencies developed in Task 6 and used in Tasks 7A and 7B, should Task 8-RoverD insights affect the frequencies. Revisions to the HRA values from Task 12 used in Tasks 7A and 7B, if/as appropriate, including any insights from the HRA dependency analysis, as a result of Task 8-RoverD insights affecting the HRA screening values.	See list of outputs below

Outputs

1) List of failed equipment for each fire compartment.

2) Model logic changes and/or temporary settings for fire in each compartment. This includes a description of how HRA events were incorporated into the model and how surrogate events were used.

3) Calculated CDF, LERF, ICDP, and ILERP results (including cutsets) for each compartment, including truncation values.

4) List of screened out compartments, including basis for exclusion.

5) Documentation of technical approach, assumptions, and conclusions, and interfaces with other tasks.

6) Recommendations for reducing compartment frequencies.

Meanwhile, a new section for Task 8-RoverD (Advanced Scoping Fire Modeling) should be added to NUREG/CR-6850 [11]. The content of this new section is similar to that of current Task 8, except for the following modifications:

- Table 8-1: For the IS bins that can be screened in Task 8, Zone of Influence (ZOI) should be calculated based on the Consolidated Model of Fire and Smoke Transport (CFAST) code outputs, including the maximum surface or inner temperature and the maximum heat flux of each target. As CFAST does not separately predict the fire-induced conditions due to individual mechanisms (i.e., flame, plume, ceiling jet, smoke layer, and flame irradiation), Figure F-2 in NUREG/CR-6850 is not applicable. Instead, the ZOI boundary is constructed by predicting the temperature and heat flux at a number of grid points around the IS (using the 98^{th} percentile of the peak heat release rate [HRR]) and comparing those outputs with the damage thresholds in Table 8-2 of NUREG/CR-6850.
- Section 8.4.1 (Inputs from Other Tasks): Since Task 8-RoverD is performed after Tasks 7B and 8, the outputs from these two tasks, such as the plant data for each fire zone and ignition source, the two work forms developed in Task 8 (the Fixed Ignition Source Form and the ZOI Form as in Appendix F of NUREG/CR-6850), and the list of fire zones unscreened in Task 7B, should be available as inputs to Task 8-RoverD.
- Section 8.4.3 (Walkdowns): As a general trend, the more realistic a fire model becomes, the more data are required as inputs. For instance, based on the observations from Phase I of this project, CFAST has approximately 50% more input parameters than the Electric Power Research Institute (EPRI) Fire-Induced Vulnerability Evaluation (FIVE) tool. The main categories of additional data for CFAST compared to EPRI FIVE are: (i) detailed information on natural/mechanical vents (e.g., x, y, and z coordinates of openings), (ii) exact location and geometry of each ignition source, and (iii) material properties of cable trays. To collect these additional data, another round of plant walkdown (in addition to the one performed to support Tasks 7B and 8) may be needed for Task 8-RoverD. The "proper DoR" associated with the fire modeling should be chosen based on the three criteria shown in #5 of Figure 1.
- Section 8.5 (Procedure): Task 8-RoverD should follow the same logical steps as Section 8.5 of NUREG/CR-6850. The Walkdown Screening Form, developed in Task 8, should be updated in terms of (i) whether the remaining ISs, unscreened in Task 8, can be screened out based on the ZOI constructed with a more realistic fire model such as CFAST and (ii) if not, on the updated value of the severity factor.

2.3 Implementation of Fire-RoverD Screening Analysis for STPNOC

This section reports applications of the Fire-RoverD screening methodology to two fire zones at STPNOC. To highlight the concept of different DoRs (related to #5 in Figure 1), the scoping fire modeling (i.e.,

NUREG/CR-6850 [11] Task 8) was conducted using two fire models: CFAST [18] and EPRI FIVE [19]. EPRI FIVE, based on engineering correlations, and CFAST, based on the 'zone modeling', represent two different DoRs for fire modeling. In quantitative screening for Fire PRA, an analyst has a choice between EPRI FIVE and CFAST in Step #5 of the Fire-RoverD methodology (Figure 1). The purpose of this analysis is to highlight how the decision regarding the proper DOR in Fire-RoverD can impact not only the realism of the risk estimation but also other factors, such as the resources required for the analysis. From the practical perspective, this section compares the current industry practice of implementing NUREG/CR-6850 Tasks 8 and 7B [11] using the engineering correlations with the RoverD-based implementation (Tasks 8-RoverD and 7-RoverD) based on more realistic fire modeling using CFAST.

2.3.1 Selection of Case Studies

As provided in Table 2-8 of the 2018 Work Scope Report [20], in total, there are 87 fire zones retained as a result of the implementation of Task 7A of NUREG/CR-6850, Vol.2 [11]. Therefore, these fire zones are considered candidates for further fire modeling and detailed risk analysis. Out of the retained 87 fire zones, two fire zones at STPNOC were chosen as case studies for the purpose of implementing the Fire-RoverD screening methodology and investigating the impact of different DoRs at the level of quantitative screening of fixed ignition sources.

The first PAU is F07Z071: "Auxiliary Shutdown Area" (hereinafter referred to as 'Z071'). This fire zone was selected based on the familiarity of STPNOC with this fire zone and STPNOC's interest in 1) the possible fire conditions and fire propagation, and 2) the required response of fire personnel.

As for the second fire zone, fire zones where ignition sources are PRA equipment were excluded from consideration, based on the guidance in Task 8: "Scoping Fire Modeling" in NUREG/CR-6850, Vol. 2 [11]. This led to reducing the number of potential fire zones to 29. Furthermore, by 1) focusing on countable fixed ignition sources (bins 1, 4, 10, 13, 14, 15, 22, 23b, and 26), and more specifically, bin 15: 'electrical cabinets,' 2) removing all non-motorized chain hoists and updating the information on the counts of this type of ignition source (bin 14: 'electric motors'), and 3) deleting zones that are just stairwells or corridors and those that have a large number of ignition sources, the following 11 fire zones are left:

- F35Z311: Spent Fuel Pool Auxiliary Area,
- F03Z116: Nonradioactive Piping Penetration Area,
- F06Z097: Outside Air Intake,
- F03Z119: Volume Control Tank and Valve Rooms,

- F02Z013: Equipment Room - Train A,
- F27Z138: Corridor and Pipe and HVAC Chase,
- F32Z103: Reactor Makeup Water and LASR Storage Tank and Pump Rooms,
- F03Z115: Radwaste Control and Counting Rooms,
- F35Z320: Spent Fuel Pool Heat Exchanger & Pump 1B,
- F27Z108: Boric Acid Tank and Pump Rooms, and
- F32Z134: Nonradioactive Pipe Chase.

With a count of 8 fixed ignition sources, F03Z115: "Radwaste Control and Counting Rooms" (hereinafter referred to as 'Z115') was selected to be the second case study. It should be noted that although 3 out of the 4 fixed ignition sources in Z071 are classified as PRA equipment and should not be screened out in Task 8, fire analysis was conducted to demonstrate the potential of utilizing zone models (i.e., CFAST) vs. engineering correlations (i.e., EPRI FIVE).

2.3.2 Fire Zones and Ignition Sources

In this section, general information, such as the geometry and material configuration, ventilation conditions, arrangement of ignition sources, and location of safety targets, is provided. This was the information used to establish the input data for fire analysis. In addition to utilizing engineering drawings for data extraction, multiple plant-walkdowns have been conducted by STPNOC to confirm the extracted data and collect additional information that was not obtained from the engineering drawings.

2.3.2.1 Fire Ignition Frequencies and Ignition Source Counts

Table 1 provides the original fire ignition frequencies and counts of ignition sources of concern for both Z071 and Z115 based on the 2018 work scope report [20] (i.e., as a result of the implementation of Task 7A). Table 1 provides the counts for electrical cabinets (bin 15) and ventilation subsystems (bin 26) for both Z115 and Z071 as they are the ignition sources that can be considered in Task 8: "Scoping Fire Modeling." Other bins, such as bin 12: 'Cable run (self-ignited cable fires)' and bin 18: 'Junction box' are not considered in the current analysis. This is consistent with the guidance in Task 8: "Scoping Fire Modeling" in NUREG/CR-6850, Vol. 2 [11].

Table 1: Original fire ignition frequencies and ignition source counts for Z071 and Z115.

Fire Zones	Z071	Z115
Total Fire Ignition Frequency (1/year)	4.25E-04	6.40E-04
Fire Ignition Frequency (1/year) for Bin 15: 'Electrical Cabinets'	3.70E-04	4.32E-04
No. of Electrical Cabinets	6	7
Fire Ignition Frequency (1/year) for Bin 26: 'Ventilation Subsystems'	0	5.56E-05
No. of Ventilation Subsystems	0	1

After conducting plant walkdowns and data collection, the original fire ignition frequencies were revised by updating the counts of the fixed ignition sources in both Z071 and Z115. The total number of electrical cabinets in each fire zone was updated based on the findings of plant walkdowns and data collection. Two electrical cabinets in Z071 (4Z351ZLP683 [NI-0045 Flux Processor] and 4Z351ZLP684 [NI-0046 Flux Processor]) were mistakenly considered to be in this fire zone and, therefore, they were removed. As for Z115, it was found that two additional electrical cabinets (480 VAC Breakers [next to ZLP-186] and ZLP-116) were not counted and, therefore, they were reconsidered as part of this fire zone. Table 2 provides the revised fire ignition frequencies and counts of ignition sources of concern for both Z071 and Z115.

Table 2: Revised fire ignition frequencies and ignition source counts for Z071 and Z115.

Fire Zones	Z071	Z115
Total Fire Ignition Frequency (1/year)	3.01E-04	7.63E-04
Fire Ignition Frequency (1/year) for Bin 15: 'Electrical Cabinets'	2.47E-04	5.55E-04
No. of Electrical Cabinets	4	9
Fire Ignition Frequency (1/year) for Bin 26: 'Ventilation Subsystems'	0	5.56E-05
No. of Ventilation Subsystems	0	1

2.3.2.2 Geometry and Material Properties

Only two types of materials have been utilized in the analysis for both case studies and whenever applicable in the utilized fire analysis tools. Table 3 provides the utilized values for a list of properties for these two materials, namely, concrete and cable jacket.

Table 3: Material properties used for case studies.

Properties [units]	Concrete Wall	Cable Jacket
Thermal Conductivity $[W/(m\,°C)]$	1.6	0.192
Density $[kg/m^3]$	2400	1380
Specific Heat $[kJ/(kg\,°C)]$	0.75	1.289
Thickness $[m]$	0.3048	0.0015
Emissivity $[-]$	0.94	0.95

The geometric configuration of the rooms within each fire zone is provided in Table 4. Figure 3 and Figure 4 provide the schematic drawing for fire zones Z071 and Z115, respectively. These figures were produced using Smokeview [21] (the magenta colored lines represent the exact locations of both natural openings and mechanical vents).

Table 4: Room dimensions for fire zones Z071 and Z115.

Fire Zone Z071

Room	Depth $[\boldsymbol{m}]$	Width $[\boldsymbol{m}]$	Height $[\boldsymbol{m}]$
015	4.5720	5.7912	7.3152
015J	10.3632	5.7912	4.2672

Fire Zone Z115

Room	Depth $[\boldsymbol{m}]$	Width $[\boldsymbol{m}]$	Height $[\boldsymbol{m}]$
217	6.5532	12.0396	5.1816
217MZ*	6.6812	7.2146	2.4384
217BZ*	2.7263	7.2634	5.1816

* MZ stands for 'mezzanine' area that is connected to room 217, and BZ stands for 'buffer zone' or the corridor at the entrance/exit of room 217.

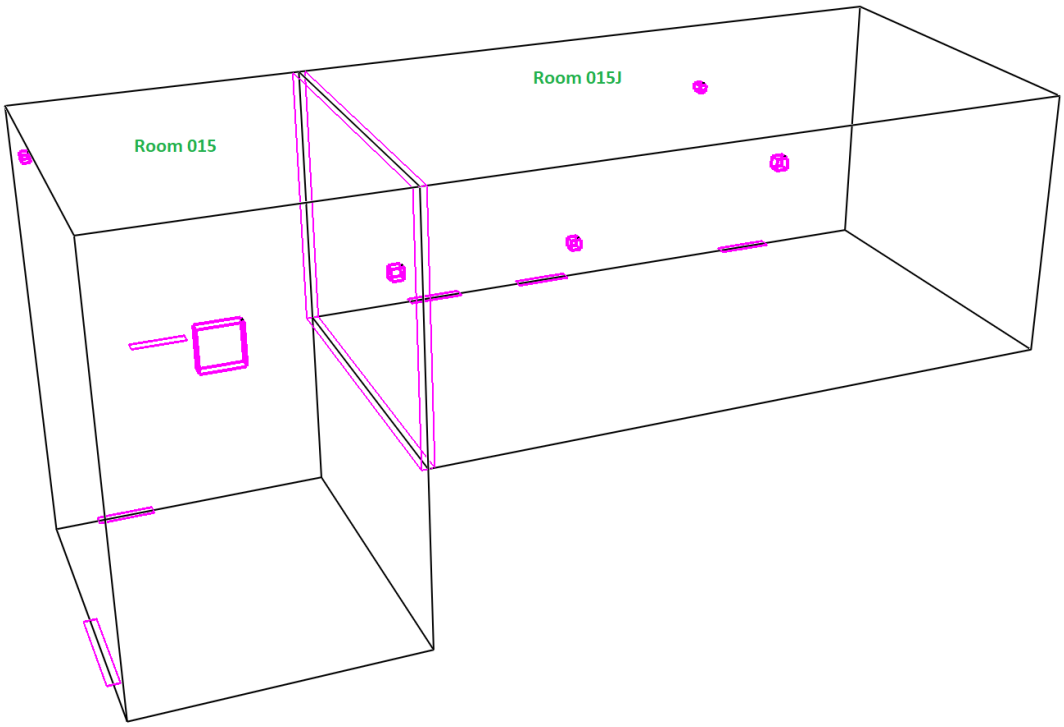

Figure 3: Schematic drawing of fire zone Z071 and its rooms.

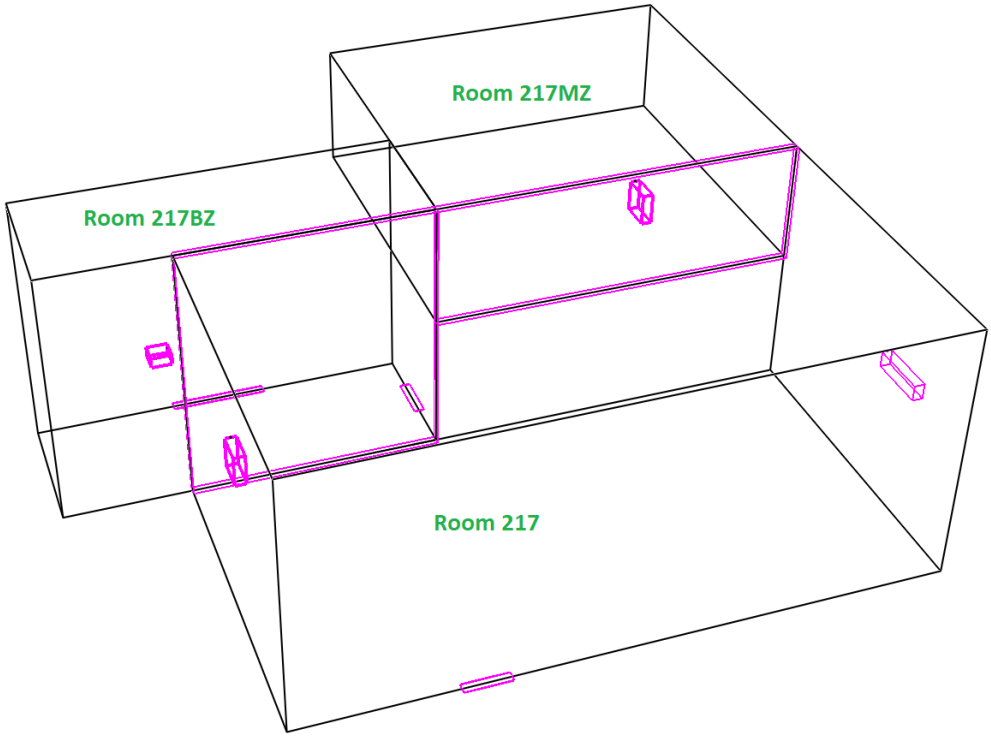

Figure 4: Schematic drawing of fire zone Z115 and its rooms.

2.3.2.3 Ventilation Conditions

Exact information about both the natural openings and mechanical vents was extracted for each fire zone. Such data is mainly intended to be used in CFAST calculations rather than for EPRI FIVE. The impact of the resolution of the representation of the ventilation conditions is discussed in more detail in Phase II of this research project (Chapter 3)[a].

All the natural openings or vents in both case studies are wall vents, i.e., there are no ceiling or floor openings in these fire zones. Table 5 provides the details of the natural vents in both Z071 and Z115 fire zones. Both fire zones contain mechanical or forced ventilation. Table 6 provides the details of the mechanical vents in both Z071 and Z115 fire zones.

Table 5: Natural openings in fire zones Z071 and Z115.

Fire Zone Z071

Vent No. & ID	Room	Elevation* of the Bottom Edge [m]	Height [m]	Width [m]
Door023†	015	0	0.0130	1.8288
Door010	015	0	0.0130	0.9144
Door093	015	3.0480	0.0130	0.9144
Door094	015J	0	0.0130	0.9144
Door095	015J	0	0.0130	0.9144
Door096	015J	0	0.0130	0.9144

Fire Zone Z115

Vent No. & ID	Room	Elevation* of the Bottom Edge [m]	Height [m]	Width [m]
Door01	217	0	0.0130	0.8900
Door02	217BZ	0	0.0130	1.8288
Door03	217BZ	0	0.0130	0.9144
NO1‡	217	2.7188	0.3048	1.1156

* The elevation is measured relative to the reference point of the room. Elevation = 0 m means the edge is at the floor level of that room.

† Door opening, i.e., the opening under the door.

‡ A natural opening that exists on one of the walls of room 217 in Z115.

[a] The different ways that can be used to define the ventilation conditions in a certain fire compartment can represent different DoRs or different variations within a single DoR depending on the utilized approach.

Table 6: Mechanical vents in fire zones Z071 and Z115.

Fire Zone Z071

Vent No.	Room	Inlet or Outlet	Vent Area [m^2]	Center Height* [m]	Flow Rate [m^3/s]
Vent1	015	Inlet	0.5110	4.2926	1.4630
Vent2	015J	Outlet	0.0413	2.1336	0.0472
Vent3	015	Outlet	0.0161	6.4770	0.0472
Vent4	015J	Outlet	0.0523	0.5715	0.0802
Vent5	015J	Outlet	0.0316	0.5969	0.0802
Vent6	015J	Outlet	0.0161	3.1496	0.0802

Fire Zone Z115

Vent No.	Room	Inlet or Outlet	Vent Area [m^2]	Center Height* [m]	Flow Rate [m^3/s]
Vent1	217BZ	Outlet	0.1594	2.1245	0.3304
Vent2	217	Outlet	0.3097	3.6830	0.6607
Vent3	217MZ	Inlet	0.3716	0.9398	0.9439

* Center height is measured relative to the floor of the room.

2.3.2.4 Arrangement of Ignition Sources

As shown in Table 2, at Z071 there are 4 countable ignition sources and at Z115 there are 10. Out of all these ignition sources, only one ignition source is classified or categorized as Ventilation Subsystems (i.e., bin 26 in NUREG/CR-6850, Vol. 2 [11]). All other ignition sources are classified as Electrical Cabinets (i.e., bin 15 in NUREG/CR-6850, Vol. 2 [11]). Table 7 provides a list of all of these ignition sources, their assigned numbers for the purpose of this report (i.e., IS number), their descriptions, tag numbers, as stated in STPNOC documents and data base [20], and the rooms in which they are located.

2.3.2.5 Location of Safety Targets (nearest cable trays)

During plant walkdowns and data collection, the nearest safety targets (cable trays) were identified. In the case of Z071, the nearest cable trays were located at a height of 3.9624 m in room 015. In the case of Z115, the nearest cable trays were located at a height of 2.7888 m in room 217. These two locations are considered conservative since they represent the nearest target to any ignition source in both respective fire zones. For example, in Z115, two possible cable trays were identified to be potential safety targets for different ignition sources, and the distance of the nearest cable tray was used for all ignition sources in that fire zone.

Table 7: List of all ignition sources in Z071 and Z115.

Fire Zone	IS No.	IS Description	Tag No. at STPNOC	Room	Bin No.
Z071	IS01	Auxiliary Shutdown Panel (ASP)	5Z341ZLP100	015	15
	IS02	Qualified Display Processing System (QDPS) APC D1 ZLP680	4Z551ZLP680	015	15
	IS03	QDPS APC D2 ZLP6801	4Z551ZLP6801	015	15
	IS04	Command Control Console – PC	9W121ECN0019	015	15
Z115	IS05	ZLP-722: Liquid waste control panel	9R301ZLP722	217	15
	IS06	ZLP-115: Reactor coolant vacuum degassing panel	9R341ZLP115	217	15
	IS07	ZLP-186: Boron recycle evap. panel	9R181ZLP186	217	15
	IS08	480 VAC Breakers (next to ZLP-186)	N/A	217	15
	IS09	ZLP-107: Boron recycle panel ZLP107	9R181ZLP107	217	15
	IS10	ZLP-185: Liquid radwaste evap. panel	9R301ZLP185	217	15
	IS11	ZLP-189: Liquid waste proc. cont. panel	9R301ZLP189	217	15
	IS12	EPL-125C (Distribution Panel)	9E521EPL125C	217	15
	IS13	ZLP-116: Gaseous waste control panel	7R311ZLP116	217	15
	IS14	VAH-025: Chemistry counting room air handling unit	8V101VAH025	217MZ	26

2.3.2.6 Determination of the Heat Release Rate

The HRR is one of the critical parameters used in the estimation of the damage caused by the fire from an ignition source. The HRR significantly affects the results of the calculated temperatures and heat fluxes which are used in the estimation of the damage to the targets. Generally, the choice of the HRR and the value of the fire diameter will determine the nature of the fire being simulated [22]. Therefore, the screening process, which is based on the ZOI and the severity factor of the simulated fire, is dependent on these two parameters. In addition, some of the non-dimensional or normalized parameters used in the evaluation process of the suitability of the ZOI model depend on the HRR (e.g., Froude Number and Equivalence Ratio). For a given ignition source within a fire zone, an HRR should be assigned based on the characteristics of the ignition source. In this section, the details of the implementation of the classification

and the determination of the peak HRR distributions for all the ignition sources in Z071 and Z115 are provided and discussed.

In total, for both Z071 and Z115, there are 13 ignition sources that are classified under bin 15: 'electrical cabinets.' Electrical cabinets are electrical enclosures that can be characterized based on the electrical function, the physical size and location, type and amount of the fuel/cable loading, and the ventilation characteristics [22]. NUREG-2178, Vol. 1 [22] provides a systematic approach for classifying electrical enclosures which can be used in determining the appropriate HRR value. In Section 3 of NUREG-2178, Vol. 1 [22], electrical enclosures are classified into four groups based on their type/function:

- Group 1: Switchgear and Load Centers,
- Group 2: Main Control Centers and Battery Chargers,
- Group 3: Power Inverters,
- Group 4: All Other Electrical Enclosures
    - Group 4a: Large Enclosures,
    - Group 4b: Medium Enclosures, and
    - Group 4c: Small Enclosures.

After the classification of the electrical enclosures based on the type/function, further classification into two types, based on the cabling type, is required. The first type includes thermoset (TS), qualified thermoplastic or synthetic insulated switchboard cables, and the second type is unqualified thermoplastic (TP) cables. For the first three groups, the ventilation type is normally assumed to be closed. For classification of electrical enclosures within Group 4, the subcategorization process is based on three additional aspects (i.e., in addition to the cabling type) which are: (i) the size of the electrical enclosure (ii) the ventilation (open or closed doors), and (iii) fuel load characterization (default, low, or very-low fuel loading). Further information on the differences among these sub-groups is provided in Section 3 in NUREG-2178, Vol. 1 [22].

For the purpose of classifying electrical cabinets (i.e., ignition sources IS01 to IS13), a conservative approach was used. After determining the classification group based on the function, the fuel type is assumed to be TP. Moreover, in the case of Group 4, the electrical cabinets are assumed to be with 'Closed Doors' and have 'Default' fueling loading whenever applicable or whenever exact data is not available. The assumptions about the ventilation for the electrical enclosure ventilation are confirmed through plant walkdowns and data collection. Other conservative assumptions helped in reducing the required resources

and time necessary to collect detailed information for each ignition source. After classifying each electrical cabinet, the recommended HRR values provided in Tables 4-1 and 4-2 of NUREG-2178, Vol. 1 [22] are assigned to each respective ignition source. Table 8 provides the classification (or categorization) and justification of all electrical cabinets in Z071 and Z115. As for IS14, VAH-025, which is classified as bin 26: 'ventilation subsystem,' the recommended HRR values for electrical fires in 'motors' specified in Table G-1 of NUREG/CR-6850, Vol. 2 [11] were utilized as per the recommendation in Table 11-1 of the same document. Table 9 shows the assigned Gamma distribution characteristics of the peak HRR for all ignition sources based on the previous classification in Table 8.

Table 8: Classification and justification of all electrical cabinets in Z071 and Z115

IS No.	Classification [22]	Justification/Comments
IS01	Group 4a	The ASP is similar to Main Control Board and only handles low voltage control power and indications (volume≥1.42 m^3)
IS02	Group 4a	The QDPS cabinets are low voltage computer cabinets (volume≥1.42 m^3)
IS03	Group 4a	
IS04	Group 4c	A small/limited size enclosure (volume≤0.34 m^3)
IS05	Group 4a	Large size electrical enclosure (volume≥1.42 m^3)
IS06	Group 4a	
IS07	Group 4a	
IS08	Group 4b	Medium size electrical enclosure (1.42 m^3≥volume≥0.34 m^3)
IS09	Group 4a	Large size electrical enclosure (volume≥1.42 m^3)
IS10	Group 4a	
IS11	Group 4a	
IS12	Group 4b	Medium size electrical enclosure (1.42 m^3≥volume≥0.34 m^3)
IS13	Group 4a	Large size electrical enclosure (volume≥1.42 m^3)

Table 9: Assigned Gamma distribution characteristics of the peak HRR for all ignition sources in Z071 and Z115.

IS No.	Peak HRR (kW) Gamma Distribution Characteristics			
	98^{th} Percentile	75^{th} Percentile	$\boldsymbol{\alpha}$	$\boldsymbol{\beta}$
IS01	400	100	0.52	145
IS02	400	100	0.52	145
IS03	400	100	0.52	145
IS04	45	15	0.88	12
IS05	400	100	0.52	145
IS06	400	100	0.52	145
IS07	400	100	0.52	145
IS08	200	50	0.52	73
IS09	400	100	0.52	145
IS10	400	100	0.52	145
IS11	400	100	0.52	145
IS12	200	50	0.52	73
IS13	400	100	0.52	145
IS14	69	32	2	11.7

2.3.2.7 Determination of the Fire Diameter

As indicated in section 2.3.2.6, the Fire Diameter (D) is another critical parameter in determining the magnitude of a certain fire. The fire diameter and the HRR are used to determine the nature of the fire [22]. A general approach for calculating the fire diameter is provided in NUREG-1934 [23], and a more detailed explanation is given in NUREG-2178, Vol. 1 [22]. The calculations of the fire diameter for all the ignition sources in Z071 and Z115 are explained in this section with further information about the different approaches provided in the relevant regulatory references.

The fire diameter is used to represent the size of the fire based on the area of the base of the fire. The fire diameter is calculated using $D = \sqrt{4A/\pi}$, where A is the assigned fire base area. Therefore, the determination of the area of the fire base determines the value of the equivalent fire diameter. There are different approaches that can be used to determine this area. The following provides a brief explanation.

- The area of the base of the fire can be assumed to be equal to the vent area [23], when vents exist on the top of the cabinet.
- The footprint area of the enclosure can be used to calculate the area of the base of the fire [22]. This is acceptable in the case of higher intensity fires (i.e., higher HRR values); however, it may violate the validation range for lower HRR values (refer to the discussion in Section 2.3.3 for the detailed discussion on the validation range).
- In the case of the fire diameter that lies outside the range of the plume correlation for the fire HRR being postulated (based on Tables 4-3 and 4-4 of NUREG-2178, Vol. 1 [22]) and where the diameter is too large, the fire diameter can be reduced to the maximum allowed value based on the validation range for Froude Number, 0.2 – 9.1 [22]. However, if the fire diameter is too small, no clear approach is identified by the research team.

Through plant walkdowns, no openings or vents on the top side of the any of the ignition sources were observed or reported. Therefore, the top footprint area of the enclosure's ignition sources is utilized as the area of the base of the fire (A). This might exclude IS04, which is a commercial PC console that has a perforated surface on the top, but the footprint area was also used for IS04 since it is a relatively small area, even without considering the perforation. Although it was observed that some ignition sources, such as the IS01, IS02, and IS03, contain vertical vents on the sides, based on [23], such vents can be used to determine the height of the fire base but not the fire base area. For the purpose of investigating the impact of data collection and plant walkdowns on the fire analysis and screening of fire scenarios, two fire areas

were assigned to IS02. These two areas are based on the footprint area, IS02_1, and on the area of the vertical vents found on the side of the cabinet, IS02_2.

Table 10 provides the top areas and the perspective Fire Diameter (D) based on the top footprint area for each ignition source. It should be noted that, based on the validation process, the Fire Diameter (D) values might need to be adjusted or modified for certain situations, such as when validation ranges are not met (see discussion on the evaluation of the suitability of fire models in Section 2.3.3) or there is a need to insert conservatism into the fire conditions.

Table 10: Fire Diameter based on the fire base area.

IS No.	Top Area (m^2)	Fire Diameter (m)
IS01	3.3445	2.0636
IS02_1	0.7452	0.9740
IS02_2	0.1316	0.4093
IS03	0.7452	0.9740
IS04	0.3513	0.6688
IS05	3.7161	2.1752
IS06	0.9290	1.0876
IS07	1.4233	1.3462
IS08	0.1776	0.4755
IS09	1.1148	1.1914
IS10	2.0903	1.6314
IS11	5.5742	2.6641
IS12	0.1673	0.4616
IS13	1.6723	1.4592
IS14	5.0649	2.5395

2.3.2.8 Determination of the Height of Fire Base

The fire location, or the fire base height, is one of the main parameters used in constructing the ZOI. Moreover, the fire location is used in the calculations of different parameters utilized in the suitability of the fire model discussed in Section 2.3.3. In this section, the height of the fire base for each ignition source is determined and justified.

A generic guidance for determining the fire base height in electrical enclosures is provided in FAQ 08-0043: "Location of Fires within Electrical Cabinets" [24]. This document recommends the approach shown in Table 11. Following this approach, the fire base heights for all the ignition sources are determined (as shown in Table 12).

As shown in Table 12, the fire base height depends on the configuration of the vents and openings in the electrical enclosure. Further explanation regarding the definition of the penetrations (i.e. sealed or unsealed openings) is provided in the FAQ 08-0043 [24], which states: "As a point of clarification, it should be noted that in the above description on penetrations, "sealed at the top of the cabinet" was not intended to imply "fire-rated." Rather the intent was that penetrations into a cabinet would be sealed such that they would not readily allow for the passage of air."

Therefore, if a cabinet has some pipes, conduits, or cables entering from the top side with a "closed/sealed" penetration, it will be considered to be sealed on the top (i.e., Cases 1 or 3 in Table 11). Section 6.5.6 in NUREG/CR-6850, Vol. 2 [11], provides a similar explanation regarding the penetration. Under Bin 15: Electrical Cabinets (Plant-Wide Components), a "well-sealed" cabinet is defined as a cabinet that does not have any open or unsealed penetrations or ventilation openings without any consideration of the fire-rating of the sealings. In addition, "well-sealed" also means that potential warping of the sides/walls of the panel would not open gaps that might allow an internal fire to escape [11]. Further information about the openings and penetrations in electrical cabinets is provided in Section G.3.3 of NUREG/CR-6850, Vol. 2 [11].

Table 11: General approach for determining the fire location in electrical enclosures per FAQ 08-0042.

Case	Approach to Determine Fire Location
Case 1: Electrical cabinets sealed on the top (without horizontal top vents or openings).	Fire location is assumed to be one foot below the top of the cabinet.
Case 2: Cabinets that are not sealed at the top.	Fire location should be the top of the cabinet.
Case 3: Vented cabinets, where the vent is either located on the side of the cabinet (vertical) or top of the cabinet (horizontal).	Fire can be located at the uppermost vent[*].
Case 4: For cabinets that are neither vented nor considered sealed.	Fire location would be assumed at the top of the door or opening which is expected to fail with fire damage[†].

[*] This is an alternative to the assumed location for the cabinets sealed on the top (i.e., an alternative to the "one foot below the top" approach).

[†] A conservative approach in locating the fire should always be considered, e.g., choosing the location nearest to the targets or choosing the higher opening. If such assumption greatly affects the results, further detailed analysis will be required.

Table 12: Fire locations (fire base heights).

IS No.	IS Physical Height (m)	Fire Base Elevation from the Floor (m)	Case or Approach (from Table 11)
IS01	2.4130	2.1082	Case 3: Cabinets that are sealed on the top with side/vertical vents (the top edge of the uppermost vent is 2.1082 m)
IS02_1	2.3368	2.1590	Case 3: Cabinets that are sealed on the top with side/vertical vents (the top edge of the uppermost vent is 2.1590 m)
IS02_2	2.3368	2.1590	
IS03	2.3368	2.1590	
IS04	0.6287	1.2192*	Case 2: The PC is considered as a cabinet that is not sealed at the top
IS05	2.2860	2.3876†	Case 1: Electrical cabinets sealed on the top (conservatively assumed to be the same height as the ignition source)
IS06	1.9812	1.9304†	
IS07	2.2860	1.8298†	
IS08	2.2860	2.3876†	
IS09	2.2860	1.8542†	Case 3: Cabinets that are sealed on the top with side/vertical vents (the top edge of the uppermost vent is 1.7526 m)
IS10	2.2860	2.3876†	Case 1: Electrical cabinets sealed on the top (conservatively assumed to be the same height as the ignition source)
IS11	2.2860	2.3876†	
IS12	2.2860	2.3876†	
IS13	2.2860	2.3876†	
IS14	NA‡	1.0000‡	NA‡

* Even if we are not sure how to classify such a case, due to the small size of the PC, low cable/fuel loading, and low probability of fire ignition, using the top of the PC as the fire location can be considered as a conservative approach. The PC is assumed to be elevated and stationed on the top of table/desk.

† IS05-IS13, Ignition sources that are located in room 217 of Z115, are elevated by a 0.1015 m (4 in) concrete base from the floor.

‡ Due to the difficulty of accessing the mezzanine area in room 217 of Z115 where IS14 is located, data about the exact height of the ignition source and other specifications were not obtainable. For the purpose of the analysis, the fire base height is assumed to be 1 m from the floor of the mezzanine area. It should be noted that, based on the collected data, the nearest target is located at a radial distance from the fire center.

2.3.3 Evaluation of Fire Model Suitability

As per NUREG-1824, Supp. 1 [25] and NUREG-1934 [23], the suitability of a fire model or fire analysis tool on a specific fire zone or ignition source should be evaluated. In the current analysis, the zone model, CFAST, and engineering correlations, EPRI FIVE, were chosen to conduct the fire modeling and analysis. Therefore, the limitations of the models should be understood and investigated in the case of both Z071 and Z115 and the ignition sources of concern.

In this section, the suitability of the zone model, CFAST, and engineering correlations, EPRI FIVE, for the ignition sources in Z071 and Z115, is established by calculating the non-dimensional/normalized parameters and comparing them to their specified validation ranges. The updated validation ranges provided in NUREG-1824, Supp. 1 [25] are utilized in the current analysis.

There are 6 non-dimensional/normalized parameters that can be used in the validation process. These parameters are:

- Fire Froude Number ($\dot{Q}^*$),
- Flame Length ($H_f + L_f$) relative to the Ceiling Height (H_c),
- Ceiling Jet Radial Distance (r_{cj}) relative to the Ceiling Height (H_c),
- Equivalence Ratio (φ) as an indicator of the Ventilation Rate,
- Compartment Aspect Ratio, and
- Target Distance (r) relative to the Fire Diameter (D).

Four of these parameters depend on the characteristics of the ignition source, namely, Froude Number ($\dot{Q}^*$), Flame Length ($H_f + L_f$) relative to the Ceiling Height (H_c), Equivalence Ratio (φ), and Target Distance (r) relative to the Fire Diameter (D). The Ceiling Jet Radial Distance (r_{cj}) relative to the Ceiling Height (H_c) is not applicable in the current analysis for Z071 and Z115 due to the exclusion of the jet targets from the analysis/simulation. The Compartment Aspect Ratio depends on the geometrical dimensions of the compartments in the fire zone and, thus, is calculated for each compartment.

2.3.3.1 Compartment Aspect Ratio

The Compartment Aspect Ratio is used as an indication for the general shape of the compartment. Two aspects, the length (L) and the width (W), are weighted relative to the ceiling height (H_c) of the compartment. The fire zone Z071 is represented by two compartments, rooms ‘015’ and ‘015J.’ The fire

zone Z115 is represented by three compartments: room '217,' an entrance area labeled '217BZ,' and the mezzanine area (above room '231') labeled '217MZ.'

The compartment aspect ratio is calculated for each compartment and for the equivalent compartment based on the total volume of the whole fire zones. Table 13 provides the values of the Compartment Aspect Ratios for Z071 and Z115 except for room '217BZ' in Z115 since this room does not contain any ignition sources or fires. However, the volume of this zone is included in the calculations of the total fire zone volume for Z115. All the values in Table 13 are within the validation range of 0.6 - 8.3 [25].

Table 13: Compartment Aspect Ratio.

Fire Zones	Compartment	Compartment Aspect Ratio	In Range?
Z071	015	$\frac{L}{H_c} = \frac{5.7912\ m}{7.3152\ m} \cong 0.792 \quad ; \quad \frac{W}{H_c} = \frac{4.572\ m}{7.3152\ m} \cong 0.625$	Yes
	015J	$\frac{L}{H_c} = \frac{5.7912\ m}{4.2672\ m} \cong 1.357 \quad ; \quad \frac{W}{H_c} = \frac{10.3632\ m}{4.2672\ m} \cong 2.43$	Yes
	Total Fire Zone Vol.	$Total\ vol = 449.8\ m^3;\ H_{c,eq} = 7.3152\ m$ $\frac{L_{eq}}{H_c} = \frac{W_{eq}}{H_c} = \frac{7.8413\ m}{7.3152\ m} \cong 1.0719$	Yes
Z115	217	$\frac{L}{H_c} = \frac{6.5532\ m}{5.1816\ m} \cong 1.2647 \quad ; \quad \frac{W}{H_c} = \frac{12.0396}{5.1816\ m} \cong 2.3235$	Yes
	217MZ	$\frac{L}{H_c} = \frac{6.6812\ m}{2.4384\ m} \cong 2.7400 \quad ; \quad \frac{W}{H_c} = \frac{6.9098\ m}{2.4384\ m} \cong 2.8338$	Yes
	Total Fire Zone Vol.	$Total\ vol = 623.9\ m^3;\ H_{c,eq} = 5.1816\ m$ $\frac{L_{eq}}{H_c} = \frac{W_{eq}}{H_c} = \frac{10.9734\ m}{5.1816\ m} \cong 1.0719$	Yes

2.3.3.2 Fire Froude Number

In this section, the calculation of the Froude Number ($\dot{Q}^*$) for the Ignition sources in Z071 and Z115 is demonstrated. The Froude Number ($\dot{Q}^*$) can be calculated using the following formula:

$$\dot{Q}^* = \frac{\dot{Q}}{\rho_\infty c_p T_\infty D^{2.5} \sqrt{g}}, \quad (2)$$

where:

$\rho_\infty = 1.2041\ kg/m^3$

$c_p = 1.012\ kJ/kg/K$

$T_\infty = 293.15\ K$

$g = 9.8\ m/s^2$

The results of the Froude Number ($\dot{Q}^*$) are provided in Table 14. It was observed that the Froude Number ($\dot{Q}^*$) is out of the validation range of 0.2 - 9.1 [25] for eight ignition sources. Furthermore, the Froude Number ($\dot{Q}^*$) for these cases was below the lower limit, i.e., fires with low Froude Number ($\dot{Q}^*$). Based on the approach suggested in NUREG-1934 [23] and NUREG-2178, Vol. 1 [22], in the case that the Fire Diameter (D) provides values out of the validation range, the fire base area or the Fire Diameter (D) can be adjusted so that the non-dimensional parameters fall within the validation range. In the case of ignition sources IS01-IS13, the safety-related damage targets are located above the top area of the ignition sources. Increasing the Froude Number ($\dot{Q}^*$) makes the fire generate more momentum-driven fire plumes; therefore, for ignition sources IS01 to IS13, this adjustment generates conservative results. The research team decided to utilize the lower value of the validation range for the Froude Number ($\dot{Q}^*$), i.e., $\dot{Q}^* = 0.2$, in order to calculate the value of the adjusted Fire Diameter (D). Although the common practice is to use the value of Froude Number $\dot{Q}^* = 1$ for similar cases to adjust the Fire Diameter (D) so that conservatism is ensured[b], the research team chose to have a more realistic representation of the fire conditions. That is not to alter the fire conditions drastically but to ensure that the changes remain conservative. Therefore, two additional cases, IS01_2 and IS01_3, in addition to the original case IS01_1, were introduced to the IS01 analysis. These two cases represent the adjustment of the Fire Diameter (D) using two different Froude Numbers ($\dot{Q}^*$), $\dot{Q}^* = 0.2$ and $\dot{Q}^* = 1$. For IS14, limited data was available to determine the exact location of the safety-related damage targets. Therefore, the severity factor will be calculated for two directions, the

[b] Both the ignition source characteristics and the location of the safety target need to be considered in order to justify conservative adjustments on the Froude Number (and thus, modifications to the Fire Diameter).

radial and axial location. The adjusted $\dot{Q}^*$ case, however, represents the case of the lower bound of the validation range, i.e., $\dot{Q}^* = 0.2$, to provide relatively extreme fire conditions above this ignition source.

Table 15 shows the values of both the original and the adjusted Froude Number ($\dot{Q}^*$) and Fire Diameter (D) for ignition sources where the original Froude Number ($\dot{Q}^*$) was below the validation limit.

Table 14: Froude Number based on HRRs in Table 9 and Fire Diameters in Table 10.

IS No.	Froude Number ($\dot{\boldsymbol{Q}}^*$)	In range?
IS01	0.0585	No
IS02_1	0.3820	Yes
IS02_2	3.3366	Yes
IS03	0.3820	Yes
IS04	0.1100	No
IS05	0.0513	No
IS06	0.2900	Yes
IS07	0.1701	No
IS08	1.1468	Yes
IS09	0.2309	Yes
IS10	0.1052	No
IS11	0.0309	No
IS12	1.2356	Yes
IS13	0.1391	No
IS14	0.0060	No

Table 15: Adjusted Fire Diameter for ignition sources with Froude Number out of the validation range.

IS No.	Original Froude Number ($\dot{Q}^*$)	Previous Fire Diameter (m)	Adjusted Froude Number ($\dot{Q}^*$)	Adjusted Fire Diameter (m)
IS01_1	0.0585	2.0636	-	-
IS01_2	-	-	0.2	1.2618
IS01_3	-	-	1	0.6628
IS04	0.1100	0.6688	0.2	0.5266
IS05	0.0513	2.1752	0.2	1.2618
IS07	0.1701	1.3462	0.2	1.2618
IS10	0.1052	1.6314	0.2	1.2618
IS11	0.0309	2.6641	0.2	1.2618
IS13	0.1391	1.4592	0.2	1.2618
IS14	0.0060	2.5395	0.2	0.6248

2.3.3.3 Flame Length Ratio

The Flame Length Ratio is the flame length ($H_f + L_f$) relative to the ceiling height (H_c) which is used to express the "size" of the fire relative to the height of the compartment. The flame length is calculated by adding the height of the fire base (H_f) and the flame height (L_f). The height of the fire base (H_f) is provided in Table 12 for each ignition source. The flame height (L_f) is calculated based on the following equation:

$$L_f = D \times (3.7 \times \dot{Q}^{*2/5} - 1.02), \quad (3)$$

Table 16 provides the values of the flame height (L_f) and the flame length ($H_f + L_f$) for each case. It should be noted that this table provides the values of the flame height (L_f) and the flame length ($H_f + L_f$) using the adjusted Fire Diameter (D) for the cases that required adjustments in Table 15.

Table 16: Flame Height, Flame Length, and Flame Length Ratio for all ignition sources.

IS No.	Flame Height (L_f) [m]	Flame Length ($H_f + L_f$) [m]	Flame Length Ratio	In range?
IS01_1	0.3476	2.4558	0.3357	Yes
IS01_2	1.1654	3.2736	0.4475	Yes
IS01_3	1.7764	3.8846	0.5310	Yes
IS02_1	1.4590	3.6180	0.4946	Yes
IS02_2	2.0350	4.1940	0.5733	Yes
IS03	1.4590	3.6180	0.4946	Yes
IS04	0.4864	1.7056	0.2332	Yes
IS05	1.1654	3.5530	0.6857	Yes
IS06	1.3431	3.2735	0.6318	Yes
IS07	1.1654	2.9953	0.5781	Yes
IS08	1.3736	3.7612	0.7259	Yes
IS09	1.2373	3.0915	0.5966	Yes
IS10	1.1654	3.5530	0.6857	Yes
IS11	1.1654	3.5530	0.6857	Yes
IS12	1.3878	3.7754	0.7286	Yes
IS13	1.1654	3.5530	0.6857	Yes
IS14	0.5770	1.5770	0.6468	Yes

For all the ignition sources in room '015' in Z071, the ceiling height (H_c) is 7.3152 m. For all the ignition sources in room '217' in Z115, the ceiling height (H_c) is 5.1816 m while ceiling height (H_c) in the case of IS14 in room '217MZ' is 2.4384 m. The Flame Length Ratio is calculated using the following relation:

$$Flame\ Length\ Ratio = \frac{H_f + L_f}{H_c}. \tag{4}$$

Table 16 shows the values of the Flame Length Ratio. In all the cases, the Flame Length Ratio is found to be within the validation range of 0.2 - 1.0 [25].

2.3.3.4 Equivalence Ratio

The Equivalence Ratio (φ) relates the energy release rate (i.e., the HRR) of the fire to the energy release that can be supported by the mass flow rate of oxygen into the compartment. It is calculated using the following equation:

$$\varphi = \frac{\dot{Q}}{\Delta H_{O_2}\, \dot{m}_{O_2}}, \tag{5}$$

where:

ΔH_{O_2}: the "heat of combustion" for oxygen ($13100\ kJ/kg$)

$$\dot{m}_{O_2} = \begin{cases} 0.23 \times 0.5\ A_o\sqrt{H_o} & (Natural) \\ 0.23 \times 0.5\ \rho_\infty \dot{V} & (Mechanical) \end{cases}$$

A_o: the effective area of the openings (m^2)

H_o: the effective height of the openings (m)

ρ_∞: the density of ambient air ($1.2041\ kg/m^3$)

$\dot{V}$: the volumetric flow rate of air into the enclosure (m^3/s)

Table 17 and Table 18 provide all the required steps for the estimation of the mass flow rate of oxygen ($\dot{m}_{O_2}$) into the fire zones Z071 and Z115, respectively.

Table 17: Mass flow rate of oxygen calculations for Z071.

Z071	
Heights of Natural Openings (H_i)	All heights for the natural openings (doors) are $0.013\ m$.
Effective Natural Opening Area (A_o)	In total for both compartments, there are 6 vertical vents/openings, and the doors of both compartments are normally closed. $A_o = \sum_{i=1}^{n=6} A_i = 0.013 \times 1.8288 + 5 \times 0.013 \times 0.9144$ $= 0.08321\ m^2$
Effective Height of Natural Openings (H_o)	$H_o = \frac{\sum_{i=1}^{n=6} A_i \times H_i}{\sum_{i=1}^{n=6} A_i}$ $= \frac{(0.013 \times 1.8288) \times 0.013 + (5 \times 0.013 \times 0.9144) \times 0.013}{0.08321\ m^2}$ $= 0.013\ m$
Volumetric flow rate of air into the enclosure ($\dot{V}$)	There is only one mechanical inlet. $\dot{V} = 1.463\ m^3/sec$
Mass flow rate of oxygen ($\dot{m}_{O_2}$)	$\dot{m}_{O_2}(Natural) = 0.23 \times 0.5 A_o \sqrt{H_o} = 0.23 \times 0.5 \times 0.08321 \times \sqrt{0.013}$ $= 0.001091\ kg/sec$ $\dot{m}_{O_2}(Mechanical) = 0.23 \times 0.5\ \rho_\infty \dot{V} = 0.23 \times 0.5 \times 1.2041 \times 1.463$ $= 0.40517\ kg/sec$ Dominant ventilation: $0.40517\ kg/sec$ (Note: if the values of natural and mechanical ventilation are comparable, it is suggested to add them).

Table 18: Mass flow rate of oxygen calculations for Z115.

Z115	
Heights of Natural Openings (H_i)	4 Natural openings that are connected to the outside. $H_1 = 0.013\ m, H_2 = 0.013\ m, H_3 = 0.013, and\ H_4 = 0.3048\ m.$
Effective Natural Opening Area (A_o)	In total, for all compartments, there are 4 vertical vents/openings, and the doors of both compartments are normally closed. $A_o = \sum_{i=1}^{n=4} A_i = 0.013 \times (0.89 + 1.8288 + 0.9144) + 0.3048 \times 1.1156$ $= 0.0116 + 0.0238 + 0.0119 + 0.340$ $= 0.3873\ m^2$
Effective Height of Natural Openings (H_o)	$H_o = \frac{\sum_{i=1}^{n=4} A_i \times H_i}{A_o}$ $= \frac{0.013 \times (0.0116 + 0.0238 + 0.0119) + 0.3048 \times 0.3400}{0.3873}$ $= 0.0002 + 0.0003 + 0.0002 + 0.1036$ $= 0.2692\ m$
Volumetric flow rate of air into the enclosure ($\dot{V}$)	There one mechanical supply vent. $\dot{V} = 0.94389\ m^3/sec$
Mass flow rate of oxygen ($\dot{m}_{O_2}$)	$\dot{m}_{O_2}(Natural) = 0.23 \times 0.5 A_o \sqrt{H_o}$ $= 0.23 \times 0.5 \times 0.3873 \times \sqrt{0.2692}$ $= 0.023108\ kg/sec$ $\dot{m}_{O_2}(Mechanical) = 0.23 \times 0.5\ \rho_\infty \dot{V} = 0.23 \times 0.5 \times 1.2041 \times 0.94389$ $= 0.1307\ kg/sec$ Dominant ventilation: $0.1307\ kg/sec$ (Note: if the values of natural and mechanical ventilation are comparable, it is suggested to sum them).

Table 19 provides the values of the Equivalence Ratio (φ) based on the above calculated mass flow rates of oxygen ($\dot{m}_{O_2}$) into the fire zones and the HRRs (the 98th percentile) provided in Table 9. The Equivalence Ratios (φ) for all the ignition sources are within the validation range of 0.0 - 0.6 [25].

Table 19: Equivalence Ratio for all the ignition sources.

IS No.	Equivalence Ratio ($\boldsymbol{\varphi}$)	In range?
IS01_1	0.0754	Yes
IS01_2	0.0754	Yes
IS01_3	0.0754	Yes
IS02_1	0.0754	Yes
IS02_2	0.0754	Yes
IS03	0.0754	Yes
IS04	0.0085	Yes
IS05	0.2336	Yes
IS06	0.2336	Yes
IS07	0.2336	Yes
IS08	0.1168	Yes
IS09	0.2336	Yes
IS10	0.2336	Yes
IS11	0.2336	Yes
IS12	0.1168	Yes
IS13	0.2336	Yes
IS14	0.0403	Yes

2.3.3.5 Radial Distance Ratio

The Radial Distance Ratio is the Target Distance (r) relative to the Fire Diameter (D) and is simply given as r/D. As an initial step in the analysis, a range for the Target Distance (r) was established based on the validation range and using the value of the Fire Diameter (D) (Table 10 for cases that did not require adjustment and Table 15 for adjusted cases) since the information about the distance of the targets was unavailable. This range was established based on the Radial Distance Ratio validation range which is 0.3 -

8.0 [25]. Table 20 shows the min. (at $r/D = 0.3$) and max. (at $r/D = 8.0$) allowable values for each ignition source and for every possible value for the Fire Diameter (D).

In later stages of the work by the research team, the distances of the nearest safety targets were collected through plant walkdowns. The nearest cable trays in Z071 and Z115 are located at the heights of 3.9624 m in room '015' and 2.7888 m in room '217,' respectively. Table 20 shows the nearest target distance (r) for each case. It is noted that all the targets are within the validation range. As for IS14, it should be clarified that the nearest target distance (r) is considered an extremely conservative estimate.

Table 20: Estimated range for radial target distance and nearest target distance for all ignition sources.

IS No.	Target Distance ($\boldsymbol{r}$) Range [m]		Nearest Target Distance ($\boldsymbol{r}$) [m]	In range?
	Min.	Max.		
IS01_1	0.6191	16.5086	1.8542	Yes
IS01_2	0.3785	10.0945	1.8542	Yes
IS01_3	0.1989	5.3027	1.8542	Yes
IS02_1	0.2922	7.7924	1.8034	Yes
IS02_2	0.1228	3.2747	1.8034	Yes
IS03	0.2922	7.7924	1.8034	Yes
IS04	0.1580	4.2125	2.7432	Yes
IS05	0.3785	10.0945	0.4012	Yes
IS06	0.3263	8.7008	0.8584	Yes
IS07	0.3785	10.0945	0.9590	Yes
IS08	0.1427	3.8044	0.4012	Yes
IS09	0.3574	9.5313	0.9346	Yes
IS10	0.3785	10.0945	0.4012	Yes
IS11	0.3785	10.0945	0.4012	Yes
IS12	0.1385	3.6926	0.4012	Yes
IS13	0.3785	10.0945	0.4012	Yes
IS14	0.1874	4.9980	0.4012	Yes

2.3.4 ZOI and Severity Factor Analysis Using CFAST

In this section, the ZOI and Severity Factor analysis using CFAST as the fire analysis tool are summarized and the results are discussed. Version 7.6.0 of CFAST was used to conduct analysis for each ignition source in Z071 and Z115.

2.3.4.1 Fire-Induced ZOI Using CFAST

The fire-induced ZOI was established using a mesh of targets/devices in CFAST to calculate the surrounding gas temperature, surface temperature, internal temperature, and the normal incident heat flux around the ignition sources. The mesh size used in the analysis is 0.1 m. Different radial directions were analyzed (mainly two directions: x-axis and y-axis) in order to ensure that the dynamics of the fire in multiple directions are captured, and the maximum radius is reported. Figure 5 shows an example of the mesh of targets or devices constructed in CFAST input files[c]. Due to the limitations on the number of the targets/devices in CFAST (a maximum of 1000 targets/devices), the analysis was conducted separately for each direction, which led to more computational time. Moreover, having more than 500 targets/devices in a single run caused issues in the device output file (.csv file), which imposed an additional computational burden. In order to handle the construction of various CFAST input files and to process the output data, Python codes, i.e., subroutines, were developed and used. These subroutines were also enhanced and integrated in the developed computational platform in Phase II of this research project (see Chapter 3 for more details). Two cases of cable material were investigated, namely, TP and TS. Damaging criteria for each case is provided in Table 21 (based on Table 1 in FAQ 16-0011 and Tables 8-2 and H-1 in NUREG/CR-6850, Vol. 2 [11]). The 98th percentile of the peak HRR is used to construct the ZOI as per NUREG/CR-6850, Vol. 2 [11]. Whenever the temperature of a device or the incident heat flux exceed the criteria at any time step, the location of that device is reported. In order to ensure conservatism, the location of the next device is used to establish the ZOI radius (R) and height (H), i.e., the location of the farthest device at which the criteria was exceeded plus 0.1 m (i.e., no interpolation was done to calculate a more accurate distance). Therefore, the reported ZOI represents the maximum ZOI possible for each ignition source over the duration of the fire. Moreover, in the case of the ZOI radius using CFAST, the ZOI radius changes with the elevation from the fire base height (i.e., from the center the fire). As part of the feedback and the efforts of the research team on Phase II of this research project, two values for the radiative fraction parameter were utilized to investigate its impact on the fire modeling for the ZOI and severity factor analysis. These two values are 0.53 and 0.35 which represent bounding limits for the radiative fraction

[c] This figure was produced using the visualization capabilities of CFAST which are based on Smokeview [21] G. P. Forney, "Smokeview (Version 6)-A Tool for Visualizing Fire Dynamics Simulation Data Volume III: Verification Guide," 2013..

parameter for materials that are categorized as electrical cables, which is the case for the safety targets in Z071 and Z115.

As seen in Figure 5, the target mesh constructed in CFAST can capture the temperature and heat flux around the fire in multiple locations and directions, which results in a more realistic representation of the ZOI that is similar to the fire visualized in this figure. An example of such representation is provided for IS07 in Figure 6 for radiative fraction = 0.35 and in Figure 7 for radiative fraction = 0.53. In these two figures, the ZOI dimensions are illustrated relative to the fire center or the fire base height (1.83 m). The ZOI is generated for each case using the four relevant damage modes that can be extracted from CFAST (i.e., surrounding gas temperature, surface temperature, internal temperature, and the normal incident heat flux). Reporting the maximum radius (shown by the dashed black lines in Figure 6 and Figure 7) provides the reported results with a substantial level of conservatism considering that, after CFAST simulation is completed, the output data can be easily processed to produce a realistic ZOI. Further discussion on the impact of the radiative fraction, target material, and damage mode is provided next. As for the simulation time, on average, the ZOI can be constructed for a specific ignition source based on a single CFAST run, which is typically 3-6 min (or 15 maximum). In order to ensure the fire behavior is captured accurately, a few runs for the same ignition source will be required (2-3 runs).

Table 21: Bounding cable damage/ignition criteria.

Cable Type	Radiant Heating	Temperature
Thermoplastic (TP)	$6\ kW/m^2$	$205\ °C$
Thermoset (TS)	$11\ kW/m^2$	$330\ °C$

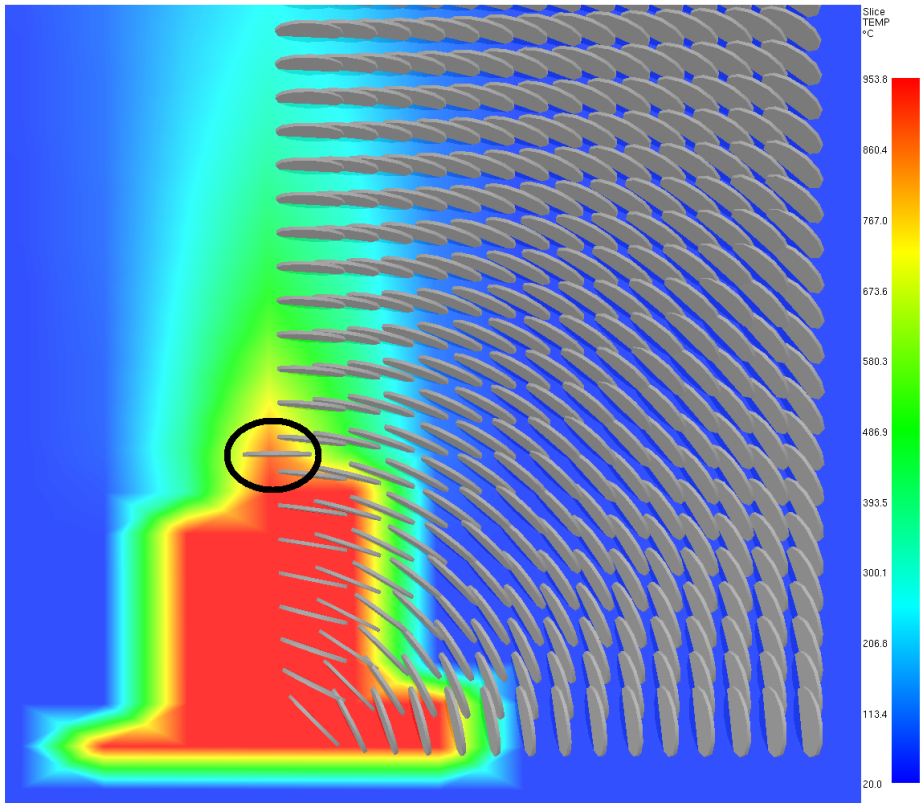

Figure 5: Example of the mesh of targets/devices used in CFAST to calculate the fire-induced ZOI for IS06.

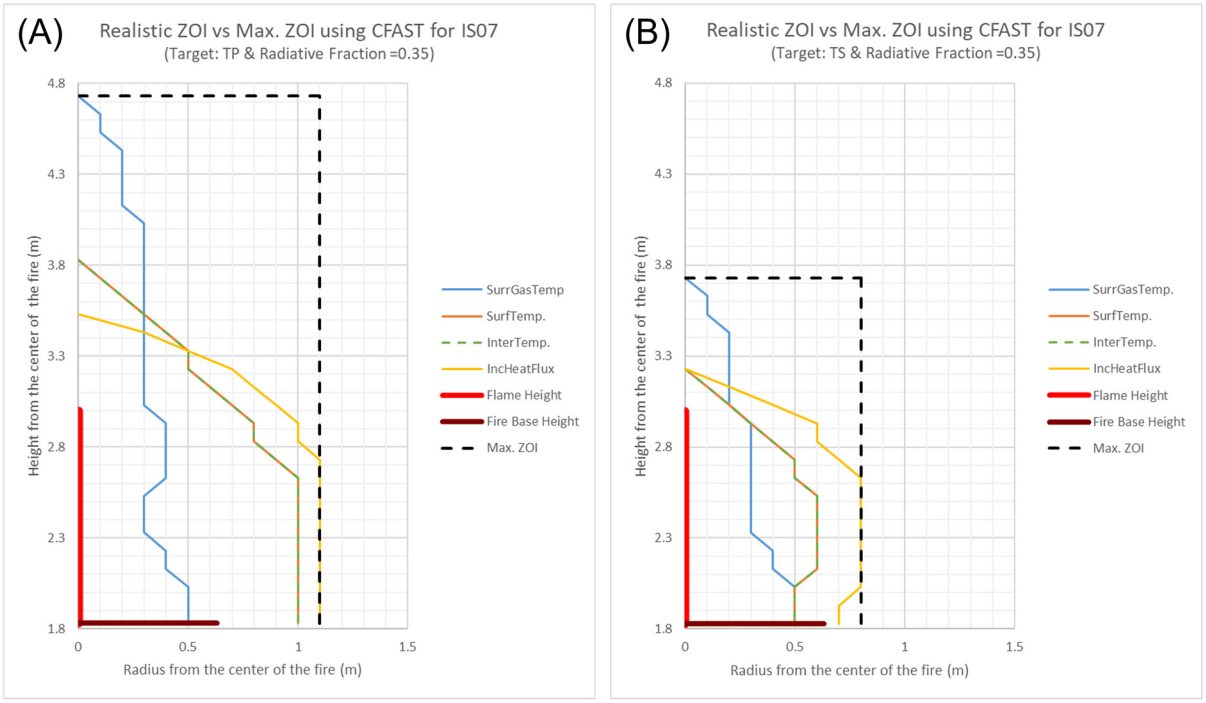

Figure 6: Realistic ZOI vs. max ZOI using CFAST for IS07 in the case of radiative fraction = 0.35 (A: the case of TP targets, and B: the case of TS targets).

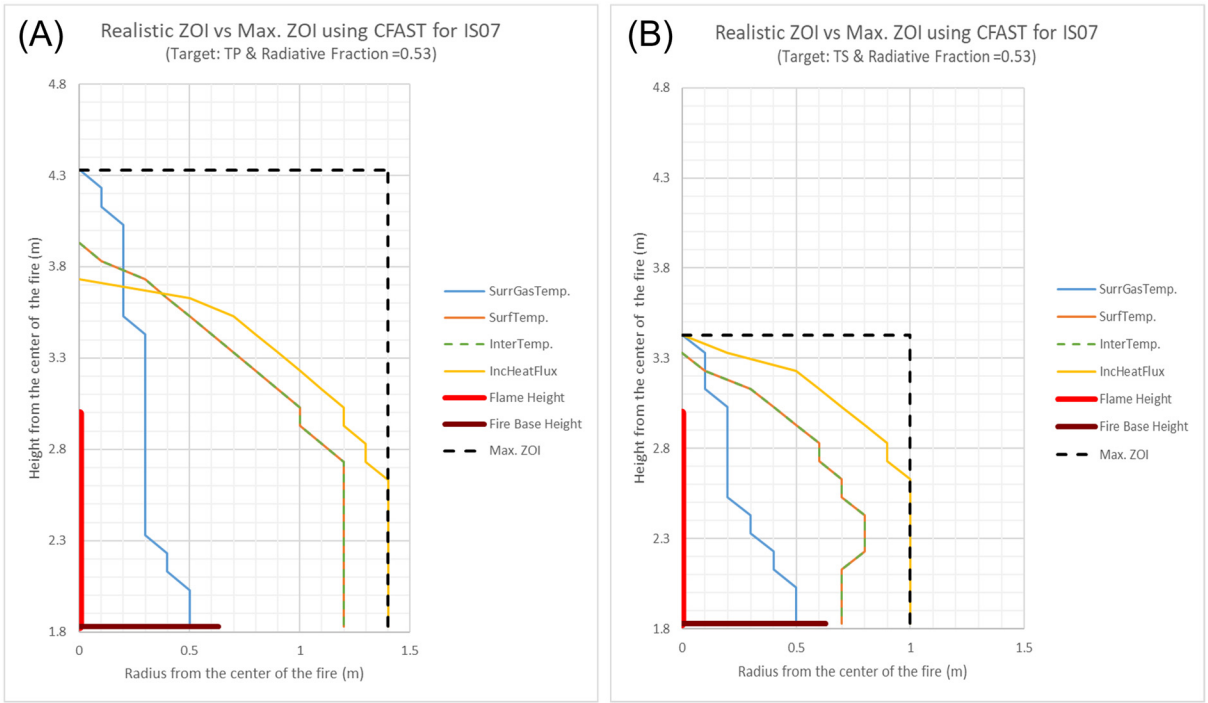

Figure 7: Realistic ZOI vs. max ZOI using CFAST for IS07 in the case of radiative fraction = 0.53 (A: the case of TP targets, and B: the case of TS targets).

Although the discussion and trends are somewhat similar for both TP and TS materials, the results are provided for both and the differences, if any, are briefly discussed. Table 22 and Table 23 provide the values of the maximum ZOI radius (R) for each ignition source and for each damaging mode for safety targets with TP material in the case of radiative fractions 0.53 and 0.35, respectively. Table 24 and Table 25 provide the values of the maximum ZOI radius (R) for each ignition source and for each damaging mode for safety targets with TS material in the case of radiative fractions 0.53 and 0.35, respectively. Table 26 and Table 27 provide the maximum height (H) for TP cables in the case of radiative fractions 0.53 and 0.35, respectively, and Table 28 and Table 29 provide the maximum height (H) for TS cables in the case of radiative fractions 0.53 and 0.35, respectively.

In general, certain trends can be observed based on the tables, using Table 22 to Table 25 for the maximum ZOI radius, and Table 26 to Table 29 for the maximum ZOI height. In the case of the maximum ZOI radius, the incident heat flux damage mode would provide the maximum radius regardless of the material of the targets or the value of the radiative fraction. These values are normally found near the fire center where the radiation part dominates in the radial direction compared to the plume temperature. This also explains why the increase in the radiative fraction will be accompanied with an increase in the maximum radius based on the incident heat flux. On average, there is an increase of about 0.2529 m and 0.1882 m, in the maximum radius based on the incident heat flux for all the ignition sources considered in this analysis, for TP and TS targets, respectively. A similar trend is observed for the surface temperature and internal temperature mode. However, in the case of surrounding gas temperature, since increasing the radiative fraction directly impacts the convection flow or plume heat, there is a slight decrease in the radius as the value of the radiative fraction increases. The average maximum differences in the maximum ZOI radius between the four damaging modes across all the ignition sources are 0.7059 m and 0.4029 m for TP and TS targets, respectively. If these latter values are examined closely with consideration of the dimensions of the fire zones and the arrangement of the ignition sources, they can be considered as significant and, thus, can impact the screening process and its outcomes.

In the case of the maximum ZOI height, since the height is calculated in the centerline of the plume right above the center of the fire, the surrounding gas temperature provides higher values compared to the other three damage modes. On average, the maximum differences across the four damaging modes were 0.8971 m and 0.4765 m for TP and TS materials, respectively. It can be observed that decreasing the radiative fraction values causes an increase in the maximum ZOI height. On average, there are 0.376 m and 0.265 m increases in the maximum ZOI for TP and TS targets, respectively, across all ignition sources.

Based on the ZOI analysis using CFAST (the results shown in Table 22 to Table 29) and the arrangement in the two fire zones being analyzed (i.e., Z071 and Z115), few ignition sources can be screened out or scoped out of the analysis. Since the safety targets are assumed to be in the centerline of the fire, right above the ignition sources, only the ZOI height is used to conduct the scoping of ignition sources based on the ZOI analysis. Therefore, IS14 can be screened out since, in reality, there are no safety targets in room '217MZ' and the assumed target distance is unrealistically conservative (refer to Section 2.3.3.5). If the safety targets are TP cables (which is the most conservative assumption in cases where there is no information or data on the materials of the safety targets), only IS04 can be screened out based on all four damage modes. However, if the safety targets are TS cables, in addition to screening out IS04, the first case of IS01, i.e., IS01_1 (which represents the actual footprint area of IS01 - see discussion in Section 0) can be screened out. Regarding the ignition sources in fire zone Z115, the arrangement of the ignition sources with the safety target did not allow for the screening of any of the ignition sources, except IS14, since the safety targets are very close to all the ignition sources (on average for ignition sources from IS05 to IS13, the target distance, r, is around 0.573 m while the maximum ZOI height ranges from the maximum possible case of 2.711 m for TP cables in the case of a radiative fraction of 0.35 to the lowest possible case of 1.622 m for TS cables in the case of a radiative fraction of 0.53). In conclusion, only IS04 and IS14 can be screened out based on the ZOI analysis and all other ignition sources are retained for further analysis for the severity factor.

Table 22: Max. ZOI radius for TP targets and radiative heat fraction = 0.53 using CFAST.

IS No.	Max. ZOI R [m] for TP with Radiative Fraction = 0.53			
	Surround Temp.	Surf Temp.	Internal Temp.	Incident Heat Flux
IS01_1	0.7	1.3	1.3	**1.4**
IS01_2	0.5	1.3	1.3	**1.4**
IS01_3	0.3	1.2	1.2	**1.4**
IS02_1	0.4	1.2	1.2	**1.4**
IS02_2	0.3	1.2	1.2	**1.4**
IS03	0.4	1.2	1.2	**1.4**
IS04	0.2	0.4	0.4	**0.5**
IS05	0.5	1.2	1.2	**1.4**
IS06	0.5	1.2	1.2	**1.4**
IS07	0.5	1.2	1.2	**1.4**
IS08	0.2	0.9	0.9	**1**
IS09	0.5	1.2	1.2	**1.4**
IS10	0.5	1.2	1.2	**1.4**
IS11	0.5	1.2	1.2	**1.4**
IS12	0.2	0.9	0.9	**1**
IS13	0.5	1.2	1.2	**1.4**
IS14	0.2	0.5	0.5	**0.6**

Table 23: Max. ZOI radius for TP targets and radiative heat fraction = 0.35 using CFAST.

IS No.	Max. ZOI R [m] for TP with Radiative Fraction = 0.35			
	Surround Temp.	Surf Temp.	Internal Temp.	Incident Heat Flux
IS01_1	0.7	1.1	1.1	**1.2**
IS01_2	0.5	1	1	**1.2**
IS01_3	0.4	1	1	**1.1**
IS02_1	0.4	1	1	**1.1**
IS02_2	0.4	1	1	**1.1**
IS03	0.4	1	1	**1.1**
IS04	0.2	0.2	0.2	**0.4**
IS05	0.5	1	1	**1.1**
IS06	0.5	1	1	**1.1**
IS07	0.5	1	1	**1.1**
IS08	0.2	0.7	0.7	**0.8**
IS09	0.5	1	1	**1.1**
IS10	0.5	1	1	**1.1**
IS11	0.7	1	1	**1.1**
IS12	0.3	0.7	0.7	**0.8**
IS13	0.5	1	1	**1.1**
IS14	0.2	0.4	0.4	**0.5**

Table 24: Max. ZOI radius for TS targets and radiative heat fraction = 0.53 using CFAST.

IS No.	Max. ZOI R [m] for TS with Radiative Fraction = 0.53			
	Surround Temp.	Surf Temp.	Internal Temp.	Incident Heat Flux
IS01_1	0.7	0.8	0.8	**1.1**
IS01_2	0.5	0.8	0.8	**1**
IS01_3	0.3	0.7	0.7	**1**
IS02_1	0.4	0.7	0.7	**1**
IS02_2	0.2	0.7	0.7	**1**
IS03	0.4	0.7	0.7	**1**
IS04	0.2	0.2	0.2	**0.2**
IS05	0.5	0.8	0.8	**1**
IS06	0.5	0.7	0.7	**1**
IS07	0.5	0.8	0.8	**1**
IS08	0.2	0.5	0.5	**0.7**
IS09	0.5	0.8	0.8	**1**
IS10	0.5	0.8	0.8	**1**
IS11	0.5	0.8	0.8	**1**
IS12	0.2	0.5	0.5	**0.7**
IS13	0.5	0.8	0.8	**1**
IS14	0.2	0.2	0.2	**0.4**

Table 25: Max. ZOI radius for TS targets and radiative heat fraction = 0.35 using CFAST.

IS No.	Max. ZOI R [m] for TS with Radiative Fraction = 0.35			
	Surround Temp.	Surf Temp.	Internal Temp.	Incident Heat Flux
IS01_1	0.7	0.7	0.7	**0.9**
IS01_2	0.5	0.6	0.6	**0.8**
IS01_3	0.3	0.6	0.6	**0.8**
IS02_1	0.4	0.6	0.6	**0.8**
IS02_2	0.3	0.5	0.5	**0.8**
IS03	0.4	0.6	0.6	**0.8**
IS04	**0.2**	**0.2**	**0.2**	-
IS05	0.5	0.6	0.6	**0.8**
IS06	0.5	0.6	0.6	**0.8**
IS07	0.5	0.6	0.6	**0.8**
IS08	0.2	0.4	0.4	**0.6**
IS09	0.5	0.6	0.6	**0.8**
IS10	0.5	0.6	0.6	**0.8**
IS11	0.5	0.6	0.6	**0.8**
IS12	0.2	0.4	0.4	**0.6**
IS13	0.5	0.6	0.6	**0.8**
IS14	**0.2**	**0.2**	**0.2**	**0.2**

Table 26: Max. ZOI height for TP targets and radiative heat fraction = 0.53 using CFAST.

IS No.	Max. ZOI H [m] for TP with Radiative Fraction = 0.53			
	Surround Temp.	Surf Temp.	Internal Temp.	Incident Heat Flux
IS01_1	**1.7**	**1.7**	**1.7**	1.6
IS01_2	**2.5**	2	2	1.9
IS01_3	**3**	2.4	2.4	2.1
IS02_1	**2.8**	2.2	2.2	2
IS02_2	**3.3**	2.6	2.6	2.2
IS03	**2.8**	2.2	2.2	2
IS04	**0.8**	0.7	0.7	0.7
IS05	**2.4**	2	2	1.8
IS06	**2.7**	2.1	2.1	1.9
IS07	**2.4**	2	2	1.8
IS08	**2.1**	1.8	1.8	1.6
IS09	**2.6**	2	2	1.9
IS10	**2.4**	2	2	1.8
IS11	**2.4**	2	2	1.8
IS12	**2.1**	1.8	1.8	1.6
IS13	**2.4**	2	2	1.8
IS14	**1**	0.9	0.9	0.8

Table 27: Max. ZOI height for TP targets and radiative heat fraction = 0.35 using CFAST.

IS No.	Max. ZOI H [m] for TP with Radiative Fraction = 0.35			
	Surround Temp.	Surf Temp.	Internal Temp.	Incident Heat Flux
IS01_1	**2.2**	1.5	1.5	1.3
IS01_2	**3**	2	2	1.6
IS01_3	**3.6**	2.4	2.4	1.8
IS02_1	**3.3**	2.2	2.2	1.7
IS02_2	**3.8**	2.6	2.6	1.9
IS03	**3.3**	2.2	2.2	1.7
IS04	**1**	0.7	0.7	0.6
IS05	**2.7***	1.9	1.9	1.6
IS06	**3.1**	2	2	1.7
IS07	**2.8**	1.9	1.9	1.6
IS08	**2.4**	1.8	1.8	1.4
IS09	**2.9**	2	2	1.6
IS10	**2.7***	1.9	1.9	1.6
IS11	**2.7***	1.9	1.9	1.6
IS12	**2.4**	1.8	1.8	1.4
IS13	**2.7***	1.9	1.9	1.6
IS14	**1.2**	0.8	0.8	0.7

* In these cases, the ceiling level is reached and, therefore, these are at the maximum height.

Table 28: Max. ZOI height for TS targets and radiative heat fraction = 0.53 using CFAST.

IS No.	Max. ZOI H [m] for TS with Radiative Fraction = 0.53			
	Surround Temp.	Surf Temp.	Internal Temp.	Incident Heat Flux
IS01_1	0.8	1.1	1.1	**1.2**
IS01_2	**1.6**	1.4	1.4	1.5
IS01_3	**2.2**	1.7	1.7	1.7
IS02_1	**1.9**	1.5	1.5	1.6
IS02_2	**2.5**	1.9	1.9	1.8
IS03	**1.9**	1.5	1.5	1.6
IS04	**0.6**	0.4	0.4	0.5
IS05	**1.6**	1.4	1.4	1.5
IS06	**1.8**	1.5	1.5	1.5
IS07	**1.5**	1.4	1.4	1.5
IS08	**1.6**	1.3	1.3	1.3
IS09	**1.7**	1.4	1.4	1.5
IS10	**1.6**	1.4	1.4	1.5
IS11	**1.6**	1.4	1.4	1.5
IS12	**1.6**	1.3	1.3	1.3
IS13	**1.6**	1.4	1.4	1.5
IS14	**0.7**	0.6	0.6	**0.7**

Table 29: Max. ZOI height for TS targets and radiative heat fraction = 0.35 using CFAST.

IS No.	Max. ZOI H [m] for TS with Radiative Fraction = 0.35			
	Surround Temp.	Surf Temp.	Internal Temp.	Incident Heat Flux
IS01_1	**1.2**	0.9	0.9	1
IS01_2	**2**	1.3	1.3	1.3
IS01_3	**2.6**	1.7	1.7	1.5
IS02_1	**2.2**	1.5	1.5	1.4
IS02_2	**2.8**	1.9	1.9	1.6
IS03	**2.3**	1.5	1.5	1.4
IS04	**0.7**	0.4	0.4	-
IS05	**1.8**	1.3	1.3	1.3
IS06	**2.1**	1.4	1.4	1.4
IS07	**1.8**	1.3	1.3	1.3
IS08	**1.8**	1.2	1.2	1.1
IS09	**2**	1.3	1.3	1.3
IS10	**1.8**	1.3	1.3	1.3
IS11	**1.8**	1.3	1.3	1.3
IS12	**1.8**	1.3	1.3	1.1
IS13	**1.8**	1.3	1.3	1.3
IS14	**0.8**	0.6	0.6	0.6

2.3.4.2 Severity Factor Analysis Using CFAST

The severity factor was calculated at the nearest target distance for each case provided in Table 20. The continuous gamma distribution characteristics provided in Table 9 were used to calculate the peak HRRs for each probability bin. The peak HRR distribution was discretized into 26 bins, and each bin has the probability weight as follows (from the lower quantile to the higher quantile): [0.20, 0.15, 0.10, 0.10, 0.05, 0.05, 0.05, 0.05, 0.02, 0.02, 0.02, 0.02, 0.02, 0.02, 0.01, 0.01, 0.01, 0.01, 0.01, 0.01, 0.01, 0.01, 0.01, 0.01, 0.01, 0.02]. The severity factor is calculated based on the guidance provided in Section 8.5.4 (Step 4: Calculation of Severity Factors) and App. E in NUREG/CR-6850, Vol. 2 [11]. Similar to the ZOI analysis, a conservative approach was used to identify the damaging bins. Once the temperature (surrounding gas temperature, surface temperature, or internal temperature) or the incident heat flux at the safety target location exceed the damage criteria provided in the relevant regulatory documents (provided in Table 21), that bin is considered to cause damage and, thus, the conditions for the next bin are calculated until the 98th percentile is reached. Table 30 and Table 31 provide the severity factor values using CFAST for TP targets in the case of radiative fraction 0.53 and 0.35, respectively. Table 32 and Table 33 provide the severity factor values using CFAST for TS targets in the case of radiative fraction 0.53 and 0.35, respectively. Cells that do not contain values are basically the cases which were screened out based on the ZOI analysis and, thus, they are not assigned severity factor values. This is specifically true for IS04 and IS14 as they have been screened out based on the ZOI analysis. In most cases where a severity factor of 0.02 is assigned, the severity factor analysis indicates that the damaging peak HRR was in the 98th percentile with the lowest possible severity factor.

Since the severity factor is typically calculated at the safety target, which is assumed to be right above the ignition source (i.e., in the centerline of the plume), the dominant mode with the highest severity factors is the surrounding gas temperature. However, this is not always true, as in some of the cases, such as ignition sources IS05 through IS09, the safety target is within the flame length (see Table 16). This is under investigation and, based on the efforts in this research project, has been identified as part of the future work of the research team. For the purpose of compartment fire frequencies, the maximum severity factor for each ignition source is utilized (see the discussion in Section 2.3.6). Additionally, it should be noted that the average simulation time for each case was ~7 min on a commercial PC setup using Python codes and subroutines to run the calculations. In Section 2.3.6, the severity factors generated will be used in the estimation of the compartment fire frequencies.

Table 30: The severity factor values for TP targets and radiative heat fraction = 0.53 using CFAST.

IS No.	Severity Factor for TP with Radiative Fraction = 0.53			
	Surround Temp.	Surf Temp.	Internal Temp.	Incident Heat Flux
IS01_1	-	-	-	-
IS01_2	0.05	0.03	0.03	0.02
IS01_3	0.13	0.07	0.07	0.04
IS02_1	0.09	0.06	0.06	0.04
IS02_2	0.17	0.11	0.11	0.07
IS03	0.09	0.06	0.06	0.04
IS04	-	-	-	-
IS05	0.3	0.55	0.55	0.55
IS06	0.25	0.3	0.30	0.25
IS07	0.17	0.23	0.23	0.21
IS08	0.55	0.45	0.45	0.4
IS09	0.19	0.25	0.25	0.23
IS10	0.3	0.55	0.55	0.55
IS11	0.3	0.55	0.55	0.55
IS12	0.55	0.45	0.45	0.4
IS13	0.3	0.55	0.55	0.55
IS14	-	-	-	-

Table 31: The severity factor values for TP targets and radiative heat fraction = 0.35 using CFAST.

IS No.	Severity Factor for TP with Radiative Fraction = 0.35			
	Surround Temp.	Surf Temp.	Internal Temp.	Incident Heat Flux
IS01_1	0.03	-	-	-
IS01_2	0.09	0.03	0.03	-
IS01_3	0.17	0.07	0.07	0.02
IS02_1	0.13	0.05	0.05	-
IS02_2	0.23	0.11	0.11	0.03
IS03	0.13	0.05	0.05	-
IS04	-	-	-	-
IS05	0.4	0.45	0.45	0.45
IS06	0.3	0.25	0.25	0.21
IS07	0.23	0.19	0.19	0.15
IS08	0.55	0.45	0.45	0.3
IS09	0.25	0.21	0.21	0.17
IS10	0.4	0.45	0.45	0.45
IS11	0.4	0.45	0.45	0.45
IS12	0.55	0.45	0.45	0.3
IS13	0.4	0.45	0.45	0.45
IS14	-	-	-	-

Table 32: The severity factor values for TS targets and radiative heat fraction = 0.53 using CFAST.

IS No.	Severity Factor for TS with Radiative Fraction = 0.53			
	Surround Temp.	Surf Temp.	Internal Temp.	Incident Heat Flux
IS01_1	-	-	-	-
IS01_2	-	-	-	-
IS01_3	0.04	-	-	-
IS02_1	0.02	-	-	-
IS02_2	0.08	0.02	0.02	0.02
IS03	0.02	-	-	-
IS04	-	-	-	-
IS05	0.21	0.35	0.35	0.45
IS06	0.13	0.15	0.15	0.17
IS07	0.08	0.09	0.09	0.12
IS08	0.4	0.3	0.3	0.25
IS09	0.1	0.11	0.11	0.13
IS10	0.21	0.35	0.35	0.45
IS11	0.21	0.35	0.35	0.45
IS12	0.4	0.3	0.3	0.25
IS13	0.21	0.35	0.35	0.45
IS14	-	-	-	-

Table 33: The severity factor values for TS targets and radiative heat fraction = 0.35 using CFAST.

IS No.	Severity Factor for TS with Radiative Fraction = 0.35			
	Surround Temp.	Surf Temp.	Internal Temp.	Incident Heat Flux
IS01_1	-	-	-	-
IS01_2	0.02	-	-	-
IS01_3	0.07	-	-	-
IS02_1	0.05	-	-	-
IS02_2	0.13	0.02	0.02	-
IS03	0.05	-	-	-
IS04	-	-	-	-
IS05	0.25	0.25	0.25	0.35
IS06	0.17	0.12	0.12	0.13
IS07	0.12	0.07	0.07	0.08
IS08	0.45	0.3	0.3	0.19
IS09	0.13	0.08	0.08	0.09
IS10	0.25	0.25	0.25	0.35
IS11	0.25	0.25	0.25	0.35
IS12	0.45	0.3	0.3	0.19
IS13	0.25	0.25	0.25	0.35
IS14	-	-	-	-

2.3.5 ZOI and Severity Factor Analysis Using EPRI-FIVE

To conduct a comparative study for utilizing CFAST vs. engineering correlations for ZOI and severity factor analysis, EPRI-FIVE tool, Rev. 2, has been used to calculate the ZOI dimensions and severity factors for all the ignition sources within this study. Whenever possible, the corresponding correlations for the relevant functions in EPRI FIVE were extracted, and the inverse function was formulated to get the distance (i.e., vertical or radial distance for ZOI analysis) and the peak HRR (i.e., for severity factor analysis) in terms of the other variables. For example, *Firr* is used to calculate radiative heat flux to a target at a distance from a point source of thermal radiation. To use this correlation to estimate the radiative heat flux (kW/m^2) at a target location, q_{trgt}, the following parameters are needed: Q_f: heat release rate of the ignition source, R: distance from the center of the heat source to the target surface, and X_r: radiative fraction, where the *Firr* correlation is expressed as: $q_{trgt}(Q_f, R, X_r) = X_r \times Q_f/(4\pi R^2)$. The distance at which the incident heat flux exceeds the damage thresholds (TP: 6 kW/m^2, TS: 11 kW/m^2) from *Firr* is obtained as $R = \sqrt{X_r \times Q_f/(4\pi \times q_{trgt})}$, where q_{trgt} represents the threshold values. The ZOI dimensions are then calculated using the 98th percentiles of the peak HRR for the ignition sources. The severity factor analysis goal is to identify the damaging Q_f from *Firr* rearranged as: $Q_{f,damage} = (4\pi R^2) \times q_{trgt}/X_r$, where $Q_{f,damage}$ is the damaging bin of the discretized peak HRR distribution (the same discretization used in CFAST calculations). This approach is used for applicable correlations. Otherwise, hand calculations using engineering guesswork or using the what-if analysis forecast feature in Excel sheets were utilized to back-calculate the ZOI dimensions and the damaging peak HRR, $Q_{f,damage}$. The following two sections summarize the demonstration of the ZOI and severity factor analysis for an ignition source at STPNOC identified as IS07.

It should be noted that since EPRI FIVE correlations utilized in this analysis are established for a specific damage mode, namely, radiative heat flux or plume temperature, they are compared to the respective incident heat flux and the surrounding gas temperature damage modes generated by CFAST.

2.3.5.1 Fire-Induced ZOI Using EPRI-FIVE

For the calculations of the radius, the following correlations were used: *FirrShokriBeyler* (radiative heat flux to a target at a distance from a source of thermal radiation considered as a cylindrical source, by Shokri and Beyler), *FirrCylinder* (radiative heat flux to a target at a distance from a source of thermal radiation considered as a cylindrical source, by Dayan and Tien), *DpHeskestad* (plume centerline temperature and plume diameter, Heskestad), and *TcjAlpert* (ceiling jet temperature correlation, by Alpert).

Table 34 provides the results for calculating the ZOI radius using these correlations and comparing them to results by CFAST for each damage mode. A brief explanation of how these correlations were utilized is provided in Table 34.

Similarly, the following correlations were used in the estimation of the ZOI height: *FirrShokriBeyler*, *FirrCylinder*, *TpHeskestad* (plume centerline temperature), *TpMcCaffrey* (plume centerline temperature), and *TcjAlpert*. Table 35 provides the results for the ZOI height (measured from the floor) using these correlations in comparison to CFAST's results for each damage mode.

On average, the ZOI radius is reduced by a factor of 0.66 using CFAST as compared to EPRI FIVE's results (around 0.79 m). Similarly, over all the cases that have been investigated, the ZOI height using CFAST is calculated to be reduced by a factor of 0.80 (around 1.76 m) relative to EPRI FIVE's results. Based on the plume temperature damage mode, however, it seems that the correlations utilized underestimate temperatures. Therefore, the CFAST results indicate a ZOI height higher by a factor of 1.03 on average (an increase of 0.16 m on average) as compared to the EPRI-FIVE results for this damage mode. Nevertheless, the estimated reduction can significantly increase if the damage modes or the target materials are identified and compared.

Table 34: CFAST ZOI radius vs EPRI-FIVE ZOI radius for IS07.

			ZOI Radius (m)			
	Target Material:		TP		TS	
	Radiative Fraction:		0.53	0.35	0.53	0.35
Mode	Tool/Correlation					
Irradiation	EPRI-FIVE	*FirrShokriBeyler* (M)*	3.01		2.15	
		FirrShokriBeyler (H)*	1.71		1.29	
		FirrCylinder (H & T_f=1500ºC)†	2.43		1.92	
		FirrCylinder (H & T_f=2000ºC)†	3.49		2.81	
	CFAST	Incident Heat Flux	1.4	1.1	1.0	0.8
Plume Temp.	EPRI-FIVE	*DpHeskestad*‡ *R:*	0.39	0.44	0.32	0.36
		DpHeskestad‡ *H:*	4.03	4.33	3.33	3.53
		DpHeskestad (max. at ceiling level)‡	0.57		0.64	
		TcjAlpert (conv.)§	1.11	1.17	1.03	1.06
		TcjAlpert (tot.)§	2.15		1.98	
	CFAST	Surr. Gas Temp.	0.5	0.5	0.5	0.5

* Using *FirrShokriBeyler*, the orientation of the target is required as an input, H: horizontal, V: Vertical, and M: Max. The total peak HRR value was used in the *FirrShokriBeyler* function without considering the radiative fraction.

† The orientation of the target is required as an input to *FirrCylinder* function, H: horizontal, and V: Vertical. Additionally, the flame temperature (T_f) is also required, two values have been chosen to represent adiabatic fires or typical and peak fires (SFPE 2016 Handbook: for most hydrocarbons, is 1327ºC, typical values are 927ºC-1727ºC, and peak values are 1127ºC-2127ºC). The total peak HRR value was used in the *FirrCylinder* function without considering the radiative fraction.

‡ Both the convection part and the total peak HRR have been used in the *DpHeskestad* function. The maximum case was calculated at the highest possible elevation, the ceiling at 5.18 m from the floor (the radius and height of the target are proportional to each other). The radius was calculated assuming the plume centerline temperature, T_{pl}, is equal to the corresponding damage threshold. The corresponding heights where the temperatures exceeded the damage thresholds are also reported.

§ Both the convection part and the total peak HRR have been used in *TcjAlpert*. These two values were used due to inconsistency in the required inputs between the EPRI-FIVE manual and the Excel sheets for the TcjAlpert correlation. The radius is calculated at the ceiling level.

Table 35: CFAST ZOI height vs EPRI-FIVE ZOI height for IS07.

			ZOI Height[*] (m)			
	Target Material:		TP		TS	
	Radiative Fraction:		0.53	0.35	0.53	0.35
Mode	Tool/Correlation					
Irradiation	EPRI-FIVE	*FirrShokriBeyler* (M)[†]	6.10		4.76	
		FirrCylinder (V & T_f=1500°C)[‡]	7.50		5.96	
		FirrCylinder (V & T_f=2000°C)[‡]	11.24		8.75	
	CFAST	Incident Heat Flux	3.63	3.43	3.33	3.13
Plume Temp.	EPRI-FIVE	*TpHeskestad*	3.96	4.31	3.28	3.53
		TpMcCaffrey[§]	5		4.14	
		TcjAlpert (conv.)[**]	3.79	4.07	3.26	3.46
		TcjAlpert (tot.)[**]	4.49		3.77	
	CFAST	Surr. Gas Temp.	4.23	4.63	3.33	3.63

[*] Measured from the floor level.

[†] Using *FirrShokriBeyler*, the orientation of the target is required as an input, H: horizontal, V: Vertical, and M: Max. The vertically oriented targets are not valid at the R=0 (the centerline). The total peak HRR value was used in the *FirrShokriBeyler* function without considering the radiative fraction.

[‡] The orientation of the target is required as an input to the *FirrCylinder* function, H: horizontal, and V: Vertical. Additionally, the flame temperature (T_f) is also required, two values have been chosen to represent adiabatic fires or typical and peak fires (SFPE 2016 Handbook: for most hydrocarbons, is 1327°C, typical values are 927°C-1727°C, and peak values are 127°C-2127°C). The total peak HRR value was used in the *FirrCylinder* function without considering the radiative fraction.

[§] The total peak HRR value was used in the *TpMcCaffrey* function assuming a buoyant plume.

[**] Both the convection part and the total peak HRR have been used in *TcjAlpert* (see relevant foot note in the previous table about the radius calculations). The height is calculated based on the plume centerline temperature at R=0.

2.3.5.2 Severity Factor Analysis Using EPRI FIVE

The severity factor was calculated using the same correlations used in the evaluation of the ZOI height since the target is located above IS07, at 2.79 m from the floor (0.959 m from the fire base). The results of severity factor calculations are shown in Table 36 for IS07. The only comparable values with CFAST are the results of the *TpHeskestad* correlations. Other values provide significantly higher severity factor estimates at the target location.

Table 36: Severity factor values using EPRI-FIVE vs CFAST for IS07.

			Severity Factor			
	Target Material:		TP		TS	
	Radiative Fraction:		0.53	0.35	0.53	0.35
Mode	Tool/Correlation					
Irradiation	EPRI FIVE	*FirrShokriBeyler* (M) *	1		1	
		FirrCylinder (V & T_f=1500°C)†	NA		NA	
		FirrCylinder (V & T_f=2000°C)†	NA		NA	
	CFAST	Incident Heat Flux	0.21	0.15	0.12	0.08
Plume Temp.	EPRI FIVE	*TpHeskestad*‡	0.19	0.23	0.08	0.11
		TpMcCaffrey	0.65		0.45	
		TcjAlpert (conv.)§	0.40	0.45	0.17	0.25
		TcjAlpert (tot.)§	0.55		0.35	
	CFAST	Surr. Gas Temp.	0.17	0.23	0.08	0.12

* At the target location, all bins of the peak HRR caused the heat flux value to be above the damage threshold.

† The *FirrCylinder*, with vertically oriented target, is not valid at the target location.

‡ Although the *TpHeskestad* correlation is not applicable for the case of the actual target location for IS07 using the 98% percentile, this condition will change while varying the peak HRR (i.e., the flame length is a function of the peak HRR value).

§ Both the convection part and the total peak HRR have been used in *TcjAlpert* (see relevant foot note in the previous table about the radius calculations). The ceiling height was assumed to be at the location of the target, which might not be a realistic representation of the case study.

2.3.6 Compartment Fire Frequencies

The fire ignition frequencies (i.e., the revised values in Table 2) for each ignition source were updated based on the ZOI analysis and severity factor analysis that was conducted using CFAST (in Section 2.3.4). The fire ignition frequency for each fire source was updated as follows:

$$\lambda'_{c,i} = \lambda_{c,i} \times SF_{c,i}, \tag{6}$$

where:

$\lambda'_{c,i}$: the adjusted fire ignition frequency for ignition source "i" in compartment "c" (1/year)

$\lambda_{c,i}$: the previous fire frequency for ignition source "i" in compartment "c" (1/year) [from Table 2]

$SF_{c,i}$: the severity factor calculated using CFAST for ignition source "i" in compartment "c" [from Table 30 to Table 33]

The maximum severity factors of all the investigated cases for each ignition source (i.e., between the different damage modes, target materials and radiative fraction values) are used to update or adjust the fire frequencies. Table 37 and Table 38 provide the updated fire ignition frequencies for each ignition source in Z071 and Z115, respectively. The original fire ignition frequencies are calculated based on the guidance provided in Task 6 of [11]. For countable ignition sources, the frequency of a certain ignition source type over the number of the ignition sources of that type (these values are calculated based on previous efforts at STPNOC [20] and based on the data collection conducted during this research project). Therefore, the total values provided in Table 37 and Table 38 are calculated for Bin 15 'Electrical Cabinets' and Bin 26 'Ventilation Subsystems.' These total values do not, therefore, include other types of ignition sources that might exist in fire zones Z071 and Z115. Using the maximum values of severity factor, there is a reduction of around 91% and 59% in the total fire ignition frequency (for both Bin 15 and Bin 26 only) in fire zones Z071 and Z115, respectively.

The updated or adjusted compartment fire frequency for each compartment (i.e., λ'_c) is then calculated as follows:

$$\lambda'_c = \sum_i \lambda'_{c,i} = \sum_i \left[\lambda_{c,i} \times SF_i\right] + others, \tag{7}$$

where λ_c' is the updated or adjusted compartment fire frequency for compartment "c" (1/year).

Equation (7) represents the summation of the updated or adjusted fire ignition frequencies for the ignition sources analyzed (Bin 15 and Bin 26 in this case). Both fire zones Z071 and Z115 contain other types (represented by the term '$others$' in Equation (7)) of uncountable ignition sources such as junction boxes and cables. Therefore, the impact of the updated or adjusted fire ignition frequencies is based on the severity factor analysis for the countable ignition sources. The updated or adjusted total compartment fire frequency (which includes other ignition sources), along with the adjusted fire ignition frequencies for the analyzed ignition sources (Bin 15 and Bin 26), are provided in Table 39. At the level of the fire zones, there is an approximate 75% and 40% reduction in the total compartment fire frequency in fire zones Z071 and Z115, respectively. The percent reduction, i.e., 75% and 40% would be directly reflected in the updated Core Damage Frequency (CDF_c') after conducting quantitative screening. Assuming that all safety targets are assigned at the minimum possible distance from any ignition source in the fire compartment and that all fire PRA component related items in that compartment would fail in case of a fire, the updated expected point-estimate, CDF_c', for compartment or scenario "c" can be simply calculated as follows:

$$CDF_c' = \lambda_c' \times CCDP_c, \tag{8}$$

where $CCDP_c$ represents the Conditional Core Damage Probability (CCDP) for compartment "c" as calculated from the PRA model. Therefore, the incorporation of the severity factor impact will lead to the same reduction in the CDF for these compartments without the quantification of the PRA model.

Table 37: Updated fire ignition frequencies for each ignition source in Z071.

IS No.	Fire Frequency (1/year) per ignition source	Max. Severity Factor	Updated Fire Frequency (1/year) per ignition source
IS01_1	6.17E-05	0.03	1.85E-06
IS01_2		0.09	**5.55E-06**
IS01_3		0.17	1.05E-05
IS02_1	6.17E-05	0.13	**8.02E-06**
IS02_2		0.23	1.42E-05
IS03	6.17E-05	0.13	**8.02E-06**
IS04	6.17E-05	0.00	**0.00E+00**
Total	2.47E-04	-	2.16E-05*

* This total represents the summation of the cases; IS01_2, IS02_1, IS03, and IS04 (in bold).

Table 38: Updated fire ignition frequencies for each ignition source in Z115.

IS No.	Fire Frequency (1/year) per ignition source	Severity Factor	Updated Fire Frequency (1/year) per ignition source
IS05	6.17E-05	0.55	3.39E-05
IS06	6.17E-05	0.30	1.85E-05
IS07	6.17E-05	0.23	1.42E-05
IS08	6.17E-05	0.55	3.39E-05
IS09	6.17E-05	0.25	1.54E-05
IS10	6.17E-05	0.55	3.39E-05
IS11	6.17E-05	0.55	3.39E-05
IS12	6.17E-05	0.55	3.39E-05
IS13	6.17E-05	0.55	3.39E-05
IS14	5.56E-05	0.00	0.00E+00
Total	6.10E-04	-	2.52E-04

* IS14 is screened out based on fire modeling with conservative assumptions and did not lead to damage to the identified safety-related targets. Hence, the severity factor of zero is assigned.

Table 39: Updated compartment fire frequencies for Z071 and Z115.

Fire Zone	Z071	Z115
Total Fire Ignition Frequency (1/year)	7.56E-05	4.60E-04
Fire Ignition Frequency (1/year) for Bin 15: 'Electrical Cabinets'	2.16E-05	2.52E-04
No. of Electrical Cabinets	3	9
Fire Ignition Frequency (1/year) for Bin 26: 'Ventilation Subsystems'	0.00E+00	0.00E+00
No. of Ventilation Subsystems	0	0

2.4 Summary

The efforts in Phase I focused mainly on the formulation and implementation of a generic streamlined approach, called the Fire-RoverD screening methodology, based on the existing NRC Fire PRA methodology in NUREG/CR-6850, Vol. 2 [11], ASME/ANS Standard RA-Sa-2009 [26], industry experience, and scientific research. The introduced Fire-RoverD screening methodology provides a generic approach for conducting screening of fire scenarios and scoping of ignition sources in Fire PRA. The quantitative screening of fixed ignition sources in Task 8: "Scoping Fire Modeling" and Task 7B: "Quantitative Screening – II" of NUREG/CR-6850, Vol. 2 [11] is used as the case study for implementing Fire-RoverD and demonstrating its steps.

In order to provide the required basis for conducting screening in Fire PRA, specifically, and PRA, in general, and based on the logic of the Fire-RoverD screening methodology, the research team worked on the conceptualization and parameterization of the DoR to express the level of the analysis and its overall requirements. The DoR was parametrized using three main attributes which are: (1) scientific credibility, (2) practical feasibility, and (3) risk overestimation or conservatism. The research has identified the need for further literature review and the need to establish a connection with the 'fidelity' principle.

As case studies, two fire zones, Z071 and Z115, at STPNOC were used for the purpose of the implementation of Fire-RoverD for conducting quantitative screening for fixed ignition sources (i.e., in the context of Task 8: "Scoping Fire Modeling" and Task 7B: "Quantitative Screening – II" of NUREG/CR-6850, Vol. 2 [11]) using two different fire analysis tools or models. These two tools reflect two different DoRs that are associated with different requirements and resources for data collection, computational analysis, and analysis validation, among other things. The quantitative screening was based on the fire-induced ZOI analysis and severity factor analysis, as described in Task 8: "Scoping Fire Modeling" of NUREG/CR-6850, Vol. 2 [11] and, then, the evaluation of the risk estimates at the level of risk scenarios, as described in Task 7 or, specifically, Task 7B: "Quantitative Screening – II" of NUREG/CR-6850, Vol. 2 [11]. The two fire analysis tools utilized for conducting the fire analysis are EPRI FIVE [19], which is an engineering correlation-based model (or hand calculations), and CFAST [18], which is a zone model. As the one of the requirements of the implementation, the research team conducted the validation analysis using the non-dimensional parameters in order to ensure the applicability and suitability of both the utilized fire analysis tools as stated in NUREG-1824, Supp. 1 [25] and NUREG-1934 [23].

Compared to EPRI FIVE, the utilization of CFAST imposed additional needs on human resources for data collection (beyond that which is required for classifying ignition sources and assignment of the

HRRs). That is mainly due to the realistic modeling of the compartment geometry, ventilation conditions, and arrangement of ignition sources. With these added computational needs, CFAST can be used to construct a more realistic ZOI. In general, for the purpose of the fire-induced ZOI analysis and severity factor analysis, it can be confirmed that the utilization of EPRI FIVE (or engineering correlation models) is more efficient since fewer data are required for achieving similar goals for both case studies. However, the utilization of CFAST seems to be efficient and practical not only when combined with certain assumptions that are mainly related to the ventilation conditions but also when utilized to analyze other terms in the risk causal equation (not just for ZOI and severity factor analyses) and the latter justified the research team's decision to further investigate the efficiency and practicality of unitizing CFAST for screening fire scenarios including multi-compartment scenarios in Phase II of this project (Chapter 3).

Based on the research in Phase I, the following is identified as needing future work:

- Additional case studies need to be incorporated in order to support the decision regarding the efficiency of a specific DoR for conducting quantitative screening in Fire PRA. This is part of generating a database of approaches used in conducting quantitative screening and for highlighting the efficiency and required resources for each approach.
- The case studies should be expanded to compare the results of the ZOI analysis and severity factor analysis of CFAST and EPRI-FIVE with that of a Computational Fluid Dynamics (CFD) model such as the Fire Dynamic Simulator (FDS) [27]. This is part of the effort to investigate the efficiency and practicality of other fire analysis tools.
- The research team has identified the importance of analyzing the associated costs of conducting the quantitative screening and its relation to the decision-making process, which can mainly impact the level of conservativism in the analysis (or for a specific DoR).
- The implementation of the generic RoverD screening methodology for other topical areas and its integration with SoTeRiA's Integrated PRA (I-PRA) algorithm is considered as part of the ongoing efforts.
- This research has identified that the conceptualization and parameterization of the DoR requires further literature review.

Page intentionally left blank

3. Methodological and Computational Developments for Fire Scenario Selection and Analysis for Multi-Compartment Fire Scenarios

This chapter reports the research outcomes from Task 2 of the project. The insights from Phase I (Chapter 2 and the interactions of the research team with the nuclear industry showed that there is a need to reduce the resources required for conducting the analyses in support of Fire Probabilistic Risk Assessment (PRA). Task 2 of the project focuses on developing the SoTeRiA-Fire platform that makes the FSS implementation more efficient by automating the pre-processing of input data, execution of a fire model, and post-processing of outputs for various tasks in the Fire Scenario Selection and Analysis (FSS). SoTeRiA-Fire can help reduce the workload of an analyst for FSS since the platform is applicable for various fire compartments or Physical Analysis Units (PAUs) as it provides the required parameters for the input file in a spreadsheet format without the need to change internal codes. The platform can also help NPPs reduce resources required for Fire PRA implementation by providing a mechanism to gradually increase the realism of FSS while screening out insignificant scenarios. The desired level of realism can be defined through multiple options for initial and boundary conditions and modeling assumptions that enable the analyst to select the level of realism based on the availability of data and resources. SoTeRiA-Fire is applied in a plant and the results are reported in this paper; however, the code is applicable for various fire compartments in nuclear power plants (NPPs) and can automate resource-efficient screening for single- or multi-compartment fire scenarios. The code would be commercially available after completing the required licensing process.

This chapter is organized as follows: Section 3.1 provides methodological and computational bases of the SoTeRiA-Fire computational tool. Section 3.2 demonstrates an application of the SoTeRiA-Fire computational tool to the selected PAUs at South Texas Project Nuclear Operating Company (STPNOC). Section 3.3 summarizes the research outcomes of this task and provides recommendations for further research.

3.1 SoTeRiA-Fire Methodological and Computational Basis

The general fire hazard logic in the SoTeRiA Fire code depicts multi-compartment scenarios involving potential ignition of secondary/intervening combustibles in NPP risk estimates. It also achieves the objectives of the FSS process as stated in the ASME/ANS RA-Sa-2009 standard [26]. The first objective of the FSS process is to determine the probability of fire damage for each selected fire scenario, including the evaluation of: (a) the fire-generated conditions with the consideration of fire spread to secondary combustibles, (b) the safety target damage likelihood, and (c) fire detection and suppression activities. The

second objective is the consideration of multi-compartment fire scenarios. The other two objectives of the FSS process; namely, selection of the fire scenarios for each unscreened PAUs for the evaluation of fire risk estimates and the characterization of the selected fire scenarios, are basically pre-requisites for the utilization of SoTeRiA-Fire. The following sequence of pivotal events is to be considered in the evaluation of the fire-induced scenario to address the first and second objectives: (1) the initial fire ignition; (2) the ignition of secondary/intervening combustibles from the initial fire which considers two types of ignition sources for initial fires. The first type includes fixed ignition sources, such as electrical cabinets and battery/battery chargers, and the second includes transient fires (both generic and transient combustible control locations). With the latter type, the Area Fraction is also considered in the estimation of the probability of fire spread from the initial transient fire to the secondary/intervening fires. The main approach of analysis in this event is the calculation of the severity factor and the corresponding Zone of Influence (ZOI); (3) safety target damage, whether it occurs due to the initial fire or due to the combined case of initial fire and secondary/intervening combustibles. Here, safety targets are assumed to be located in the adjacent compartment, i.e., the exposed compartment in the multi-compartment scenario; (4) failure of the detection and suppression system in the compartment that contains the initial fire and secondary/intervening combustibles, i.e., the exposing compartment in the multi-compartment scenario; (5) the failure of the fire barriers, such as penetration seals, fire doors, and ventilation dampers, between the compartments, i.e., the exposing and exposed compartments; and (6) failure of the suppression system in the adjacent compartment where safety targets are located, i.e., the exposed compartment in the multi-compartment scenario.

Figure 8 shows the general event tree that was utilized as the basis for developing SoTeRiA-Fire. The event tree is based on the above sequence of events but excludes failure of the fire barrier event (pivotal event #5). SoTeRiA-Fire conducts the required fire modeling to evaluate end states D, H, and L which, together, constitute the total frequency for a multi-compartment scenario. In addition, the platform incorporates the failure probability of fire barriers after the frequencies of the end states have been evaluated (Table 11-3 of NUREG/CR-6850, Vol. 2 [1]).

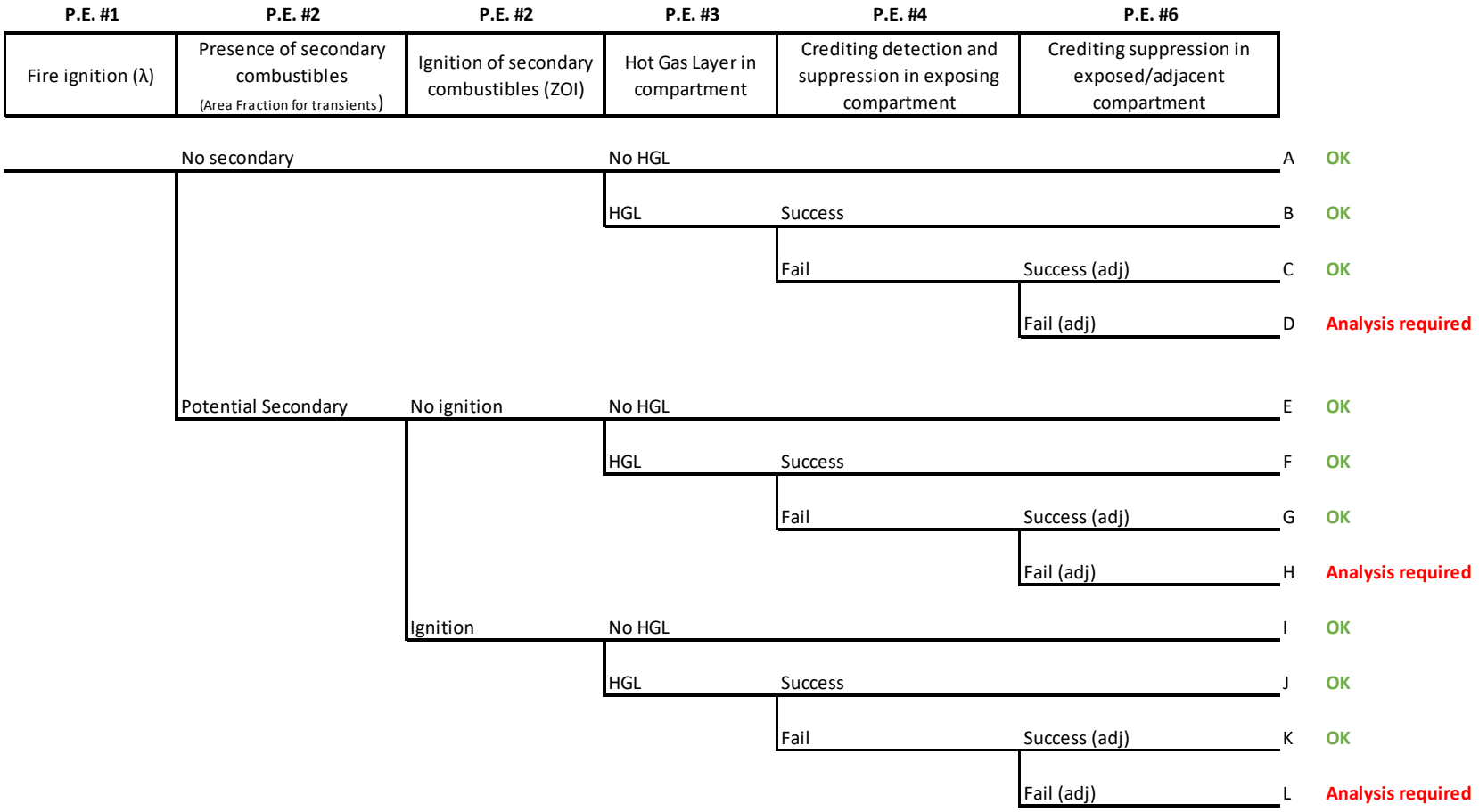

Figure 8: General event tree of the fire hazard scenario for the SoTeRiA-Fire platform.

For pivotal event #1 in Fig. 1, two types of initial ignition sources are considered, namely, electrical enclosures modeled using NUREG-2178, Vol. 1 [28]; and transient fires modeled using NUREG-2233 [29]. For pivotal event #2, the Consolidated Model of Fire and Smoke Transport (CFAST) [30] predicts temperature and heat flux at the locations of the secondary combustibles used to construct a ZOI for these combustibles and to estimate the probability of a secondary combustible ignition. For now, the platform is limited to the treatment of cable trays as the only type of secondary or intervening combustible. The platform is also capable of modeling fire spread in multiple configurations of cable trays utilizing the FLAme Spread over Horizontal CAble Trays (FLASH-CAT) model documented in NUREG-7010, Vol. 1 [31]. Currently, SoTeRiA-Fire utilizes the CFAST code for fire modeling; however, the structure is designed to accommodate other fire simulation tools as well. Another important aspect of SoTeRiA-Fire is the incorporation of the Validation and Verification (V&V) process for CFAST as a fire model in the nuclear industry (NUREG-1824, Supp. 1 [32] and NUREG-1934 [33]).

For pivotal event #3, the Hot Gas Layer (HGL) temperature and heat flux computed by CFAST are compared with the cable damage thresholds to estimate the time to a damaging HGL for safety targets. For pivotal events #4 and #6, the platform is equipped with a detection-suppression event tree and a non-suppression curve adopted from NUREG-2169 [34] to estimate the non-suppression probability based on the time to damaging conditions computed by CFAST. Currently, SoTeRiA-Fire allows the user to utilize two detection and suppression event trees to calculate the total non-suppression probability, namely, the event tree provided in Appendix P, NUREG/CR-6850, Vol. 2 [1] and the event tree provided in NUREG-2230 [35] for electrical cabinet fires. For pivotal event #5, the failure probability of fire barriers is inherently incorporated by multiplying the scenario frequency with the corresponding probabilities for the defined type of fire barriers.

One of the main goals of SoTeRiA-Fire is to provide its users with the ability to determine the desired Degree of Realism (DoR) to conduct FSS within the context of NUREG/CR-6850 [1] and ASME/ANS RA-Sa-2009 [26]. The DoR reflects the various boundary conditions and modeling assumptions defined by the user for the analysis. In addition, the platform provides the users with the ability to control the definition of the fire hazard scenario and the associated top events by either excluding or including certain events in the analysis. For instance, the user can limit the analysis to conducting severity factor and ZOI analysis to support Task 8 of the NUREG/CR-6850 Fire PRA methodology: “Scoping Fire Modeling” while turning off the analyses for the other top events.

3.1.1 SoTeRiA-Fire Computational Flowchart

The computational flowchart of SoTeRiA-Fire is shown in Figure 9. SoTeRiA-Fire reads the input file (spreadsheet) using two modules: The *Platform* module (Block #1) and the *InpP* module (Block #2). The *InpP* module reads the input file and assigns the values for the variables, matrices, and other parameters. Next is the *V&V* module (Block #3), where the non-dimensional parameters of concern are evaluated, and Block #3.a where the applicability of CFAST is checked . In case some of the non-dimensional parameter values are out of the predefined V&V ranges, the platform checks whether there is the possibility of adjusting them in a conservative manner that complies with the already established regulatory and industry practices in Block #3.b. If the problem under consideration remains beyond the predefined V&V ranges, the platform stops the analysis and reports the status. However, if there is the possibility to adjust certain parameters so that they remain within the V&V ranges, then these changes are made in Block #3.c and the V&V process begins anew.

The development of the input files of the specified fire simulation tool begins through the *InpFG* module, Block #4. This module links and establishes the required communication between various modules used to define parts of the input files in the fire simulation tool. For the definition of the ventilation conditions in the *Vent* module, Block #4.e, the platform allows for user-defined ventilation conditions. It also provides the user with the ability to define the equivalence ratio, φ, as a single value, or a range of values, in order to define corresponding natural ventilation conditions.

The *MainF* module defines the initial or primary fire specifications and characteristics (Block #4.f). For the definition of the secondary fire in intervening secondary cable trays, in the *SecondF* module, Block#4.g, the platform utilizes an approach based on the FLASH-CAT model [31] for modeling fire spread in multiple configurations of cable trays. In complex configurations that have combinations of horizontal and vertical cable trays, CFAST is used iteratively to define fire propagation through the initial propagation period of the secondary fire (i.e., ignition of the first few cable trays). If secondary or intervening combustibles exist, they are not analyzed or incorporated in the analysis until the initial primary ignition source is analyzed in Block #5: Fire Analysis/Simulation. This is to confirm, through ZOI analysis and HGL analysis, whether the secondary or intervening combustibles ignite.

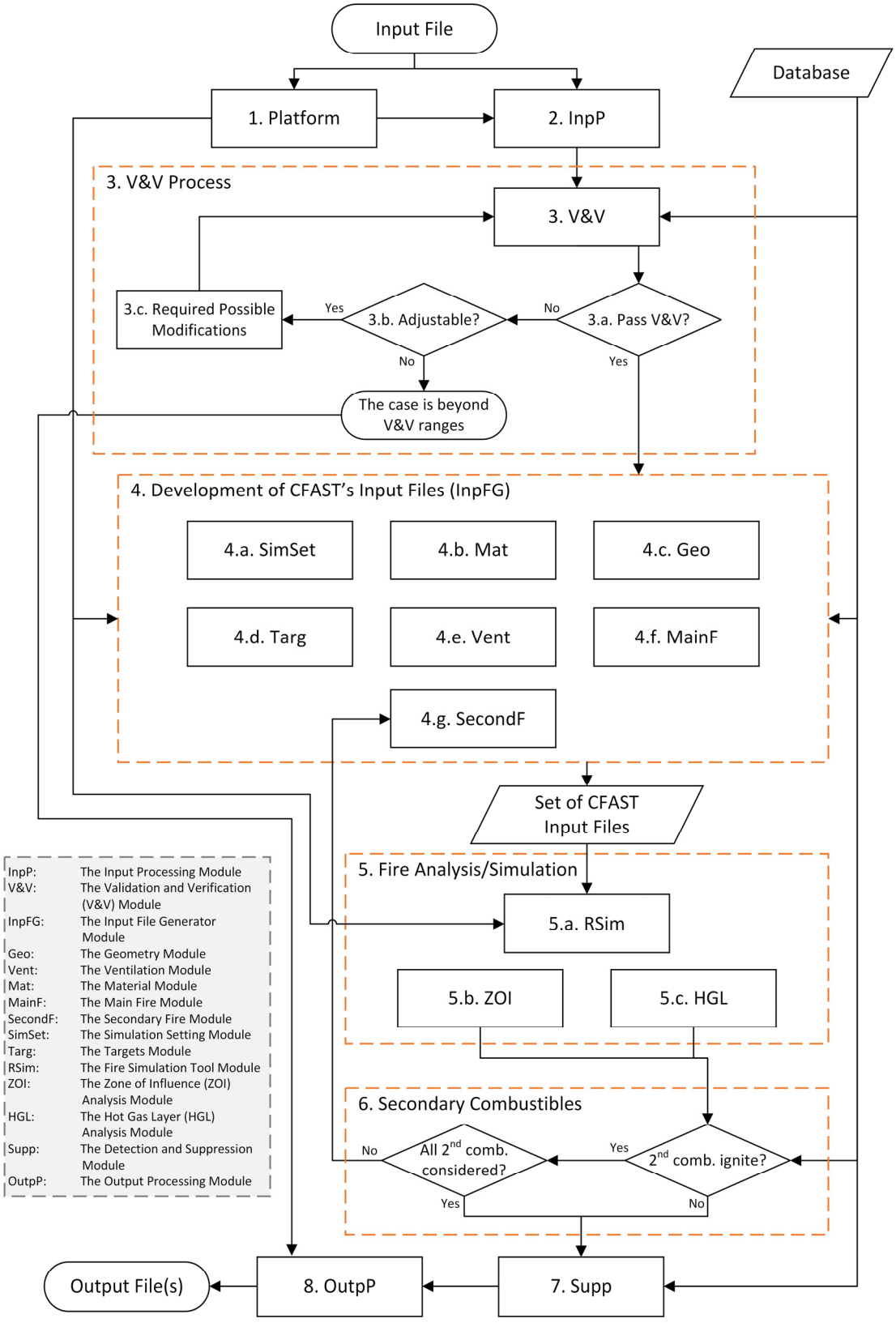

Figure 9: Computational flowchart for the SoTeRiA-Fire platform.

After generation of the required set of the fire simulation input files (i.e., CFAST), the RSim module, Block #5.a, executes the required command to run the simulation tool to generate the fire analysis results and the temperature and heat flux evaluation as the key performance measures. Currently, the ZOI module conducts the ZOI analysis in the vertical direction only. This approach is based on one of the assumptions of the FLASH-CAT model where the fire is assumed to be beneath the lowest tray. Therefore, to reduce any unnecessary use of computation time, the ZOI module only develops a vertical ZOI in the case of cable trays. In this case, the ignition criteria for bulk cable/tray ignition criteria provided in FAQ 16-0011 [36] is used in the ZOI analysis. For the severity factor calculation in the ZOI module, the whole probability distribution of the peak heat release rate (HRR) for the main fire source is considered for the estimation of the damaging HRR value, which is used to calculate the severity factor. The platform provides one approach for the treatment of the peak HRR distributions for the purpose of ZOI analysis. The peak HRR probability distributions are discretized into the 15 bins suggested in relevant regulatory documents (except for the probability distributions for the transient fire where a suggested discretization was suggested by the authors). In future versions of the platform, a flexible user-defined discretization approach and a sampling approach from the continuous peak HRR distributions will be introduced to improve the realism. The HGL analysis is conducted in the *HGL* module by analyzing the temperature of the HGL developed in the compartment. One critical output from the fire analysis/simulation, Block #5, is the estimated time for a damaging HGL to occur. This time-to-damaging HGL is calculated using the bounding cable damage/ignition criteria provided in both NUREG/CR-6850, Vol. 2 [1] and FAQ 16-0011 [36]. The heat-soak method [37] is used to calculate the time-to-damaging conditions by accounting for the fire exposures as a function of time until the safety targets (i.e., safety cables) fail.

Once the time-to-damaging HGL is obtained, the *Supp* module, Block #7, uses it to estimate the non-suppression probability. The relevant detection and suppression event tree is solved, and the non-suppression probability associated with that defined fire scenario is estimated. Both pivotal events, #4 and #6, of the sequence of events in the fire hazard scenario (Figure 8) are evaluated here. That is, the failure of the detection and suppression system in the compartment containing the initial fire and secondary/intervening combustibles, and the failure of the suppression system in the adjacent compartment where the safety targets are located, are calculated through the *Supp* module. The *OutpP* module, Block #8, conducts the last step in SoTeRiA-Fire by generating the required output files (e.g., tabulated data, graphics, and reports). This includes reporting the total frequency for the fire hazard scenario by evaluating end states D, H, and L in Figure 8.

Currently, the input file or input data spreadsheet is an Excel spreadsheet file that incorporates all the required input data for conducting FSS with consideration of defined cable trays as secondary fires. The

main sections in the input data file mirror the main sections in the CFAST input. Although Excel spreadsheets lack interactive features for constructing input files, they are commonly used in PRA applications and do not require syntax or formatting rules. Moreover, for each parameter in the input data spreadsheet, detailed commentary, and descriptions, including its suggested values and specified measurement units, are provided. SoTeRiA-Fire generates different outputs for each case analyzed. These output files include CFAST files, tabulated data for the various physical parameters, such as the time profile for the HGL temperature, the time profile for chemical species in the HGLs, and various graphical representations for the physical parameter time profiles.

3.2 Application of SoTeRiA-Fire Tool for a Nuclear Power Plant Case Study

Two PAUs have been chosen for case studies to demonstrate the capabilities of SoTeRiA-Fire. These two fire zones are part of multi-compartment scenarios that have been identified at STP. The description, type of main ignition sources, configuration of intervening combustibles, and the fire ignition frequencies are provided in Table 40.

Table 40: Fire Zones at STP that are utilized as case studies.

	F02Z001	**F71Z007**
Fire Zone Description	Channel II Dist. Room	Elec. Chase, Train B
Main Ignition Source	Battery Chargers	Transient Fire
Intervening Combustibles (Electrical Cables)	1 stack × 1 cable tray	2 stacks × 3 cable trays
Fire Ignition Frequency (1/year)	3.86E-04	2.84E-05

It should be noted that the intervening combustibles, i.e., the electrical cable trays, are assumed to extend horizontally from the one side of the compartment to the other, which does not necessarily reflect their actual configuration at the plant. However, the engineering approach used ensures conservatism in this representation, e.g., the cable trays are longer and, thus, contain more fuel and if they are not perfectly aligned vertically, they are assumed to be aligned which ensures faster propagation of fire and the applicability of the FLASH-CAT model. In the case of fire zone F71Z007, one stack is investigated due to the substantial horizontal spacing between the two cable trays (one is longer, and the other is shorter). In

addition, due to the similarity in the configuration, analysis of the longer configuration can be used to make conclusions on the shorter stack (in a conservative manner).

The analysis of the real fire zones, based on the plant data, lead to the conclusion to screen out these two fire zones as there is no anticipated damage that can occur in an adjacent compartment from the HGL generated in these fire zones. In F02Z001, the main fire can ignite the cable trays, with a severity factor of 0.02 based on the 98th percentile peak HRR. However, since there is only one cable tray above and, due to the large volume of the fire zone, the generated HGL does not lead to damage to safety targets (i.e., the damage integral does not reach the unit over the duration of the fire). In F71Z007, the main fire is relatively small, i.e., a transient fire assumed to have a fire base height of 1 m, which is relatively high for a transient fire, and was not enough to ignite the cable trays. Thus, no damage is anticipated in this case, either. For the purpose of demonstrating the capabilities of SoTeRiA-Fire using these 2 fire zones, the configuration was adjusted conservatively to induce scenarios that can generate damaging HGL. The reference information for both F02Z001 and F71Z007 is provided in Appendix A. Furthermore, Appendix B provides the data about the materials and cable trays that are shared between all the cases investigated here. Utilizing the same approaches and techniques that are incorporated in SoTeRiA-Fire, all the following results should be reproducible.

In F02Z001, two adjusted cases were investigated. In the first case, F02Z001-A, the height of the lowest cable tray was reduced from 2.74 m to 2.3 m. In this case, the combined fire of the main ignition source and the single cable tray did not lead to a damaging HGL; however, the severity factor values increased. In the second case, F02Z001-B, a second cable tray identical to the first cable tray is added to the configuration in case F02Z001-A with a 0.45 m spacing distance. In this case, a damaging HGL developed. There is, therefore, the probability of damaging safety targets in the adjacent compartment[d]. Table 41 shows the severity factor, ignition time of the lowest cable tray in the cable trays, the time-to-damaging HGL, and the non-suppression probability for four damaging modes. In this analysis, the cable trays and safety targets are assumed to be thermoplastics (TP). There is no difference in the severity factor and the ignition time between the two cases as there were no changes in the main ignition source elevation or the height of the lowest cable tray. However, in case F02Z001-B, the addition of a second cable tray led to a combined fire that caused a damaging HGL. The non-suppression probability is calculated using a value of $\lambda = 0.098$ [min^{-1}] for the rate of fire suppressed.

[d] It is assumed that a damaging HGL in the exposing compartment is enough to damage some safety target in the adjacent exposed compartment, i.e., $P\left(ST_{exposed} \middle| HGL_{exposing}\right) = 1$, where, $ST_{exposed}$ is the probability of a safety target in the exposed compartment being damaged, and $HGL_{exposing}$ is the probability that a damaging HGL exists in the exposing compartment.

In F71Z007, three adjusted cases are investigated. The scenario was adjusted by assuming the height of the transient fire base to be 1.5 m from the floor and lowering the height of the lowest cable tray from 5.33 m to 3 m. Two cases out of the three were conducted using two values for the equivalence ratio, namely, 1.1 and 0.7. These two cases had two different HRR time profiles. The first profile was established using data from NUREG-2233 (Appendix A.4 WPI Waste Bag Test) [29], where the growth time is 218 sec, the peak duration is 56 sec, and the decay duration is 1295 sec. The second profile was established using the case study in Appendix E, NUREG-1934 [38] as a reference. In this case, the growth time is 480 sec, the peak duration is 320 sec, and the decay duration is 800 sec. Table 42 provides the results of the three investigated cases.

In these three cases, the cable trays and safety targets are assumed to be thermoplastics (TP) and the rate of fire suppression is $\lambda = 0.111$ [min^{-1}]. First, comparing cases F71Z007-B and F71Z007-C, we can observe that lowering the value of the equivalence ratio led to a relatively longer time-to-damaging HGL and, thus, it lowered the non-suppression probability. Second, comparing F71Z007-A and F71Z007-B, we can see that since the peak HRR profile progresses faster in case F71Z007-A, the time-to-damaging HGL is shorter and, thus, the non-suppression probability is increased.

Similar cases and those that are dissimilar, e.g., the zone-of-influence analysis discussed in Phase I, can be handled using the SoTeRiA-Fire computational tool. Beyond the discussion in this report, the sensitivity analysis module is capable of generating ample results for multiple combinations of various parameters. On average, based on the cases analyzed in this case study, SoTeRiA-Fire takes 7.5 sec to process input data, prepare required variables, and construct CFAST input files. It takes 37.2 sec to run a single case for severity factor analysis using CFAST, and about 51.6 sec to run a single case for HGL analysis and generate the non-suppression probability.

Table 41: Two adjusted cases for F02Z001 investigated in the case study.

Case: F02Z001-A (Equivalence Ratio: 1, Lower Oxygen Limit: 0.01, Radiative Fraction: 0.35)				
Damage Mode	Severity Factor	Lowest Cable Tray Ignition Time (sec)	Time-to-Damaging HGL (sec)	Non-Suppression Probability
Surrounding Gas Temperature	0.06	645	NA	NA
Surface Temperature	0.06	510	NA	NA
Internal Temperature	0.06	510	NA	NA
Incident Heat Flux	0.06	480	NA	NA
Case: F02Z001-B (Equivalence Ratio: 1, Lower Oxygen Limit: 0.01, Radiative Fraction: 0.35)				
Damage Mode	Severity Factor	Lowest Cable Tray Ignition Time (sec)	Time-to-Damaging HGL (sec)	Non-Suppression Probability
Surrounding Gas Temperature	0.06	645	2790	0.005730
Surface Temperature	0.06	510	2580	0.008455
Internal Temperature	0.06	510	2580	0.008455
Incident Heat Flux	0.06	480	2535	0.009190

Table 42: Three adjusted cases for F71Z007 investigated in the case study.

Case: F71Z007-A (Equivalence Ratio: 1.1, Lower Oxygen Limit: 0.01, Radiative Fraction: 0.35) (Main Fire HRR: growth: 218 sec, peak: 56 sec, and decay: 1295 sec)				
Damage Mode	Severity Factor	Lowest Cable Tray Ignition Time (sec)	Time-to-Damaging HGL (sec)	Non-Suppression Probability
Surrounding Gas Temperature	0.06	210	990	0.1602
Surface Temperature	0.03	285	1065	0.1394
Internal Temperature	0.03	285	1065	0.1394
Incident Heat Flux	0.03	285	780	0.2362
Case: F71Z007-B (Equivalence Ratio: 1.1, Lower Oxygen Limit: 0.01, Radiative Fraction: 0.35) (Main Fire HRR: growth: 480 sec, peak: 320 sec, and decay: 800 sec)				
Damage Mode	Severity Factor	Lowest Cable Tray Ignition Time (sec)	Time-to-Damaging HGL (sec)	Non-Suppression Probability
Surrounding Gas Temperature	0.06	435	1200	0.1086
Surface Temperature	0.03	510	1275	0.0945
Internal Temperature	0.03	510	1275	0.0945
Incident Heat Flux	0.03	510	780	0.2362
Case: F71Z007-C (Equivalence Ratio: 0.7, Lower Oxygen Limit: 0.01, Radiative Fraction: 0.35) (Main Fire HRR: growth: 480 sec, peak: 320 sec, and decay: 800 sec)				
Damage Mode	Severity Factor	Lowest Cable Tray Ignition Time (sec)	Time-to-Damaging HGL (sec)	Non-Suppression Probability
Surrounding Gas Temperature	0.06	435	1350	0.0823
Surface Temperature	0.03	525	1455	0.0678
Internal Temperature	0.03	525	1455	0.0678
Incident Heat Flux	0.03	525	915	0.0184

3.3 Summary

This chapter reports the outcomes of Task 2 of the project. The methodological and computational bases of the SoTeRiA-Fire platform, an automated environment for the FSS process in fire PRA of NPPs, have been developed (Section 3.1). SoTeRiA-Fire helps investigate the impacts of certain input parameters and modeling approaches that contribute to the efficiency of the FSS process. This platform facilitates resource-efficient screening for single- or multi-compartment fire hazard scenarios. The platform can help NPPs reduce resources required for Fire PRA implementation by providing a mechanism to gradually increase the realism of FSS while screening out insignificant scenarios. The desired level of realism can be defined through multiple options for initial and boundary conditions and modeling assumptions that enable the analyst to select the level of realism based on the availability of data and resources. SoTeRiA-Fire has been applied to two PAUs at the STPNOC plant, demonstrating the applicability and efficiency in practical Fire PRA applications (Section 3.2).

Based on the results and experience gained in Task 2 of the project, potential directions of future work include:

- Expanding uncertainty quantification and sensitivity analysis in SoTeRiA-Fire. To operationalize the statistical computations, existing risk analysis software tools, such as RAVEN developed by INL, could be integrated with SoTeRiA-Fire.
- Treating combustibles near penetrations, such as natural vents, in multi-compartment scenarios.
- Utilizing other methods for providing input data for SoTeRiA-Fire (other than Excel spreadsheets), e.g., a graphical user interface.
- Conducting thorough validation and verification on SoTeRiA-Fire.
- In addition to utilizing CFAST, integrating other fire simulation tools with different levels of resolution, such as Fire Dynamic Simulator (FDS) and the EPRI FIVE tool, respectively.
- Developing a module for the estimation of the local and real-time damage for safety targets in the exposed compartment, based on fires initiated in the exposing compartment.

Page intentionally left blank

4. Experimental Validation of Agent-based Fire Crew Performance Model

This chapter reports the research outcomes of Phase III of the project. One of the main tasks of Fire Probabilistic Risk Assessment (PRA) is determining the probability of fire-induced equipment damage. This probability depends on several competing factors. One of these factors is the non-suppression probability, which represents the probability that a fire will not be suppressed before damage to the target equipment occurs. Different types of fire detection and suppression systems are in place at nuclear power plants (NPPs). In some scenarios, fire crew intervention is required to suppress the fire; for instance, if automated suppression systems are insufficient or unavailable. The longer the fire crew takes to suppress the fire, the higher the probability of target damage would be; hence, it is essential to quantify the fire crew response time. The response time depends on the actions required to control and suppress the fire and the amount of time needed for each action. The first action performed by the fire crew after entering the room is the identification of the fire location. The time to locate the fire can be lengthy, particularly when it is a high-intensity fire that can generate smoke and low visibility and when it occurs in a closed compartment with various interconnected systems.

Due to the importance of quantifying this response time, a methodology was developed to utilize Agent-Based Modeling (ABM) to simulate the fire crew performance in locating and suppressing a compartment fire and to incorporate the ABM fire crew simulation into the Fire PRA of NPPs [7]. The purpose of incorporating the ABM model into PRA is to enhance the realism of the fire crew performance assessment and, ultimately, to obtain more realistic risk estimations; however, the uncertainties in Fire PRA introduced by the ABM fire crew simulation should be quantified. If the ABM fire crew model has a large bias, resulting in underestimation or overestimation of the response time, it can induce a large bias in the point estimate of the plant risk. Meanwhile, if the output of the ABM fire crew model has a large uncertainty bound, it may induce a large epistemic uncertainty for the plant risk estimates. It is important to validate the newly developed ABM fire crew model using uncertainty as a measure of the degree of validity.

The objective of Phase III is to validate the ABM fire crew performance model by quantifying the bias and uncertainty in the prediction of the fire crew response time. The validation methodology suggested by the U.S. Nuclear Regulatory Commission for validating fire models [39] is adopted for the purpose of this study.

The remainder of this chapter is organized as follows: Section 4.1 provides the mathematical background of the validation methodology and clarifies the assumptions utilized in its derivation process. Section 4.2 describes the experimental setup for the fire crew performance test conducted in this study.

Section 4.3 describes the agent-based fire crew model developed for the validation case. Section 4.4 shows the implementation of the validation methodology to the agent-based fire crew model and discusses the results of the validation study. Section 4.5 summarizes the research outcomes, discusses the limitations of this study, and provides suggestions for future research.

4.1 Validation Methodology

This study adopts the validation methodology recommended for the validation of fire models supporting Fire PRA of NPPs [39]. This section summarizes the validation methodology and its mathematical formulation.

The aim of the validation in this research is to quantify the predictive uncertainty of the ABM fire crew model by statistical analysis based on a pair-wise comparison of experimental data and model outputs. In a (hypothetical) case where the model perfectly represents reality, the model outputs and experiment data align perfectly. Obviously, this is not the case in any mathematical or computational models because discrepancies between model outputs and experimental observations can be generated. These include:

- Uncertainties in the measured quantity of interest in the experiment
- Uncertainties in the set of conditions used in the experiment. If the experimental conditions are not set exactly the same as those that are modeled, they can generate discrepancies between the model output and the experimental observation.
- Uncertainties of the model itself, due to the use of assumptions and approximations.

The effects of the three sources of uncertainties listed above are shown in Table 43, where Qc and Qe represent the calculated and experimental quantity of interest, respectively. $\in_{\mathrm{Qe}}$ represents uncertainties in the measured quantity of interest. $\in_{\mathrm{model}}$ represents uncertainties in the model itself. $\in_{\mathrm{input},i}$ represents uncertainties in condition i of the experiment. P_i represents a dependency factor, which reflects how a change in condition i of the experiment produces a change in the measured output.

Considering the effects of the uncertainty sources in Table 1, the model uncertainty $\in_{\mathrm{model}}$ can be computed when the following quantities are known:

- Uncertainties in the measured quantity of interest ($\in_{\mathrm{Qe}}$)

- Uncertainties of the reported experimental conditions that are used as inputs to the model ($\in_{\text{input},i}$)
- Understanding how uncertainties in the individual experimental conditions propagate to the experimental output (P_i)

Table 43: Effects of uncertainties on the differences between model output and experimental observation.

ID	Type of uncertainties	Effects	Mathematical representation
0	Everything is perfect (no uncertainties at all)	N/A	$\text{Qc} = \text{Qe}$
1	Uncertainties in the measured quantity of interest in the experiment	The difference between calculated and measured quantity of interest will be due to uncertainties in the measured quantity itself	$\text{Qc} - \text{Qe} = \in_{\text{Qe}}$
2	Uncertainties in the description of the set of conditions used in the experiment.	The differences between calculated and measured quantity of interest will be due to uncertainties in the experimental conditions (those that will be used as inputs in the model), leading to different experimental and model output	$\text{Qc} - \text{Qe} = \sum_i \in_{\text{input i}} * P_i$
3	Uncertainties associated with the model itself due to the use of assumptions and approximations	The differences between calculated and measured quantity of interest will be due to uncertainties in the model itself	$\text{Qc} - \text{Qe} = \in_{\text{model}}$

The aim of the mathematical procedure is to quantify the model uncertainty using two metrices; the bias in the model prediction ($\hat{\delta}$) and the degree of scatter in the true value representing model uncertainty ($\widehat{\omega_M}$). The formula to calculate the bias and model uncertainty, derived by the maximum likelihood estimation method [39], is shown in Equations (9) and (10), respectively.

$$\hat{\delta} = \exp\left(\frac{1}{n}\sum_{i=1}^{n} ln\left(\frac{M_i}{E_i}\right) + \frac{s^2 - {\omega_E}^2}{2}\right) \tag{9}$$

$$\widehat{\omega}_M = \exp\left(\frac{1}{n}\sum_{i=1}^{n} ln\left(\frac{M_i}{E_i}\right) + \frac{s^2 - {\omega_E}^2}{2}\right)\sqrt{s^2 - {\omega_E}^2} \tag{10}$$

where:

$\hat{\delta}$	:	Bias of the model
$\widehat{\omega}_M$	:	Relative uncertainty in the model
n	:	Number of experiments
M_i	:	Model output corresponding to experiment *i*
E_i	:	Output of experiment *i*
s^2	:	Sample variance given in Equation
ω_E	:	Relative uncertainty in the experiment

$$s^2 = \frac{1}{n-1}\sum_{i=1}^{n}\left[ln\left(\frac{M_i}{E_i}\right) - \frac{1}{n}\sum_{i=1}^{n} ln\left(\frac{M_i}{E_i}\right)\right]^2 \tag{11}$$

Aside from the pairwise data of the model outputs and experimental observations (M_i,E_i), the relative experimental uncertainty ω_E is required to calculate $\hat{\delta}$ and $\widehat{\omega}_M$, using Equations (9) to (11). Referring to Table 43, ω_E accounts for the combination of the uncertainty in the measured quantity of interest in the experiment and the impact of the uncertainty in the experimental conditions. Mathematically, ω_E can be represented by Equation (12) [39].

$${\omega_E}^2 = {\omega_0}^2 + \sum_j {p_j}^2 {\omega_j}^2 \tag{12}$$

where ω_0 represents the relative uncertainty in the measured output, ω_j represents the relative uncertainty in the reported experimental condition j (where these conditions are required as an input to the model), and p_j represents the dependency factor associated with experimental condition *j*. The probability density of

the quantity of interest (θ), conditional on the value of its model prediction (M), can then be obtained using Equation (13):

$$\theta|M \sim N\left(\theta, \left(\frac{\theta}{\hat{\delta}}\right)^2 \left(\frac{\widehat{\omega}_M}{\hat{\delta}}\right)^2\right) \tag{13}$$

The calculation of ω_0, ω_j, and p_j requires an in-depth understanding of the experimental settings. Section 4.2 provides a detailed description of the experimental settings and the potential uncertainty.

4.2 Experimental Setup of Fire Crew Performance Test

To generate the fire crew performance data, experiments were conducted by the Illinois Fire Service Institute (IFSI) to observe the fire crew response to a fire initiating in a closed compartment. Those experiments were conducted in a room with the same structure as Room 015 in the fire zone Z071 at the South Texas Project Nuclear Operating Company (STPNOC) plant. Room 015 is connected to a mezzanine level, Room 015J, where the safety-related cables are installed. Within the scope of this project, the IFSI test room focuses on Room 015, while Room 015J is included in the experimental setup. The research team has chosen not to include Room 015J in the experimental setup due to practical considerations. including budget and time constraints. In spite of the simplification in the room geometry, this study is designed carefully to provide a proof of concept for experimental validation of the ABM fire crew performance model and the treatment of associated uncertainty in support of Fire PRA of NPPs. The following subsections describe the detailed experimental setup inside the room.

4.2.1 Room Geometry

The structure of Room 015 is displayed in Figure 10. Room dimensions are given by a width (x) of 4.572 m, a length (y) of 5.791 m, and a height (z) of 7.315 m. There are three electrical cabinets in the room, including (i) two Qualified Display Processing System cabinets (QDPS, 0.9779 m × 0.762 m × 2.3368 m) and (ii) an Auxiliary Shutdown Panel (ASP, 3.6576 m × 0.9144 m × 2.413 m). The height and width of the door are 1.829 m and 2.134 m, and the desk located in front of the door is 0.787 m × 1.067 m × 0.711 m. Table 44 summarizes the room geometry and dimensions of the objects in the room.

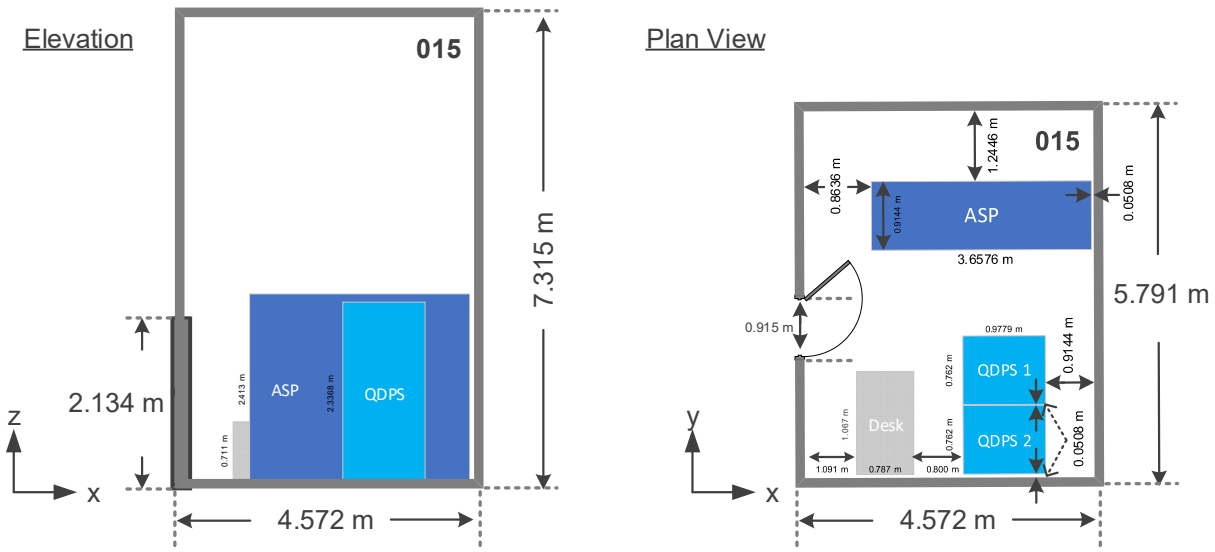

Figure 10: Drawing of Fire Compartment in the IFSI Experiment.

Table 44: Room geometry and dimensions of the objects inside the room.

Object	Width (x)	Length (y)	Hight (z)
Room	4.572	5.791	7.315
QDPS	0.9779	0.762	2.3368
ASP	3.6576	0.9144	2.413
Door	1.829	NA	2.134
Desk	0.787	1.067	0.711

4.2.2 Fire ignition sources

There are two types of electrical cabinets and cable trays in the room that can be considered as ignition sources. In the series of IFSI experiments, a fire source is created by a digital fire attack system, rather than by using a live fire. The fire locations in the experiments are shown in Figure 11.

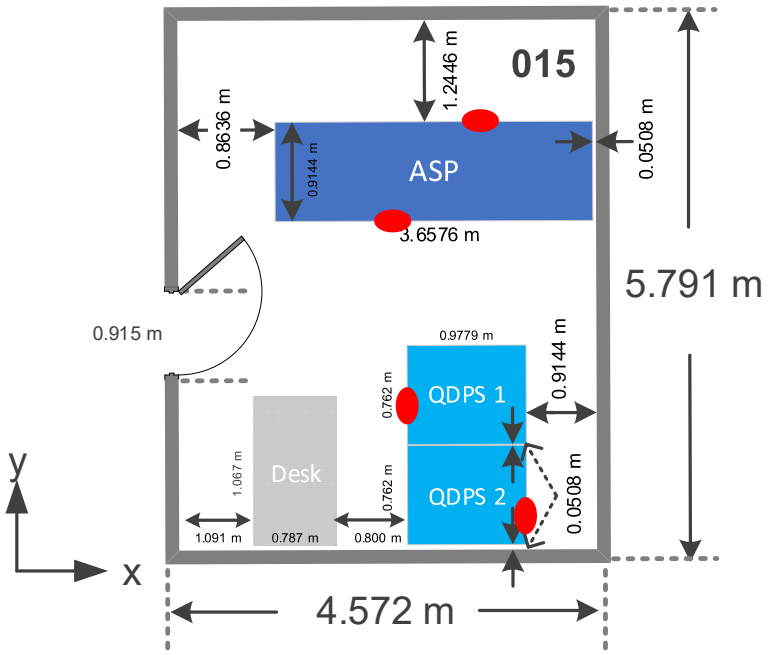

Figure 11: Locations of fire in the IFSI experiments (shown by red ellipses).

4.2.3 Procedure and Equipment for Fire Crew Response

Fire gear goggles with polarized lenses are given to the fire crew to simulate the obscuration level due to smoke. The polarized lenses allow the experiment to set visibility to any smoke condition to provide specific obscuration measures proportional to fire growth and help ensure replicability of the experimental conditions. The use of polarized lenses also allows for tracking the fire crew's movements from above with a motion-capture camera, without the actual concern of obscuration due to smoke.

The fire crew is tasked with searching and suppressing the fire in the room. The fire crew is dispatched to respond to an alarm with restricted information; thus, before the room entry, the exact location of the fire and event progression are unknown to the fire crew members. Manually operated, hand-held fire extinguishers are given to the fire crew. When the command tells the fire crew, "You are on the scene," the fire crew opens the door and proceeds to search and suppress the fire. Based on the level of visibility and familiarity/experience, the fire crew decides whether to crawl or walk during their fire search. After arriving at the fire location, the fire crew suppresses the fire using the hand-held extinguishers.

4.2.4 Time Measurement of Fire Crew Response

Time stamps of fire crew response are measured by the IFSI test staff with a stopwatch. The times provided by the experiment staff are the time to knock the fire (i.e., the time when water is initially applied to the fire

source) and the time to strike the fire (i.e., the time when the fire is fully suppressed based on the report from the fire crew). When the fire crew arrives at the fire location and the water is applied, the fire crew communicates with the commander over the radio, “Fire is knocked.” Once the fire is fully out, the fire crew communicates with the commander again over the radio, “Strike the fire.” Based on these radio communications, the test staff records the time to knock the fire and the time to strike the fire. The time to locate the fire is not reported by the test personnel but can be calculated based on the preparation time, entry time, and the time to knock the fire using Equation (14).

$$t_{\text{locate}} = t_{\text{knock}} - t_{\text{entry}} - t_{\text{preparation}}, \quad (14)$$

where:

t_{locate} : Time to locate the fire

t_{knock} : Time to knock the fire measured by the test staff

t_{entry} : Time needed to enter the room (estimated from the video recordings)

$t_{\text{preparation}}$: Preparation time for fire suppression (estimated from the video recordings)

4.3 Agent-based Fire Crew Model

The fire crew performance model is developed using ABM. ABM is a bottom-up modeling approach, where a system is viewed as a collection of independent entities known as "agents." A typical ABM formulation begins with an agent and defines the agent's behavior rules regarding timing, decisions, and interactions with other agents and environments in the modeled system. The modeling formulation and structure in this study are based on Bui et al. [7], while the ABM inputs are updated to simulate the specific fire compartment used in the IFSI experiments. The NetLogo software tool is used to operationalize the fire crew performance model. The following subsections describe computational settings in the ABM fire crew performance model.

4.3.1 Modeling Assumptions

The fire search process is modeled on a set of assumptions and decision rules based on the bouncing-off procedure.

- The fire crew’s decision regarding whether to walk or crawl is based on three main conditions: experience, visibility, and temperature in the room. Higher experience and visibility increase the

tendency to choose walking, while higher temperature increases the likelihood of selecting crawling. Within the scope of this study, the movement mode (walking vs. crawling) of the fire crew in the ABM simulation is predefined based on the experimental observation for each trial of the IFSI test.

- It is assumed that the fire crew always begins the fire search process from the right side of the room. This assumption is made based on the common firefighting practice that the fire search under degraded visibility is conducted using a specific direction so that the fire crew does not become spatially disoriented.
- The model assumes that, once the fire crew begins to move in a certain direction, they will keep moving in that direction with a constant speed unless i) an obstacle (e.g., electrical cabinet) is found in their path, and its distance from the fire crew reaches a predefined value or ii) they reach a dead end, such as a wall.
- The simulation stops when the fire location falls within the visible range of the fire crew. The angle of their range of vision is assumed to be 120 degrees [40].

Considering the limitation in the numbers of grid cells that can be simulated in the NetLogo software, the room dimensions are rounded to the first decimal digit. The time step is set to 0.1 seconds.

4.3.2 Governing Equations

This section describes equations that govern the fire crew movement in the ABM model.

4.3.2.1 Walking and crawling speeds

As stated above, two movement modes are considered for the fire crew: walking and crawling. In cases where the fire crew crawls, the average speed of crawling on hands and knees is assumed to be 0.84 m/s, based on the measurement result in Ref. [41]. In cases where the fire crew walks, the traveling speed of the fire crew is modeled by Equations (15) and (16) representing the walking speed as a function of smoke density.

$$Speed_{smoke} = -0.1364 \times \ln(C_s) + 0.6423 \tag{15}$$

$$C_s = -\ln\left(1 - \left(\frac{OSU}{100}\right)\right) \tag{16}$$

where OSU is the percentage of obscuration. For a given value of OSU, we can determine the optical density from Equation (16) and then use Equation (15) to determine the walking speed of the fire crew. The equations above are used in cases where smoke exists in the room and can impact the fire crew performance. Meanwhile, if there is no smoke in the room, the walking speed is determined using a normal distribution with a mean and a standard deviation of 1.2 and 0.15, respectively [42].

4.3.2.2 Visibility Correlation

Visibility in a room under smoke-filled conditions is encoded in the model using Equation (17):

$$V = k\frac{1}{C_s} \tag{17}$$

where C_s represents the optical density, and k is calculated as a function of a set of physical parameters [43]. The visibility computed by Equation (17) is used in the ABM model to define the minimum distance from the fire source that the fire crew should reach to locate the fire source.

4.3.3 Limitations of the ABM fire crew model

The fire crew model developed in this study has potential limitations. Further research is required to evaluate the impact of these potential limitations on the results and insights of the validation of the ABM fire crew model.

- The room geometry is modeled in two dimensions (on the X-Y plane) rather than three dimensions; therefore, modeling of human behavior in the height (Z-) direction is beyond the scope of the current model.
- The same obscuration level is assumed for all locations in the room. This assumption is introduced in the ABM model to reproduce the visibility conditions of the IFSI tests, where the obscuration level due to smoke is generated using the polarized lenses that generate a constant obscuration level for the fire crew throughout the entire time of each test run. Although the visibility in black smoke and white smoke can be different, the type of smoke is not explicitly considered in the model or in the IFSI experiments.
- The smoke-induced obscuration level is assumed to be the dominant mechanism of interactions between the fire crew and fire progression. In reality, other physical factors in the fire room such as heat flux and toxic gas can also impact the fire crew performance.

4.4 Validation of the ABM-based Fire Crew Performance Model

In this section, the validation methodology discussed in Section 4.1 is applied to the ABM-based fire crew performance model. Experimental uncertainties are first introduced. An explanation of the different cases considered for validation is then provided, followed by a discussion of the results obtained.

4.4.1 Experimental uncertainties

As shown in Equation (12), there are two sources of uncertainty in the experiment. The first source is related to uncertainty in the measured quantity of interest to which the model output is compared ($\omega_0{}^2$ in Equation (12)). The measured quantity of interest in the IFSI experiments is the time needed for the fire crew to locate the fire source. As stated in Section 4.2.4, this quantity of time is measured using a stopwatch and, in this research, the delay in the reaction by a person using the stopwatch is the largest source of uncertainty for the experimental measurement. According to Ref. [44], the uncertainty in reaction time for a stopwatch-operated start and stop experiment can be modeled by the normal distribution N(0, 0.102). The second source of uncertainty is related to uncertainties in the experimental conditions that are used as inputs to the model, represented by the second term on the right-hand side of Equation (12). Experimental conditions related to the IFSI experiments that represent this source of uncertainty include:

- Room geometry and dimensions
- The exact location of the fire
- Experience level of the fire crew
- Obscuration level

To calculate Equation (12), each of the experimental conditions above requires estimations of the relative uncertainty ω_j and the dependency factor p_j. To estimate p_j, a direct relation (such as a physical equation) connecting a given condition (input) to the output quantity of interest is needed. In Ref. [39], the dependency factor was estimated based on engineering correlations that are widely used in fire protection engineering. In this research, however, it has proven to be challenging to compute the dependency factor by relying on a pre-defined, deterministic input-output relationship since human actions are not governed by simple mathematical equations. This study, therefore, assumes that uncertainties associated with the experimental conditions are zero. This assumption ($\omega_j = 0$) results in a more conservative estimation of the bias and the relative uncertainty of the model and, ultimately, leads to a conservative risk estimation. This point can be proved mathematically. By substituting $\omega_j = 0$ in Equation (12), a lower value of ω_E is

obtained. Since ω_E in Equations (9) and (10) is subtracted from the standard deviation s, the lower value of ω_E generates an upper (conservative) estimation of the model bias and relative model uncertainty. The larger the amount of time for fire search is, the larger the non-suppression probability becomes since longer suppression time results in a higher probability of exceeding the time to target damage; hence, this assumption ultimately leads to a conservative risk estimation.

By the assumption of $\omega_j = 0$, Equation (12) is reduced to Equation (18).

$$\omega_E{}^2 = \omega_0{}^2 \tag{18}$$

The bias in the model prediction ($\hat{\delta}$) and the degree of scatter in the true value ($\widehat{\omega}_M$) are calculated by Equations (9) and (10) using the model outputs (M), experimental outputs (E), and uncertainties in the experiment $\omega_E{}^2$. This study considers two cases for the value of ω_E. The first case assumes that the experiments have no uncertainty and represents the real world which will mean that the differences in the model output and the experiment will be solely due to uncertainties in the model. This assumption produces the upper bounds for $\hat{\delta}$ and $\widehat{\omega}_M$; thus, it is considered as a bounding assumption.

In the second case, it is assumed that the experiment involves the measurement uncertainty (ω_0), while, as stated above, the uncertainty for the experimental conditions is ignored ($\omega_j = 0$). ω_0 is calculated using Equation (19) below, where σ is the standard deviation in the time measurement. This study uses $\sigma = 0.102$ as suggested in Ref. [44] and assumes that it is constant for all the experiment trials.

$$\omega_0{}^2 = \frac{\sigma^2}{measured\ time} \tag{19}$$

Since we have multiple time measurements, we consider two sub-cases for the measured time in the dominator of Equation (19). The first subcase (2.a) uses the longest time recorded (which will produce the lowest ω_0), while the second subcase (2.b) uses the average time recorded (which will produce the average ω_0). Table 45 summarizes the different cases that will be utilized for the validation purposes.

Table 45: Different Cases of Experiment Relative Uncertainty Considered in Validation.

Case ID	Experiment Relative Uncertainty
1	$\omega_E{}^2 = 0$
2.a	$\omega_E{}^2 = \omega_0{}^2$ where $\omega_0 = \frac{0.1}{longest\ time}$
2.b	$\omega_E{}^2 = \omega_0{}^2$ where $\omega_0 = \frac{0.1}{average\ time}$

4.4.2 MATLAB Code

A MATLAB code is developed for the implementation of model validation using the methodology discussed in Section 4.1. The steps utilized in the code are summarized below.

1. Import inputs from an excel sheet. The inputs include:
    a. Model output for each trial M_i
    b. Experiment output for each trial E_i
2. Set the value of $\omega_E{}^2$. This value is changed depending on the cases analyzed (Table 45).
3. Compute the value of s^2 utilizing the values of M_i and E_i using Equation (11)
4. Compute the bias in the model using Equation (9)
5. Compute the uncertainty in the model using Equation (10)

For verification of the MATLAB code, the code has been run for an arbitrary dataset where the bias and relative uncertainty are known. The data is artificially generated using the following steps:

1. Set values for the experiment's relative uncertainty ω_E, model relative uncertainty ω_M and model bias δ. These values are used to generate the hypothetical data.
2. Generate 1000 uniformly distributed random values θ_i between 0 and 1000. These values are assumed to be the true values of the quantity of interest.
3. For each of the true values θ_i generated in the second step, randomly select a value that represents a hypothetical experimental measurement, E_i, from a normal distribution whose mean is the true value θ_i and whose standard deviation is equal to $\omega_E * \theta_i$

4. For each of the true values θ_i generated in the second step, randomly select a value that represents a hypothetical model prediction, M_i, from a normal distribution whose mean is $\delta * \theta_i$ and whose standard deviation is equal to $\omega_M * \theta_i$

The data generated in the steps above are used to verify the MATLAB code. The code takes these data as input and calculates the bias and relative uncertainty as an output. Since the results of the bias and model uncertainty calculated by the MATLAB code agreed with the assumed values, the MATLAB code is verified. The results of the code verification are shown in Table 46.

Table 46: Verification results of the MATLAB code

		Assumed	Calculated
TEST 1	Bias	1.5	1.4989
	Uncertainty	0.1	0.0978
TEST 2	Bias	1	1.0031
	Uncertainty	0.2	0.2074
TEST 3	Bias	0.5	0.5004
	Uncertainty	0.01	0.0102

The estimates of bias and model uncertainty, Equations (9) and (10) respectively, are based on normality approximations, and are derived using a Taylor series approximation [39]. Section 4.4.3 provides a test that validates the applicability of the normality assumption to the data used in this study. The MATLAB code is then used to analyze the real data obtained from the experimental measurements and model predictions in Section 4.4.4.

4.4.3 Normality Test

This section describes the test utilized to validate the applicability of the normality assumptions to the data used in this study. Equation (20), shown below, provides an opportunity to test the normality assumption [39].

$$\ln\left(\frac{M_i}{E_i}\right)|E_i \sim \mathrm{N}\left(\ln(\delta) - \frac{\omega_M^2}{2\delta^2}, \frac{\omega_M^2}{\delta^2} + \omega_E^2\right) \quad (20)$$

The K-S goodness of fit test is used to test the hypothesis of the normal distribution in Equation (20). Total number of pairwise points (E,M) is 9 (four for "Behind ASP" and 5 for "Behind QDPS"). Table 47 shows the results of the test. As can be seen from Table 47, the hypothesis passed the K-S test.

Table 47: Result of the K-S goodness-of-fit test to check applicability of the normality assumption to the data being analyzed.

Sample (i)	$ln(M/E)$	Empirical Cdf †		Hypothesized Cdf †	Differences	
		$S_n(t_i)$	$S_n(t_{i-1})$	$F(t_i)$	$\lvert F(t_i) - S_n(t_i)\rvert$	$\lvert F(t_i) - S_n(t_{i-1})\rvert$
1	-0.31886	0.1111	0	0.0002	0.1109	0.0002
2	0.06791	0.2222	0.1111	0.0376	0.1846	0.0735
3	0.07067	0.3333	0.2222	0.0387	0.2946	0.1835
4	0.23287	0.4444	0.3333	0.1540	0.2904	0.1793
5	0.49960	0.5556	0.4444	0.5824	0.0268	0.1380
6	0.65733	0.6667	0.5556	0.8248	0.1581	0.2692
7	0.83718	0.7778	0.6667	0.9609	0.1831	0.2942
8	0.99853	0.8889	0.7778	0.9939	0.1050	0.2161
9	1.207357	1	0.8889	0.9997	0.0003	0.1108
					MAX (Differences)= 0.294	
					Rejection Region $D_9(\alpha = 0.05)$ = 0.430	
					MAX < Rejection Region = TRUE Normality Test = PASS	

† "Cdf" in this table stands for "cumulative distribution function."

4.4.4 Validation Results

For the cases where the fire source is in front of the ASP or in front of QDPS, the observed time to locate the fire, obtained from the IFSI experiments, is quite short. When compared to the length of time required for other activities (including time for the preparation and time for suppression) performed by the fire crew, the search time for these two locations is insignificant. For this reason, these two locations are not included

in the validation analysis shown in this section. The bias and relative uncertainty for the model calculated for the other two fire locations (Behind QDPS and Behind ASP) are shown in Table 48. For each case of experimental uncertainty treatment (Cases 1, 2.a, and 2.b listed in Table 45), the bias and relative uncertainty are computed by (i) treating data for each fire location separately; and (ii) combining the data for both fire locations (Behind QDPS and Behind ASP).

Table 48: Validation results for three cases of experimental uncertainty.

Case	Location	Model bias	Model Relative uncertainty
Case 1	Behind QDPS	2.263	0.608
	Behind ASP	1.019	0.210
	Combined	1.756	0.819
Case 2.a	Behind QDPS	2.263	0.607
	Behind ASP	1.019	0.210
	Combined	1.756	0.819
Case 2.b	Behind QDPS	2.262	0.606
	Behind ASP	1.019	0.210
	Combined	1.756	0.819

As can be seen from Table 48, the bias and relative uncertainty of the model are location dependent. Table 6 indicates that the ABM fire crew model tends to overestimate the time for fire search for "Behind QDPS," while the model prediction for "Behind ASP" has less bias (over-/under- estimation) indicated by the model bias closer to unity. It should be noted that the number of data points for each ignition source was four for "Behind ASP" and five for "Behind QDPS." The 95% confidence interval for the model bias estimated for each ignition source, "Behind QDPS" and "Behind ASP", is greater than 50% and 40% of the corresponding point estimate, respectively.

In Table 48, by comparing Cases 1, 2.a, and 2.b, it can be seen that the uncertainty in the experimental output has no significant effect on the calculated bias and relative uncertainty of the model.

This is explained by the fact that the time uncertainty associated with utilizing the stopwatch is less than the time to locate the fire by an order of magnitude.

The bias and relative model uncertainty provided in Table 48 can be used alongside the model output to generate a distribution of the time required by the fire crew to locate the fire. This distribution can then be used in the calculations of the non-suppression probability as input to the Fire PRA of NPPs.

4.5 Summary

The aim of Phase III of this project is to estimate the relative uncertainty and bias associated with the ABM-based fire crew model to generate a probability distribution of the time to locate the fire source in a given compartment. Note that locating the fire is only the first step in the fire crew response. Other activities in the fire crew response, such as suppressing the fire, are not included in the scope of validation in this research. Additionally, the validation of the ABM-based fire crew model did not consider the subroutine in the model that is used to determine the fire crew's decision to walk or crawl. Instead, this decision was treated as a predefined input based on the movement mode observed in the IFSI experiment.

The uncertainty in the experimental conditions is not explicitly considered in this study (Section 4.1) due to difficulties in estimating the dependency factor associated with each condition based on existing engineering correlations or experimental data. The assumption of the zero experimental condition uncertainty leads to conservative estimates of the model bias and relative uncertainty. If the fire crew performance is identified as the critical risk contributor or the dominant uncertainty source, the realism of the model uncertainty quantification for the ABM model should be improved by conducting additional fire crew experiments to derive empirical relationships between each experimental condition and its effect on the output quantity of interest.

Page intentionally left blank

5. Fire Probabilistic Risk Assessment for Advanced Nuclear Power Reactors: Literature Review and Gap Analysis

This chapter reports the research outcomes from Task 3 of the project. Probabilistic Risk Assessment (PRA) is an important tool for analyzing the safety of nuclear power plants (NPPs). The insights derived from PRA can be highly utilized in each stage of the lifecycle of NPPs and are considered by the U.S. Nuclear Regulatory Commission to be one of the key pillars in the risk-informed decision-making process. After the near-miss fire event at the Browns Ferry NPP in 1975, fire protection and regulation at NPPs in the U.S. experienced dramatic changes. Deterministic and prescriptive requirements were established by 10 CFR 50.48 and Appendix R [45]. In parallel with the development of the deterministic and prescriptive fire protection regulations, in 1977, the U.S. NRC initiated fire risk analysis research which resulted in the development of a systematic and structured methodology for estimating the fire-induced risk to NPPs. This Fire PRA methodology was implemented in several PRA projects. The Fire PRA approach, developed in the 1980s, was used as a foundation for the EPRI/NRC-RES Fire PRA Methodology NUREG/CR-6850 [1], developed by the Office of Nuclear Regulatory Research of the U.S. Nuclear Regulatory Commission (NRC) and the Electric Power Research Institute (EPRI). NUREG/CR-6850 is the main guidance followed to conduct Fire PRA quantification for the current generation of operating reactors. It is worth noting that standardization and generality, to the extent possible, were considered during the development of NUREG/CR-6850. The contents of NUREG/CR-6850, however, were mainly influenced by the experience and research developed for the current fleet of Light Water Reactors (LWRs).

In recent years, various advanced reactor designs have emerged, each with its specific design features that can differ significantly from the currently operating reactors. In general, the applicability of the Fire PRA methodology (NUREG/CR-6850) for advanced reactors could be questioned if the fire phenomena and their impacts on the systems, structures, and components (SSCs) involved underlying processes that differ from those of the existing fleet or if the Fire PRA data collected from the existing plants (e.g., historical fire event database, manual suppression data) have a low level of relevancy. For instance, since the potential for metal fires is a unique risk in the liquid metal cooled reactors, external and internal fire scenarios that could accelerate the metal fire risk could be classified as one of the major contributors to the plant risk. The existing light water reactors, however, do not typically use liquid metal; thus, the fire event data collected from the existing plants are not relevant to metal fires, and the existing fire models (especially the ones relying on engineering correlations) may need additional validation or calibration. Currently, there are no regulatory or industry documents that outline the entire Fire PRA procedure for advanced reactors.

The objective of this study is to analyze the applicability of the existing Fire PRA methodology based on NUREG/CR-6850 and the subsequent NUREG documents (in this chapter, the methodology is referred to as the "NUREG/CR-6850 Fire PRA methodology") for advanced reactors and to evaluate potential challenges, gaps, and special considerations when the NUREG/CR-6850 methodology is applied to advanced reactors. To the authors' knowledge, there is no existing study that has reviewed or analyzed the current Fire PRA methodology in the context of advanced reactors. This research provides crucial insights for the development of a methodological basis for the Fire PRA of advanced reactors.

The remainder of this chapter is organized as follows: Section 5.1 describes the methodology used for conducting the literature review, detailing the research questions addressed in this study. Section 5.2 provides an overview of the worldwide advanced reactors and a detailed description of the databases used, the keyword selection, keyword combinations, and some statistical insights of the results obtained. Section 5.3 provides a detailed review of the existing Fire PRA studies for advanced reactors. Section 5.4 provides a detailed description of all the features of advanced reactors that might generate challenges when applying the NUREG/CR-6850 procedure for Fire PRA and how the existence of these features will affect different tasks of NUREG/CR-6850. Each of the challenges identified in the literature review was mapped with the corresponding task(s) of NUREG/CR-6850. Section 5.5 provides a summary and suggestions for future work.

5.1 Methodology of Literature Review

This research defines "advanced reactors" as the nuclear fission reactors that are categorized under at least one of the following classes: (i) Small Modular Reactor (SMR), (ii) Supercritical Water-cooled Reactors (SCWR), (iii) High Temperature Gas-cooled Reactor (HTGR), (iv) Very High Temperature Reactor (VHTR), (v) Gas-cooled Fast Reactor (GFR), (vi) Sodium-cooled Fast Reactor (SFR), (vii) Lead-cooled Fast Reactor (LFR), and (viii) Molten Salt Reactor (MSR). To achieve the objective of this study, the following five research questions are generated, and the relevant literature is analyzed from the viewpoint of these research questions.

- RQ1: What is the status of advanced nuclear power reactors around the world? The answer to this question will provide an understanding of the current status of advanced reactors worldwide. The knowledge gained from this question helps with selection of the keywords that are used to address other research questions.

- RQ2: For which advanced nuclear power reactors has the Fire PRA quantification already been performed?
    - RQ2.1 Which type of advanced reactor was analyzed?
    - RQ2.2 As an output of PRA, what risk metric was computed?
    - RQ2.3 What fire-induced risk scenario(s) was analyzed?
    - RQ2.4 What are the assumptions used, deviations or gaps found, and difficulties faced by the analysts during the quantification of fire risks?
    - RQ2.5 Are any regulatory/industry standards and guidance referenced for the Fire PRA methodology being used?
    - RQ2.6 Is any discussion provided regarding the comparison of the Fire PRA of advanced reactors with the Fire PRA of existing reactors?
- RQ3: What references are there that discuss the challenges of Fire PRA quantification for advanced reactors? What are the challenges listed in these references?
- RQ4: What NUREG/CR-6850 Fire PRA task(s) could potentially be affected by the challenges specific to each advanced reactor design?

Based on the research questions above, this report analyzes the applicability of the NUREG/CR-6850 Fire PRA methodology for advanced reactors and the methodological advancements and modifications that are required for the NUREG/CR-6850 Fire PRA tasks to be applied to advanced reactors.

To address the above research questions, several steps have been performed (Figure 12). First, an understanding of the advanced reactors in the world is established. Based on the different types of advanced reactors, a set of keywords is selected and then used to perform a comprehensive search for any Fire PRA studies conducted specifically for advanced reactors. As a result, two reference types are identified. The first type is the reference indicating that a Fire PRA study was performed for one of the advanced reactors and that plant risk metrics were quantified (e.g., Core Damage Frequency [CDF], Frequency of Large Release). The second type is the reference that indicates potential challenges in performing Fire PRA for some of the advanced reactors but with no quantification of the plant risk metrics. These two types of references support RQ2 and RQ3, respectively. The insights from the literature obtained in these steps, combined with a detailed review of NUREG/CR-6850, are used to provide answers to RQ4.

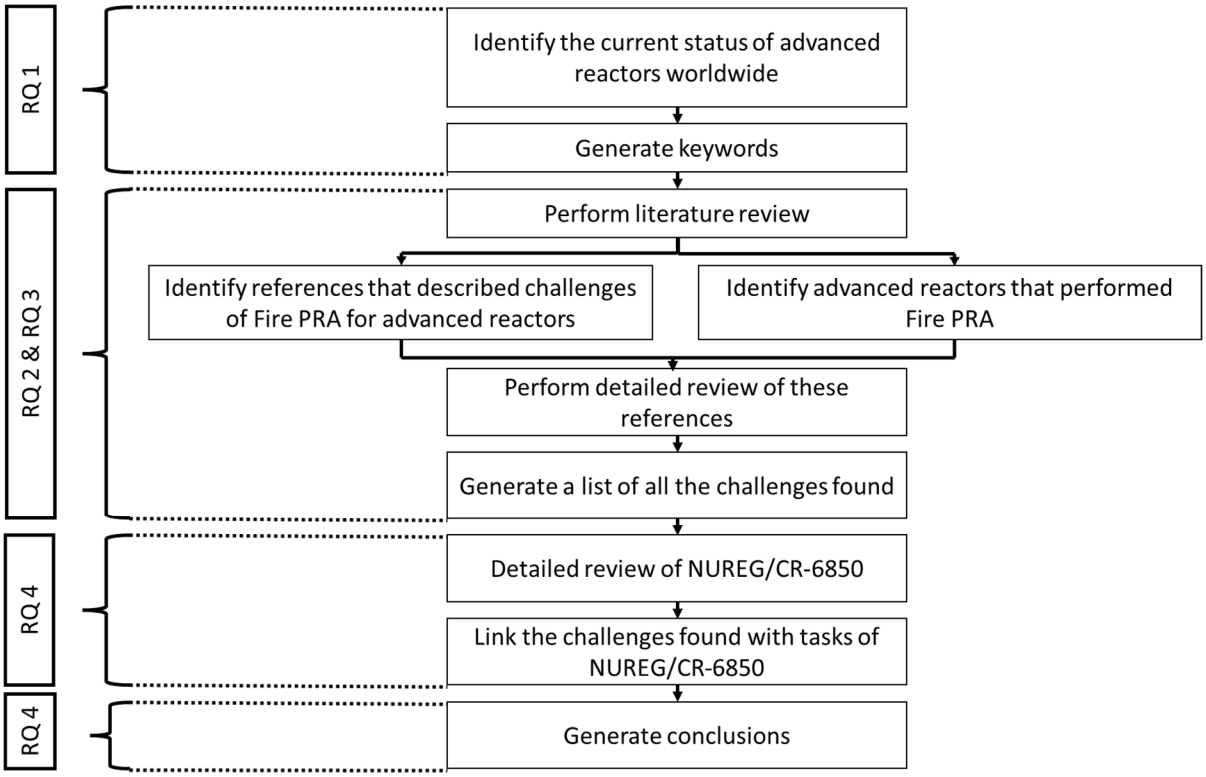

Figure 12: Literature Review Flowchart.

5.2 Overview of advanced reactors and selection of keywords

The first step in this study is to establish an understanding of the status of advanced reactors worldwide. For this purpose, various resources and databases are reviewed, including the Advanced Reactor Information System (ARIS), a database designed and, since 2009, maintained by the International Atomic Energy Agency (IAEA) [46]. Other databases, such as the advanced nuclear directory developed by the U.S. Department of Energy (DOE) under the Gateway for Accelerated Innovation in Nuclear (GAIN) framework[e], were reviewed.

Based on the types of advanced reactors identified, a set of keywords is generated for searching literature relevant to the research questions (RQ 1 to 4). The literature search in this study uses two of the most well-known and frequently used search databases – Scopus and Google Scholar. These two websites provide a versatile option for keyword selection and methods of combining different keywords using the Boolean operators "AND" and "OR." In addition, other databases, such as the NRC's Agencywide

[e] https://gain.inl.gov/SitePages/Home.aspx

Documents Access and Management System, Idaho National Laboratory website, DOE website, and official webpages of advanced reactor companies are used.

The keywords are divided into different groups, and the keywords within each group are connected using an “OR” logic, while the groups are connected using an “AND” logic. The groups of keywords are shown in Table 49. All combinations of these groups are used in the two databases: Scopus and Google Scholar. The surveyed period was from the year 2005 to 2021. The year selected to begin the literature review (2005) was because this was the year that NUREG/CR-6850 was officially released. The total number of references surveyed in this study is approximately 1,700. To ensure that the literature review is comprehensive, additional searches are performed using the keywords “NUREG/CR-6850” and “ANS RA-S-1.4-2021.” All the references are then reviewed in detail and linked with the RQs in this study.

Table 49: Keywords and Groups Used in Literature Search.

Group 1 keywords (combined with OR operator): “Fire PRA”, OR “Fire PSA”, OR “Fire probabilistic risk assessment”, OR “Fire probabilistic safety assessment”, OR “Fire probabilistic risk analysis”, OR “Fire probabilistic safety analysis.”	**Group 3 keyword:** “nuclear”
Group 2 Keywords (combined with OR operator): “Fire AND PRA” OR “Fire AND PSA” OR “Fire AND probabilistic AND risk AND assessment” OR “Fire AND probabilistic AND safety AND assessment” OR “Fire AND probabilistic AND risk AND analysis” OR “Fire AND probabilistic AND safety AND analysis”	**Group 4 Keywords:** "Small Modular Reactor" OR "SMR" OR "Sodium-cooled" OR "Fast Reactor" OR "High Temperature Gas Cooled Reactor" OR "HTGR" OR "Gas-cooled" OR "Fast Reactor" OR "Molten Salt" OR "Supercritical" OR "Lead-cooled" OR "microreactor"
	Group 5 Keywords: "Sodium-cooled" OR "Fast Reactor"
	Group 6 Keywords: "Small Modular Reactors" OR "SMRS"
	Group 7 Keywords: "High Temperature Gas Cooled Reactor"

5.3 Review of the Existing Fire PRA Studies for Advanced Reactor Designs

Based on the literature review, three categories of advanced reactor designs are found to have Fire PRA quantification performed to quantify the plant risk metrics: sodium-cooled fast reactors, a high temperature gas-cooled reactor, and light water-cooled advanced reactors. This section reviews the existing Fire PRA studies for each advanced reactor design and provides the answers to RQ2.

5.3.1 Existing Fire PRA Studies for Sodium-Cooled Fast Reactors

In literature, there are two types of sodium-cooled fast reactors for which Fire PRA was conducted to compute the plant risk metrics: (i) the Prototype Gen-IV Sodium-cooled Fast Reactor (PGSFR), which is a sodium-cooled fast reactor under development by the Korea Atomic Energy Research Institute (KAERI); and (ii) the China Experimental Fast Reactor (CEFR), which is a fast reactor, located at the China Institute of Atomic Energy and will be used as the technical basis for the advanced reactor CFR-1000.

5.3.1.1 Existing Fire PRA Studies for the PGSFR Reactor

Kim et al. [47] provided a preliminary Fire PRA analysis for the PGSFR. The reference highlighted two important differences between the currently operating NPPs and the PGSFR design in terms of Fire PRA implementation: (i) the amount of equipment required in advanced reactor designs which may be far less than that for the current generation of LWR reactors, (specifically, the amount of Fire PRA equipment for PGSFR vs. commercial NPPs is 592 vs. 1177), and (ii) the introduction of new ignition sources such as sodium. Ref. [47] followed the NUREG/CR-6850 methodology, but some of the tasks were either not performed or lacked detailed descriptions.

Also, several assumptions were used in their analysis. It was assumed that if there is a fire, all equipment and cables in the fire zone are lost. This assumption conforms with what is stated in Task 7 of NUREG/CR-6850 but, at the same time, it indicates that the analysis stopped at this stage with no further detailed analysis or modeling.

It was also assumed that the ignition frequency of PGSFR is less by a factor of (592/1177) compared to ignition frequencies in an LWR. This assumption was based on the difference in the total amount of equipment, and no consideration was given to the types of equipment. The ignition frequency caused by the sodium leak was estimated based on sparse historical data from one reactor (BN-600 SFR); namely, the number of fire events that occurred over a period of 30 years. However, the degree of relevancy of the BN-600 SFR ignition data to the specific reactor design being studied (PGSFR) was not explicitly

analyzed; for instance, the differences in the sodium inventory and additional safety features and how they can impact the ignition frequency estimation. Their analysis also assumed that the fire ignition probabilities are identical for all the fire areas where a sodium flow path exists without considering the differences between each fire area in terms of the complexity of the sodium piping system.

A follow-up study was published in 2018 [48], which described a level 1 PRA for the PGSFR. The authors followed the same methodology as in the previous study but increased the realism of the analysis by calculating the sodium fire frequency based on the probability of sodium fire given a leakage. This probability is also based on the historical data of BN-600. The ignition frequency due to the sodium leakage was then apportioned to each fire area by multiplying the total sodium fire ignition frequency by the length of the sodium pipes passing through that fire area, divided by the total length of the sodium pipes in the entire reactor.

For the calculation of the fire ignition frequency in the Main Control Room (MCR), it was assumed that the MCR contains two electrical cabinets. The ignition frequency for the MCR was calculated based on the generic ignition frequency of electric cabinets multiplied by a factor representing the percentage of cabinets in the MCR to the total number of cabinets in the PGSFR. This frequency was then multiplied by the factor of 592/1177 that represents a smaller number of components than for the operating LWRs. The second multiplication factor, however, is based on the number of PRA components in general and is not specific to electrical cabinets. A table was provided showing the percentage of CDF for each fire area. The area with the longest sodium piping pass was found to be the most important area followed by the MCR. This differs from the preliminary analysis [47] where the MCR was the most important area.

In Ref. [49], the authors discussed the effects of the assumptions used in the two previous analyses [47, 48]. First, the authors used a different approach to estimate the ignition frequency of sodium fires. That is, the sodium piping leakage rate (3.0E-9/ft/h) obtained from Ref. [50] was used to estimate the sodium fire ignition frequency for each compartment rather than using the approach used in the two former analyses. As a result, CDF was reduced by 51%. Second, the authors decided not to consider the multiplier of 592/1177 when estimating the fixed and transient ignition frequencies. As a result, the CDF increased by 27%. Third, the authors decided to double two of the Human Error Probabilities (HEPs) during the MCR fire. These two HEPs are related to i) “Operator’s Failure to use Remote Shutdown Panel” and ii) “Failure to Manually Open PDRC Damper.” As a result, CDF increased by 13%. Deviations from the previous analyses showed that the assumptions made during the analysis can significantly affect the PRA results and more care should be taken when any assumptions that are not used in the current Fire PRA methodology for the operating LWRs need to be applied.

5.3.1.2 Existing Fire PRA Studies for the CEFR Reactor

Song et al. [51] developed and applied Fire PRA to the CEFR. They compared the SFR designs with the LWR design in terms of Fire PRA requirements, and potential gaps were identified, including:

- Estimation of sodium ignition frequency with consideration of the leakage probability, rate, and location rather than assuming a fixed location and quantity;
- Peak heat release rate distribution for sodium fires. NUREG/CR-6850 and the subsequent relevant NUREGs for light-water reactors do not provide the heat release rate estimation for sodium fires. The heat release rate of sodium fires can be impacted by various physical factors, such as crack size and shape;
- Non-thermal effects of sodium fires on availability of safety equipment and human actions, for instance, aerosol settlement, chemical corrosion, and toxicity of the products;
- Treatment of the detection and suppression systems designed for sodium fires. The sodium fire-specific fire protection systems differ from those used for other types of fires at LWRs. The reliability and availability of these sodium fire-specific fire protection systems need to be evaluated as part of the Fire PRA performed for sodium reactors.

5.3.2 Existing Fire PRA Studies for High Temperature Gas-Cooled Reactor

In literature, there is one type of high temperature gas-cooled reactor for which Fire PRA was conducted to compute the plant risk metrics: The High Temperature GCR - Pebble-Bed Module (HTR-PM), which is the first demonstration plant of a helium-cooled, graphite-moderated High Temperature Gas-Cooled Reactor in China, designed by Tsinghua University.

Wang et al. [52] discussed the challenges faced when applying the NUREG/CR-6850 Fire PRA methodology to perform Fire PRA for a switchgear room fire scenario in the HTR-PM reactor, such as:

- Selection of the plant risk measures for HTR-PM. Those used in NUREG/CR-6850 for LWRs, such as CDF and Large Early Release Frequency (LERF), were not applicable for the HTR-PM, based on the discussion provided in Tong et al. [53]. To overcome this challenge, the cumulative frequency of the beyond design-basis accident sequences causing an off-site individual effective dose exceeding 50 mSv was selected as a new plant risk metric.
- Fire frequency bins and generic frequencies available in the fire event database for LWRs may not be applicable for new reactor-specific ignition sources since the ignition frequencies from the new

reactor-specific equipment cannot be found on the recommended list in the database. Due to unavailability of operational data and limited information available under the construction phase of the HTR-PM at the time, Wang et al. [52] suggested that, for the ignition source types in the HTR-PM plant that also exist in the operating LWRs, those ignition sources be mapped to the NUREG/CR-6850 ignition source bins so that the corresponding plant-level generic fire frequencies could be used. For the ignition source types in the HTR-PM plant that cannot be mapped to any of the NUREG/CR-6850 bins, the component-level fire ignition frequency was estimated based on generic data from similar facilities, including non-nuclear facilities. These generic data will then be updated by Bayesian updating when the HTR-PM-specific operating records become available.

- In Fire PRA for the existing LWRs, engineering correlations (such as the Fire Dynamics Tool by the U.S. NRC) and a zone fire model (such as the Consolidated Model of Fire Growth and Smoke Transport [CFAST] code) are commonly used for fire modeling. The advantage of the engineering correlations and CFAST, compared to more sophisticated fire modeling tools, such as the Fire Dynamics Simulator (FDS), is that they can provide reasonably accurate predictions of fire-induced conditions with less data collection effort and lower computational cost. However, it should be noted that, so far, these fire models have been validated only for the range of ignition sources and fire conditions anticipated at the existing LWRs, for instance, see NUREG-1824 [32] for the validation of five fire models by the U.S. NRC. Wang et al. [52] recognized this potential challenge and proposed applying a combination of CFAST and FDS in HTR-PM Fire PRA to utilize FDS for new types of non-LWR fire scenarios by taking advantage of the greater resolution of the FDS while balancing the realism of fire modeling with computational burden. The feasibility of the suggested approach was illustrated by applying it to a switchgear room fire scenario of HTRPM.

5.3.3 Existing Fire PRA Studies for Water-Cooled Advanced Reactor

In literature, there are two types of water-cooled advanced reactors for which Fire PRA was conducted to compute the plant risk metrics: (i) the System-integrated Modular Advanced Reactor (SMART), which is a light-water cooled and moderated SMR designed by KAERI; and (ii) NuScale Power Module™ (NuScale NPM-20), which is a light-water cooled and moderated SMR designed by NuScale Power, Inc. and is currently in the Standard Design Approval/Pre-Application stage with the U.S. NRC.

5.3.3.1 Existing Fire PRA Studies for the SMART Reactor

Kang and Jin [54] provided an overview of Fire PRA conducted for the SMART reactor. Lack of information related to circuit design, cable routing, and position of the Fire PRA equipment were among the challenges during their application of the NUREG/CR-6850 methodology to SMART. Specifically, the main issues were related to quantifying the i) severity factors which, based on NUREG/CR-6850, requires fire modeling that, at the time, was not possible for SMART due to the lack of information and ii) the probability of fire-induced spurious operation of equipment. The guidance in NUREG/CR-6850 was used for most of the Fire PRA tasks, while the severity factors and fire-induced spurious operation probabilities were assigned values based the EPRI Fire PRA Implementation Guide.

In relation to the previous study, Kang and Han [55] and Kang et al. [56] introduced an interface program for constructing a zone effect table (IPRO-ZONE) with the results of its application to Fire PRA of SMART. In their analysis, all equipment and cables in the fire zone were assumed to be damaged due to a fire. Also, when power supply cables and control cables for a given component exist in the same zone, it was assumed that control cables would fail first, causing spurious operation of the equipment, and the electric cables would follow. Multiple Spurious Operations (MSOs) were not considered because the MSO scenarios were determined to be non-significant contributors to the CDF as the safety-related equipment and circuits at the SMART reactor are physically separated and electrically isolated. Engineering judgment and Appendixes J and K of NUREG/CR-6850 were used for the estimation of fire-induced component spurious operation. Within the scope of their study [55, 56], the IPRO-ZONE had no function for addressing human failure events; hence, the effects of fire-induced instrumentation failures on human failure events were not analyzed. The malfunctions of these instrumentations and controls, however, could have had a great effect on the operators' situation awareness and judgment during emergencies.

In a later study, Park et al. [57] summarized the status and results of Level-1 and Level-2 PRA for internal events, internal fire events, and internal flooding events at full power operation mode for the SMART reactor. The methodology used for the internal Fire PRA in their study was based on NUREG/CR-6850 and NUREG/CR-6850 Supplement 1. Fire ignition frequency for SMART was evaluated by applying the fire ignition frequency estimation method in NUREG/CR-6850 and the fire ignition frequency data from NUREG-2169 derived from LWR operating experience.

5.3.3.2 Existing Fire PRA Studies for the NuScale Reactor

For the NuScale NPM-20, a Standard Plant Design Certification Application was submitted to the U.S. NRC in 2020 [58] and included the internal Fire PRA for at-power operations for a single NuScale Power

Module (NPM). The Internal Fire PRA followed the NUREG/CR-6850 methodology. A description was provided for the methodological and modeling aspects along with key results for the CDF, LRF, and conditional containment failure probability. The main issue faced during the Fire PRA analysis was related to the unavailability of detailed design information. For example, detailed cable configuration and routing information were not established for design certification. So, cable routing was assumed based on the physical location of equipment and engineering judgment. However, since safety systems are passive in nature, the loss of power to these systems due to cable fire was considered less concerning. To handle the lack of detailed information, conservative assumptions were used in the Fire PRA analysis. For example, fire-induced failures other than spurious actuations were assigned a probability of 1.0. Additionally, no suppression (automatic or manual) was credited within individual fire compartments and, if fire growth occurred, these fires were conservatively assumed to damage all the equipment in the room. Also, fires in the MCR, including fires affecting the main control board, were conservatively assumed to damage all the equipment in the room. Despite the use of conservative and bounding assumptions, results showed that fire risk is extremely low. It was argued that the reason for the lower risk is due to the passive features of the NuScale design.

Since the NuScale design can consist of multiple modules, multi-module risk estimation is needed. Current Fire PRA methodology does not consider multi-module risk analysis; thus, a systematic approach was developed for the assessment of multi-module risk by leveraging the single-module full-power internal-event PRA. Parametric adjustments to the single module were made at the cutset level using multi-module adjustment factors and multi-module performance shaping factors.

5.4 Potential Challenges and Gaps in the NUREG/CR-6850 Fire PRA Methodology When Applied to Advanced Reactors

Based on the review in Section 5.3, potential challenges and gaps in Fire PRA for advanced reactors (especially when the NUREG/CR-6850 methodology is applied) are classified into six categories:

- Introduction of new ignition sources that do not exist in the operating LWRs (Section 5.4.1)
- Analysis of the operating conditions different from the operating LWRs (Section 5.4.2)
- Modeling of new types of Fire PRA scenarios (Section 5.4.3)
- Modeling of Passive Safety Systems (Section 5.4.4)
- Analysis of radioactive inventories outside of the reactor core (Section 5.4.5)

- Inapplicability of the existing LWR data and assumptions (Section 5.4.6)

The following subsections discuss each of the potential challenges and gaps.

5.4.1 Introduction of new ignition sources

Some advanced reactors introduce new ignition sources that are not considered for the Fire PRA based on NUREG/CR-6850. When applying the NUREG/CR-6850 methodology to advanced reactors, these new ignition sources may generate challenges associated with 1) calculation of the ignition frequencies, 2) estimation of the reliability of fire protection measures, 3) fire modeling, and 4) analysis of fire-induced consequences unique to the advanced reactors (e.g., radioactive material release by sodium fires at fast reactors).

The treatment of new ignition sources that are not listed in the predefined ignition source bins was briefly included in Task 6 of NUREG/CR-6850: "*It is possible that unique ignition source types are identified that may not be reflected in the generic frequency model ignition source.*" Then, NUREG/CR-6850 provides guidance on what information should be gathered about the new ignition sources and suggests that "ignition frequency associated with the source should be developed and justified, using such information sources as the vendor, other industries, or, ultimately comparing the source to others with known ignition frequencies." However, no detailed procedure is provided as to how this suggested method can be applied to new ignition sources. Moreover, this current guidance in NUREG/CR-6850 only addresses the calculation of the ignition frequencies, while other aspects, including estimation of the reliability of fire protection measures, fire modeling, and analysis of advanced reactor-specific consequences are not provided.

Four examples of the new ignition sources that could pose a challenge in performing Fire PRA for advanced reactors are provided below.

Example 1: Graphite

One of the initiating events specific to the MSR design, identified by Pyron [59] using a Master Logic Diagram, was a graphite fire that could be caused by the Wigner effect or oxygen ingress into the primary loop. Additionally, salt penetration in graphite can cause thermal decomposition of graphite-oxide, which increases the release of flammable CO, leading to poor thermal stability and generation of a fire hazard [60]. The pebble bed designs of VHTRs and HGTRs also include graphite that should be considered as an ignition source. The fire hazard that originates from the production of graphite dust during normal

operation in the pebble bed designs of VHTRs and HGTRs was highlighted by Denman et al. [61]. Graphite dust can be produced by abrasion between pebbles in the reactor core or abrasion between pebbles and the fuel handling system [62].

Example 2: Hydrogen

Hydrogen is already considered in the NUREG/CR-6850 methodology (Ignition Source Bins 19 and 34). In advanced reactors, however, hydrogen might exist in locations and configurations different from those at the operating LWRs. For example, the VHTR and HGTR reactor designs may be operated in conjunction with a hydrogen production facility, which itself poses a new challenge in assessing the hydrogen fire and explosion risks [61].

As another example, in sodium-cooled reactors, a sodium leak in the secondary water loop could lead to the production of sodium hydroxide and hydrogen that could cause hydrogen explosions [63]. Also, sodium may react with the concrete, in case of sodium leakage, and the sodium-concrete reaction can generate hydrogen that can accumulate in a compartment and lead to detonation [64]. When hydrogen detonation occurs, the blast wave characteristics may challenge nuclear safety barriers and structures in ways that are different from the typical fire damage, for example, with thermal and smoke impacts [65].

Some of the MSR designs with fluoride salts use hydrogen and metal fluoride additions to control the chemistry of the molten salt; hence, hydrogen fire and explosion risks should be considered in Fire PRA. Attention should be given to inventory, layout, and consequences of fires and explosions if the hydrogen is released outside of the main molten salt loop [65].

Example 3: Sodium

In SFRs, the presence of sodium poses fire risks different from those for the conventional fires analyzed in other types of reactors. For loop-type SFRs, in the event of a coolant or fuel leak, sodium will ignite upon contact with air [61]. Compared to the fire sources that are already considered in Fire PRA of operating LWRs, sodium fires have distinct characteristics:

- When sodium burns, large quantities of oxide aerosols are released. Radioactive sodium in these emissions poses a significant health hazard to plant workers and firefighting personnel; hence, the location of a primary loop sodium leak may be difficult or impossible to reach [65, 66]. Also, sodium fires can generate a thick smoke layer that can adversely impact the plant shutdown procedures and emergency response activities [63]. The potential effects of the release of

radioactive sodium aerosols on human performance needs to be reflected in the HEPs used in Fire PRA.

- Compared to the other types of typical ignition sources at NPPs, sodium fires burn at higher temperatures [66] and generate highly corrosive aerosols [63, 65]. The higher temperatures and the corrosive aerosols could represent a threat to SSCs, such as pipes, valves, and tanks, not normally considered vulnerable to fire-induced damage. The highly corrosive aerosols can cause consequential hazards away from the seat of the fire and result in blockages of equipment such as pumps, filters, and general instrumentation damage [65, 67]. This aspect should be considered in the component selection and screening process and the fire-induced damage criteria in Fire PRA for SFRs.
- Potential for core voiding and its impact on PRA scenarios. Large-scale sodium-cooled fast reactors may have a positive void reactivity coefficient; thus, if sodium is voided, it will cause the power level of the reactor to rapidly increase and might directly lead to a core meltdown. Sodium fires could lead to sodium being voided if an undercooling event is initiated without scram (reactor shutdown). A severe leak in the secondary system coupled with cable fires could lead to this situation [66]. This introduces a new scenario that might not be considered in the internal events PRA upon which the Fire PRA is based. Analysts should ensure that this scenario is included in the Fire PRA and is not overlooked.

Example 4: Volatilized gases in off-gas systems

Off-gas from the fluorination process in the MSR includes volatilized UF6 [68]. Ignition of the activated carbon in the charcoal beds (utilized as a functional barrier) due to volatile organic materials in the off-gas stream may reduce the efficiency of this functional barrier and could lead to radioactivity release. Ignition Source Bin 20 in NUREG/CR-6850 is related to the off-gas/H2 recombiner in Boiling Water Reactors; however, the relevancy and applicability to the off-gas system in each advanced reactor design need to be evaluated.

Among the four examples of new ignition sources above, the one that has been most extensively studied is sodium fires. Subsection 5.4.1.1 summarizes the status of the existing insights on sodium fires. Based on the insights from the sodium fire-related studies, Subsection 5.4.1.2 analyzes which tasks in the NUREG/CR-6850 procedure may be impacted by the newly introduced ignition sources in advanced reactor designs.

5.4.1.1 Available Insights on Sodium Fires

For the calculation of ignition frequencies of sodium fires, historical data are available from older SFR designs; however, there are certain factors that should be accounted for when utilizing the historical database of sodium fires:

- The difference in sodium inventories between advanced and older sodium reactor designs which can directly impact the ignition frequency calculations
- Piping and structural designs that could affect the sodium leakage probability and the sodium ignition frequency.
- Any changes in operation and maintenance procedures

Additionally, new prevention and mitigation measures in advanced reactor designs that did not exist in the older designs should be considered. Potential design improvements to prevent and mitigate sodium leaks include nitrogen injection, pressure release valve, catch pan, and drain system for leaked sodium [69]; utilization of secondary piping and inert atmospheres and the use of low pressure in the primary coolant loop, use of ductile materials to reduce the likelihood of brittle failures, and the detection of small sodium leaks before they convert into large leaks [64-66]; and the use of cold traps to remove oxygen and other impurities from sodium coolant [66]. Aside from the design improvements, the enhancement of administrative programs, fire protection programs, and procedures and training can also contribute to prevention and mitigation of sodium fires [67, 70]. The reliability and effectiveness of these preventive and mitigative measures should be explicitly considered in the ignition frequency calculations.

From the viewpoint of fire modeling, when compared to conventional fires at operating LWRs, sodium fires are unique in terms of high temperatures and the production of corrosive aerosols. To enhance the realism of sodium fire modeling, several experiments were conducted, and sodium fire codes were developed. Application of these codes will require some additional model development and validation work since most of these experiments were performed years ago and cannot be used to support model development today [66]. Several codes have been under development for sodium fire analysis. A code named CONTAIN was introduced by Sandia National Laboratories in 1982. The Japan Atomic Energy Agency (JAEA) built on that code and developed CONTAIN-LMR for application to a probabilistic risk assessment of liquid metal fast reactors [71]. The Department of Energy (DOE) initiated a multi-year program to incorporate sodium fire and containment modeling capabilities residing in the dormant code CONTAIN/LMR into the MELCOR computer code [61]. Another computer code called SPHINCS was developed, which is a computer code that solves coupled phenomena of thermal hydraulics and sodium fire,

based on a multi-zone model [72]. The code solves other phenomena associated with sodium fires such as chemical reactions, gas and aerosol transfer, energy transfer, pressure and temperature in the air and at the walls and structures [64]. This code then was added to a system of codes developed by JAEA. The system has various computational programs including the ASSCOPS code for sodium spray and pool fire analysis in two-cell geometry, the SPHINCS code for simultaneous spray and pool fire analysis in multi-cell geometry, the AQUA-SF code for three-dimensional analysis of an atmospheric gas region, and the other computational modules for individual phenomenon such as equilibrium chemical reaction and sodium aerosol behavior [73]. The SPHINCS code was used to analyze various sodium fires in the steam generator room to evaluate the performance of the candidate sodium fire measures [69]. Other codes for sodium fire analysis are SOFIRE II, CORIUM-2D, and ECART [67].

Verification and Validation of computer codes provides a very important criterion for considering the codes applicable for the analyses of sodium fires. One important method to develop a validation matrix is called the Phenomena Identification and Ranking Table (PIRT) exercise. The PIRT exercise was performed at SNL and an experimental and modeling program was designed based on the PIRT results [74, 75]. The aim of the exercise was to identify the phenomena of interest in two scenarios involving sodium fires. The PIRT exercise was also used to identify the validation matrix of important phenomena for the sodium fire analysis codes SPHINCS and AQUA-SF [76, 77]. However, for sodium fire model performance, there are no systematic comparisons that use a recognized set of scenarios [65].

5.4.1.2 Potential Impacts on NUREG/CR-6850

The NUREG/CR-6850 tasks potentially affected by these newly introduced ignition sources in advanced reactors include:

- Task 1 (PLANT BOUNDARY DEFINITION AND PARTITIONING): Some of the advanced reactor designs will be utilized in connection with a hydrogen production facility. There is a decision to be made in regard to the plant boundary definition. The decision is whether to consider the hydrogen production facility inside the boundary definition of the nuclear power plant or to consider it as an external hazard source. This might affect the method of analysis.
- Task 2 (FIRE PRA COMPONENTS SELECTION): it was stated in NUREG/CR-6850 that "Because a key emphasis of the Fire PRA Component List is to identify and track relevant cables in Task 3 that could be affected by fires in the plant, the list need not contain passive/mechanical equipment (i.e., non-electrical components) deemed by the analyst to be unaffected by fires." It is important that care shall be taken when identifying the components that might be affected by fire

in advanced reactors. For example, in the case of sodium fires with high temperatures, the structures such as pipes might be affected, unlike the cases considered before in the analysis of LWRs. This might be overlooked by the analysts due to their pre-existing assumptions derived from their experience in previous generations of reactors where these assumptions held true. Also, care should be taken by the analysts in performing this task since the task is only concerned with equipment identification, but in advanced reactors, fires might affect not only equipment but also the assumed conditions for some of the reactor systems. This is better explained by the effects of fires on the ultimate heat sink temperature assumed for a passive decay heat system to deliver its function. A new category may be added for components that might not cause initiating events but are important as barriers to limit radioactive releases.

- Task 5 (FIRE-INDUCED RISK MODEL): This task relies on the Internal Events PRA models. As discussed in task 2, there might be a new criterion for the selection of important equipment to be considered in the fire PRA. So, the analyst should verify that the PRA logic model reflects, as intended, the effects of fire-induced equipment failures.
- Task 6 (FIRE IGNITION FREQUENCIES): as commented previously, the new types or configurations of ignition sources are not listed in the NUREG/CR-6850 ignition frequency bins. The estimation of the ignition frequencies might represent a challenge due to the lack of historical data.
- Task 8 (SCOPING FIRE MODELING): In NUREG/CR-6850 it states that "A set of conservative fire modeling calculations are performed for predicting fire conditions near a target in order to assess if target damage or ignition can occur. The analyst can then be confident that an ignition source can be screened out if no relevant targets receive thermal damage." As explained in this report, the new ignition sources might introduce effects other than the thermal effects that are damaging. Consideration of these effects is important in the analysis of some advanced reactors such as sodium reactors. The analyst should not consider thermal damage as the sole reason for component damage. Changing the damage criteria, in turn, might also affect the calculations of severity factors used to update the ignition frequencies calculated in task 5. Additionally, Table 8-1 in NUREG/CR-6850 recommends Zone of Influence (ZOI) and severity factor calculation methods for the ignition sources listed in NUREG/CR-6850. Some of these methods might not be based on fire modeling. The applicability of these methods shall be validated for the use of ZOI calculations for new ignition sources. All of the issues explained here should be considered when performing task 8 for advanced reactors containing new ignition sources not listed in NUREG/CR-6850.

- Task 11 (DETAILED FIRE MODELING): NUREG/CR-6850 states that when performing task 11 the analyst shall "Identify and characterize fire ignition sources to be analyzed in terms of location within the compartment, type, size, initial intensity, growth behavior, severity/likelihood relationship, etc." Application of the quoted statement might be challenging for advanced reactors. For example, in case of sodium fires due to sodium leakage from pipes, the location and the size of the fire are not fixed because these two characteristics depend on the location of the leak and the crack size in the pipes. Additionally, NUREG/CR-6850 states that the analyst shall "identify fire detection and suppression features such as smoke and heat detectors, continuous fire watch, automatic and manual fixed suppression systems and fire brigade capabilities." New methods or systems might be used for fire detection and suppression in advanced reactors, such as automated Firewatch and sensory detectors utilizing machine learning. Reliability calculations of these systems might be challenging to the analyst especially if these systems are new with a scarcity of available failure data. Also, new challenges might exist for the fire brigade due to the existence of new ignition sources creating hazards other than the fire risk itself. For example, sodium fires generate smoke that has dangerous chemicals and that might also contain radioactive materials that will affect the health of the fire brigade. Unlike those fires where chemical and radioactivity risks are not present, sodium fires can reduce the brigade's capabilities to handle fires efficiently. Modeling of the fire brigade capabilities to handle fires with the existence of these risks might be challenging and should be considered when performing task 11 for advanced reactors. Another quote from NUREG/CR-6850 states that "The analysis does not explicitly try to quantify the risk contribution of seismic-induced fires. Hence, the conditions that may be encountered during a post-earthquake fire are not considered in the discussions provided for fire modeling." Quantification of the risk contribution of seismic-induced fires is not considered in NUREG/CR-6850 due to the assumption that these seismic-induced fires have a very low probability. This might be true for LWRs but for sodium reactors this assumption might not be valid. This is due to the fact that seismic events can cause a crack in the pipes leading to the release of sodium which would ignite, unlike the case of a pipe break in LWRs where the coolant flowing through the pipes is water. Another concern when performing task 11 is related to fire growth and propagation analysis. Special consideration might be needed in performing this step for the ignition sources introduced in this report since the fire growth and propagation analysis codes might require some modifications to enable analysis of the new ignition sources.
- Task 12 (POST-FIRE HUMAN RELIABILITY ANALYSIS): A suggestion is provided in NUREG/CR-6850 in Task 12 about the need to account for the crew's lack of familiarity in dealing with possible fires, when compared to other internal events, in assessing the impact of training.

Similarly, for advanced reactors with new ignition sources, operators and the fire brigade might be less familiar with fighting fires from the new ignition sources, especially sodium fires, than they are with other ignition sources found in the current generation of reactors. This means that the analyst should pay attention when performing this task to consider applicability and suitability of training or experience of operators and the fire brigade.

5.4.2 Analysis of the operating conditions that differ from those of operating LWRs

Some advanced reactors operate under high temperature conditions that differ from those found in the LWRs; however, the LWR data are used as a base in the Fire PRA methodology of NUREG/CR-6850. The high operating temperatures may represent a challenge in the calculation of ignition frequency even for the same combustible materials found in current reactor designs. In other words, the ignition frequency bins found in NUREG/CR-6850 may need some modification to account for the differences in operating conditions between current designs and advanced reactor designs. Higher temperatures in advanced reactors might increase operating temperatures in the room to levels exceeding the auto-ignition temperature of exposed combustibles [78]. Other effects of higher temperatures were discussed in several references, and examples are provided in the following paragraphs.

In MSRs, there are risks of high operating temperatures and thermal inertia of the molten salts, which may originate from a primary loop leak leading to heat being transferred to combustible materials or high flashpoint fluids, causing fire and explosions. To cope with these risks, the new designs shall consider the inventories, layout, and storage arrangements of molten salts in relation to combustible materials and fluids [65]. Another risk associated with higher operating temperatures is the polymerization of lubricants leaked into the primary side leading to blockages and accumulation of fission products in filters that can result in consequential fires and activity releases due to the decay heat [65].

5.4.2.1 Potential Impacts on NUREG/CR-6850 Tasks

The examples discussed above will generate scenarios that were not previously considered when performing Fire PRA for current LWRs. This will introduce different challenges when performing several tasks of NUREG/CR-6850 for advanced reactors. Tasks of NUREG/CR-6850 affected by these new scenarios are:

- Task 5 (FIRE-INDUCED RISK MODEL): This task relies on the Internal Events PRA models. As discussed above, the different operating temperatures may generate new scenarios to be considered

in the Fire PRA; therefore, the analyst should ensure that these new scenarios are added to the PRA logic model.

- Task 6 (FIRE IGNITION FREQUENCIES): as stated above, higher operating temperatures may affect the ignition frequency of combustible materials. This should be considered by the analyst when calculating the fire ignition frequencies.
- Task 11 (DETAILED FIRE MODELING): In cases where the high temperature molten salt has leaked, combustible materials coming into contact with the leaked molten salt may ignite. Depending on the location and amount of the molten salt leak, there is a possibility that multiple ignition sources ignite simultaneously. This possibility should be considered by the analyst when performing task 11 of NUREG/CR-6850.

5.4.3 Modeling of new types of Fire PRA scenarios

Advanced reactor designs may produce fire events and scenarios not previously considered for the current generation of reactors. An example of these scenarios is associated with sodium leak events. In Appendix A of NUREG/CR-6850, it states that "sequences not very relevant to fire scenarios may be eliminated on the basis of low probability of coincidental events; for example, a fire and a loss of coolant accident (LOCA) at the same time." In contrast to what is stated in NUREG/CR-6850, in cases where there is a sodium leak, fire induced by sodium leaks should be modeled in the event trees and fault trees corresponding to the events that might cause the sodium leak. For example, if sodium is used as the coolant, a leak in sodium would mean the initiation of fires and, at the same time, a loss of coolant event.

Extra attention should be given when combustible materials are in areas where sodium leakage and fire may occur because sodium fires may spread and ignite them. Different mitigation measures are used for sodium fires than for other types of fires. Water-based sprinklers are normally used to contain fires of combustible materials; however, if this firefighting intervention method is used, the sodium will react with the water to produce enough sodium hydroxide and hydrogen gas to result in hydrogen explosions [61]. The joint occurrence of sodium fires and normal fires should be considered in the design of mitigation and suppression systems for sodium reactors and special consideration should be given to this while performing Fire PRA analysis.

Another scenario is related to seismically induced fires. Task 13 of NUREG/CR-6850 states that "This procedure does not provide a methodology for developing models and quantifying risk associated with fires caused by a severe seismic event. This is due to a combination of limitations in the state of the art and the perceived low level of risk from these fires." For LWRs, an earthquake might lead to coolant

leakage, but since the water is the coolant, the potential risk significance of seismically induced fires has generally been judged to be low. On the other hand, seismically induced fires might be of significant importance in sodium or metal cooled reactors where large-scale sodium leaks resulting from a seismic event would likely result in the initiation of fire events that can affect multiple systems. A quantification of the potential risk significance of seismically induced fires for metal cooled reactors would be required [66].

Smoke is one of the factors used in the Fire PRA analysis to judge the habitability of the MCR as well as the time to evacuate. Smoke generated as a result of fires in different reactor areas might be transferred to the MCR through the HVAC system [66]. The final decision to abandon the control room is assumed to depend on habitability conditions listed in NUREG/CR-6850. In cases where smoke generated by sodium fires is transported to the MCR, the final decision to abandon the control room must take into consideration the effects of this smoke that are not listed in the habitability conditions in NUREG/CR-6850. An example of one such effect is that the smoke from sodium fires might be toxic and radioactive, which may pose significant challenges to MCR habitability.

Another scenario is related to multi-compartment analysis. The compartment boundaries in Fire PRA are defined by the fire barriers that can prevent the fire spread to other compartments. As stated in NUREG/CR-4840, “the analyst may use a screening barrier failure probability of 0.1. For scenarios that do not screen out, a more realistic barrier failure probability may be used.” In the design of barriers in lead-fast reactors, consideration should be given to the potential for high mechanical loadings from molten lead releases and the rate of temperature rises on the ‘back face’ of fire barriers. [65] state that releases of molten lead at a primary circuit temperature of ~ 500 ºC may result in unacceptably high temperatures on the other side of barriers. These mechanical loads and higher temperatures might affect the failure probability of the barriers indicated in NUREG/CR-4840. These effects should be considered by the analyst when performing Fire PRA for multi-compartments. Also, for SMRs, considering the relatively smaller footprint, the fire load densities may be higher than those of current conventional reactors. This means that the fire dynamics, considering the smaller floor areas, may result in having a higher heat impact on fire barriers [78].

In advanced reactors, there are some latent issues that can pose risks that will not be immediately apparent. An example of these risks is that sodium metal aerosols can be deposited in cold spots during normal operation where inert gas is present. These deposits will not ignite directly because of the existence of the inert gas. Later, during post operation, for example, several areas of the reactor may return to an air atmosphere, with the associated increased risk of fire initiation. Inspection and maintenance on sodium fast reactor components may require cleanout of this residual [65]. This issue introduces a new scenario that

was not previously considered but should be when performing Fire PRA, especially during plant shutdown and maintenance phases.

Tasks of NUREG/CR-6850 that will be affected by the new scenarios and associated modeling challenges include:

- Task 2 (FIRE PRA COMPONENTS SELECTION): as indicated above, new scenarios might be introduced in advanced reactors. Analysts should consider all the possible scenarios in order not to overlook any important component during the Fire PRA analysis. Additionally, when performing this task, the analyst should not focus on components alone. Instead, consideration should be given to the assumed conditions for the reliable operation of safety related systems.
- Task 5 (FIRE-INDUCED RISK MODEL): This task relies on the Internal Events PRA models. As discussed above, scenarios that are new and were not previously analyzed may exist for advanced reactors; therefore, the analyst should ensure that the new scenarios are added to the PRA logic model.
- Task 11 (DETAILED FIRE MODELING): The detailed fire modeling for the new scenarios, such as the scenarios cited in this report, may represent a challenge for the analyst.

5.4.4 Modeling of Passive Safety Systems

Care shall be taken by the analyst in performing Task 2 of NUREG/CR-6850 when identifying important components to be considered in Fire PRA analysis. The task is only concerned with equipment identification but, in advanced reactors, fires might affect not only equipment but also assumed conditions for some of the systems utilized in advanced reactors. Specific examples include the fire potential related to the liquid metal and graphite and the effects of these fires on the passive safety systems. An example of this would be when a fire occurs, there is an increase in the temperature of the ultimate heat sink which causes a decrease in the reliability of passive decay heat removal systems. Identification of potential side effects or failures of the passive systems, as a result of fires, will be necessary [66, 79, 80]. Both internal and external fires can affect passive safety systems. JAEA has developed a safety design approach to external hazards for sodium fast reactors. One external hazard analyzed was forest fire and a new methodology was developed to assess forest fire hazards on a decay heat removal function. The methodology is based on two parts - the first part is concerned with the development of a hazard curve that maps the intensity of the hazard with the frequency of the hazard and the second part is concerned with the effects of forest fire on the reliability of the decay heat removal function of an SFR reactor. An example of the effects of forest fire on the decay heat removal function is the air temperature (ultimate heat sink) and

the existence of smoke and debris that may block the air flow filters, adversely affecting the system's ability to function [81-85]. Also, serious concerns are being raised after the Fukushima accident regarding external hazards in the safety of NPPs. In their study, [85] identified combinations of hazards, if occurring in specific order, that can damage the air cooler for decay heat removal of an SFR. External fire was one of the hazards analyzed in their study. The authors suggest that the procedures developed for the analysis will be applicable to other passive safety systems as well.

Tasks of NUREG/CR-6850 affected by the issues included in this section are:

- Task 5 (FIRE-INDUCED RISK MODEL): the existence of passive safety systems in advanced reactors will introduce new criteria for the selection of important equipment to be considered in the Fire PRA. So, the analyst should verify that the PRA logic model reflects, as intended, the fire-induced effects on the reliability of the passive safety systems.
- Task 11 (DETAILED FIRE MODELING): this task is related to fire modeling and simulation in order to calculate the failure probability of targets due to a given fire. The failure probability of a target is calculated by comparing the temperature at the target location with a predetermined threshold temperature above which damage will occur to the target. For some passive safety systems, the situation is somewhat different. For example, for the passive decay heat removal system, we are interested in the ultimate heat sink temperature. Due to fire initiation, the room temperature will vary depending on the distance from the fire source and the height of the room. This would mean that the temperature to be used in the calculation of the reliability of the decay heat removal system is a variable and not a constant across the room. This is something the analyst should take into consideration during the detailed fire modeling stage.

5.4.5 Analysis of radioactive inventories outside of the reactor core

Chisholm et al. [68] speak of the possibility of the existence of significant inventories of radioactive materials in locations other than reactor core or primary cooling systems, for example, in the MSRE off-gas and in the MSRE fuel salt processing systems. In the case of sodium fires, even if the fires do not lead to core damage, if the sodium vapor generated from the fires is released into the environment, it can become a source term and could represent a health threat to the general public [63, 66].

Since the final aim of PRA is to calculate the frequency of release of radioactivity into the environment, PRA analysis should include other initiating events that might cause a radioactive release from inventories other than the inventories commonly analyzed, such as reactor core. The link of this to

fire PRA can appear during the partitioning tasks and screening of ignition sources and compartments. For example, if the existence of these inventories is not considered by the Fire PRA analyst, the compartments that include these inventories might be screened out.

Tasks of NUREG/CR-6850 affected by the issues named in this section include:

- Task 2 (FIRE PRA COMPONENTS SELECTION): since advanced reactors may contain radioactive inventories outside of the reactor core and the primary system, the focus of the analyst when performing task 2 of NUREG/CR-6850 should shift from "components important to prevent core damage" to "components important to prevent radioactive releases." As indicated in section 2 of this report, some advanced reactors do not even consider core damage frequency as an applicable end state for PRA analysis. An example of such an advanced reactor is the HTR-PM reactor.
- Task 4 (QUALITATIVE SCREENING): the analyst should be vigilant and not screen out any compartment that contains radioactive inventories that could be released due to a fire.
- Task 5 (FIRE-INDUCED RISK MODEL): This task relies on the Internal Events PRA models. PRA analysis of the current generation of reactors utilizes core damage as an end state. Due to the existence of radioactive inventories outside the reactor core, other end states have been utilized by some advanced reactors. During the development of the fire-induced risk models, the analyst may need to consider new event trees with new end states not usually considered in the current generation of reactors.
- Task 7 (QUANTITATIVE SCREENING): the screening criteria in NUREG/CR-6850 is based on the CDF value, while some advanced reactors have different end states which may require new screening criteria.

5.4.6 Inapplicability of the existing LWR data and assumptions

Since the methodologies and data provided in NUREG/CR-6850 are based on the experience of LWRs inside the USA, some challenges and issues may arise when using the data in NUREG/CR-6850 for advanced reactors. Examples of such challenges are provided below:

- The list of MSOs provided in NUREG-CR-6850 is based on LWR experience in the U.S [86]. This list might need some modifications for new designs to identify any possibilities for MSO scenarios that might not have been identified.
- In NUREG/CR-6850, failure modes of electrical circuits are screened out based on the electrical design standards followed by U.S industry. For example, 3-phase proper polarity hot shorts on

grounded three-phase AC power systems [86]. The electric circuit design in new advanced reactors shall be reviewed against the assumptions listed in NUREG/CR-6850.

- Generic fire ignition frequencies listed in NUREG/CR-6850 are influenced by the design, maintenance, and practice in U.S. industry that operates under a specific set of rules and requirements [86]. Any deviations in these rules and requirements might have an impact on the ignition frequencies for fixed and transient ignition sources. An example of such practices that can affect the ignition frequency is housekeeping.
- Applicability of Heat Release Rates (HRRs) provided in the NUREG/CR-6850 should be verified before utilization for advanced reactors, considering deviations in combustible loading, configuration, ventilation, and cable materials from those used in the generation of HRR data in NUREG/CR-6850 [86].
- An investigation should be performed to find any significant deviations that could render the use of cable damage criteria provided in NUREG/CR-6850 invalid for advanced reactors. For example, the generic bin for the control room is assumed to be applicable to the main control room for some advanced reactors even though the main control room design may be completely digital as opposed to the traditional electromechanical design [52].
- Lack of plant-specific information during the design phase and lack of operational experience are common issues for advanced reactors [52]. Based on Ref. [87], pilot studies were being performed for: HTR-PM, Power Reactor Innovative Small Module (PRISM), Traveling Wave Reactor, ANL/KAERI Sodium Cooled Fast Reactor, Xe-100 HTGR, and MCFR. Lack of design and operational details for pre-operational PRA development and lack of experience with non-LWR PRA were some of the challenges faced by these pilot projects. Since some of the information required for Fire PRA quantification may not be available for advanced reactors, especially in early stages of the design and licensing, analysts may limit the scope of the Fire PRA to some parts of the internal events PRA. Exclusion of or not crediting certain equipment might sometimes lead to a nonconservative result. This is a very important point since some advanced designs might adopt the conservative assumption of not crediting many components, leading to an insufficient analysis that might miss important sequences.

NUREG/CR-6850 tasks affected with the issues cited above include:

- Task 1 (PLANT BOUNDARY DEFINITION AND PARTITIONING): As stated in NUREG/CR-6850, this task requires “substantial knowledge of the plant layout, the characteristics of compartment boundary elements, and the general location of plant systems and equipment.” This

information might not be available during the design stage for advanced reactors. It was also specified in NUREG/CR-6850 that "Partitioning decisions should not, however, be finalized until one or more confirmatory walkdowns have been performed." This may not be possible during the design and licensing stages, which would represent a challenge for the analysts.

- Task 6 (FIRE IGNITION FREQUENCIES): NUREG/CR-6850 states that "at least one walkdown of the entire plant or unit is recommended to identify ignition sources in each fire compartment identified in Task 1, map the components to the frequency bins of Table 6-1, facilitate the equipment count and identify their locations." This may not be possible during the design and licensing stages for advanced reactors. Also, the generic fire ignition frequencies in NUREG/CR-6850 reflect the fire protection and housekeeping practices of the nuclear industry in the United States. Quoted from NUREG/CR-6850: "The generic frequency model utilizes fire location/ignition source bins to estimate fire ignition frequencies. Each bin represents a set of operating experience events at a particular location/ignition source in U.S. NPPs." Based on the above statement, an update of the frequencies provided in NUREG/CR-6850 may be required if these frequencies are to be utilized for advanced reactors located outside of the USA. If these frequencies are to be used for advanced reactors, protection and housekeeping practices for these advanced designs should not deviate from the industry standards. Additionally, Section 6.5.4 in NUREG/CR-6850 is related to mapping plant-specific locations to generic locations. The tagging and location mapping might be difficult for advanced reactors since the design of these reactors may deviate significantly from LWR designs and that will introduce new locations and systems not previously considered in the analysis of LWRs.
- Task 11 (DETAILED FIRE MODELING): as stated in NUREG/CR-6850, it is recommended that the analyst verify that the parameters influencing the HRR are appropriate for the scenarios being analyzed before using the HRRs provided in NUREG/CR-6850. Another issue regarding task 11 is related to fires in the MCR. In modeling fires in the MCR, the data provided in NUREG/CR-6850 is based on a probabilistic model presented in Appendix L. This model is based on information obtained from EPRI's Fire Events Database and a series of cabinet fire experiments reported in NUREG/CR-4527. If the data listed in NUREG/CR-6850 is to be used for advanced reactors, the analyst should verify that the cabinet configurations and loads are the same as those in the experiments used to generate the data. Regarding the modeling of the detection and suppression of fires, it is worthwhile noting that the data provided in NUREG/CR-6850 consists of reported fire response durations in commercial U.S. NPPs. The non-suppression probability curves in NUREG/CR-6850 may not be applicable to advanced reactors due to several factors, such as the

use of new detection and suppression systems (e.g., automated fire watch), different fire brigade capabilities in countries outside of the USA, and the fact that the data of events used to generate non-suppression probability curves in NUREG/CR-6850 do not include information on sodium or newly introduced ignition source fires.

5.5 Summary

In Task 3 of the project, a literature review and gap analysis have been performed to determine the applicability, challenges, gaps, and special considerations when applying current Fire Probabilistic Risk Assessment methodologies for quantifying fire risks in advanced reactors. A literature review is completed on Fire PRA for advanced reactors, and the methodology for the literature review is explained. A discussion of the references found is provided, and this discussion focuses on comparing the methodology used for Fire PRA with the methods suggested by NUREG/CR-6850 in order to identify all the assumptions used and understand all the difficulties faced by the analysts in applying Fire PRA for advanced reactor designs. The literature also covers other issues related to fire risk in advanced reactors and the connection of these issues with Fire PRA was established. During the literature review, it showed that there was a very wide range of advanced reactor designs in different areas of the world. Most of these designs are not mature and neither internal events PRA nor Fire PRA were performed for them. A lot of assumptions were used in the surveyed references to cover for the lack of the data which decreases the realism of the analysis and might skew the insights driven from the PRA analysis. Also, some of these assumptions might not actually be valid and further evaluation and research might be needed (for example, the calculation of ignition frequencies for sodium fires).

In this chapter, differences between current reactors and advanced reactors that might affect Fire PRA are discussed in detail with specific examples provided for each difference. Based on the discussion, it is concluded that several challenges would exist in Fire PRA for advanced reactors and that, in their current form, some of the tasks in NUREG/CR-6850 may be challenging or require caution if they are to be applied for conducting Fire PRA for advanced reactors. In general, the applicability of the current Fire PRA methodology for advanced reactors would be questioned (i) if the fire phenomena and their impact on structures, systems, and components (SSC) involve the underlying physical processes and human action different from those of the existing plants, or (ii) if the Fire PRA data collected from the current reactors (e.g., historical fire event database, manual suppression data) have a low level of relevancy.

The research team has identified that the I-PRA methodology developed in this project could contribute to the risk-informed design and licensing of advanced reactors in multiple ways, for instance:

- The Fire RoverD methodology developed in Phase I (Chapter 2 of this report) can help increase the confidence in the Licensing Basis Events (LBEs) selection. This is because Fire RoverD provides a coherent quantitative screening mechanism to screen out non-significant scenarios using the combination of deterministic and risk-informed analyses. While qualitative methods such as Failure Mode and Effect Analysis (FMEA) and Hazard and Operability Study (HAZOP) can identify a complete set of potential LBEs, the RoverD methodology can provide a risk-informed, quantitative way to screen out non-significant LBEs. The iterative procedure of RoverD, where the degree of realism is gradually increased, can facilitate the design process of advanced reactors, where the safety analyses should be progressively refined as more data and insights become available.
- The SoTeRiA-Fire computational tool developed in Phase II (Chapter 3 of this report) can help conduct a detailed analysis of fire scenarios while balancing the realism of the fire scenario analysis with the availability of design data and the resources required for the analysis. As highlighted in Section 5.4, advanced reactors may introduce new ignition sources that do not exist in the operating reactors. Additionally, new fire-induced failure modes for hardware equipment and human action could be caused by the new ignition sources at advanced reactors. In such cases, higher resolution models, e.g., a CFD-based fire model, might be required, instead of relying on the existing data-driven models such as engineering correlations; however, the use of high-resolution models in PRA could be challenging for advanced reactors (especially in the design and licensing phases) due to lack of detailed design data and the need for quick results for iterative design processes. SoTeRiA-Fire, developed in Phase II, provides an automated process for using simulation models in support of Fire PRA while reducing data requirements and analysis burdens using scientifically justified conservative simplifications in inputs and modeling assumptions.
- Phase III of this project can address the second challenge mentioned above, i.e., how test data and operational experience from existing reactors can be leveraged for risk-informed analysis of advanced reactors. In the current Fire PRA methodology, the fire crew performance in manual suppression is credited using a non-suppression curve derived from the Fire Event Database collected from the existing plants. However, the data-driven non-suppression curve may not be fully applicable to advanced reactors due to design-specific conditions and procedures different from the operating plants. In such a situation, the advanced fire crew model, developed in the Fire I-PRA framework, can help understand how the design-specific conditions and procedures can impact the fire crew's performance. One of the critical challenges is the validation of the fire crew model, provided that the design-specific operating experience is unavailable or quite limited for advanced reactors. To address this challenge, Phase III of this project has conducted a fire crew

performance test and demonstrated how the limited test data could be utilized to evaluate the validity of the simulation model using the uncertainty quantification-based method.

Page intentionally left blank

6. Conclusion

The objective of this project is to improve the operational efficiency of Nuclear Power Plants (NPPs) by improving the realism of Fire Probabilistic Risk Assessment (PRA). Co-PI Mohaghegh and her team, in previous work to enhance the Fire PRA realism associated with fire progression and damage modeling and the modeling of interactions between fire progression and manual suppression, developed an Integrated PRA (I-PRA) methodological framework [2, 3]. This latest academia-industry collaboration project advances the Fire I-PRA methodological framework, focuses on the current Fire PRA challenges in the nuclear industry, and scales up Fire I-PRA to a full-scope plant. In this report, a comprehensive description of the work conducted is provided, including theoretical bases, methodologies, results, and products.

In order to enhance the methodological and practical values of Fire I-PRA, this Department of Energy (DOE)-funded academic-industry project, in collaboration with South Texas Project Nuclear Operating Company (STPNOC), started in 2019. This project has been conducted in three phases:

Phase I focuses on developing a streamlined approach to perform more efficient screening of fire zones and ignition sources in Fire PRA (Chapter 2 of this report). The RoverD methodology for Fire PRA (Fire-RoverD) is developed, including a theoretical basis and an algorithm for practical implementation. The Fire-RoverD methodology is mapped to the NUREG/CR-6850 procedure to demonstrate that Fire-RoverD can be seamlessly merged with the current Fire PRA procedure. The implementation of the Fire-RoverD methodology is demonstrated by case studies using two fire zones at South Texas Project Nuclear Operating Company (STPNOC).

Phase II consists of two tasks:

- For the first part, based on the discussion among the research team and the communication with a contractor of the parallel STPNOC Fire PRA Upgrade project (Jensen-Hughes), an enhancement of the Multi-Compartment Analysis (MCA) for Plant Analysis Units (PAUs) involving transient ignition sources has been selected as the primary scope. A methodological and computational platform called, “SoTeRiA-Fire,” is developed to automate the Fire Scenario Selection and Analysis (FSS) supporting MCA in the Fire PRA of NPPs (Chapter 3 of this report). Although SoTeRiA-Fire reflects the guidelines of NUREG/CR-6850 and ASME/ANS RA-Sa-2009, it can help NPP reduce resources required for Fire PRA implementation by (a) automating the pre-processing of input data, execution of a fire model, and post-processing of outputs for various tasks in the FSS and (b) providing a mechanism to gradually increase the realism of FSS while screening

out insignificant scenarios. The fire hazard propagation event tree in SoTeRiA Fire includes multiple pivotal events: (1) initial fire ignition, (2) ignition of secondary combustibles and fire spread, (3) formation of damaging conditions for target equipment and cables, (4) failure of detection and suppression systems in the exposing compartment containing the initial fire source, (5) failure of fire barriers, and (6) failure of a suppression system in the exposed compartment. The SoTeRiA-Fire assembles the input parameters, conducts required input data processing, and constructs the input files for the Consolidated Model of Fire and Smoke Transport (CFAST) fire simulation program. It then analyzes various combinations or ranges of key input parameters based on the fire propagation event tree logic and prepares the outputs to be post-processed for FSS. The applicability and practical values of the SoTeRiA-Fire computational tool are demonstrated by case studies for two PAUs at the STPNOC plant.

- The second part of Phase II analyzes the applicability, challenges, gaps, and special considerations when applying the existing Fire PRA methodologies, developed for light-water reactors, to advanced nuclear power reactors (Chapter 5 of this report). A systematic literature review on Fire PRA for advanced reactors is performed. A detailed review of the relevant references is performed to compile a list of the features of advanced reactors that could generate challenges when applying the current Fire PRA methodologies. The potential challenges identified in the literature review are mapped with the corresponding task(s) of the NUREG/CR-6850 procedure. As an outcome, this study provided recommendations for future work to extend the applicability of the current Fire PRA and the Fire I-PRA methodologies to advanced reactors.

Phase III performs experimental validation of an agent-based fire crew model, developed by Co-PI Mohaghegh and her team in their previous work [7]. The fire crew performance tests are conducted by leveraging the fire testing capabilities at the Illinois Fire Service Institute (IFSI). This research is the first effort to validate the probabilistic simulation of the fire crew performance at NPPs using the test data and to connect the coupled fire-human test data to the system-level PRA scenarios. As the validation methodology, this study adopts the uncertainty quantification-based approach recommended by the U.S. Nuclear Regulatory Commission (NRC) for the validation of fire models in support of Fire PRA.

6.1 Publication List

The publications generated in this project (as of March 17, 2022) are listed below.

Conference Papers:

1) Alkhatib, S., Sakurahara, T., Reihani, S., Kee, E., Ratte, B., Mohaghegh, Z., "Academia-Industry Collaboration to Advance Screening Process in Fire PRA of Nuclear Power Plants," Proceeding of the 30th European Safety and Reliability Conference (ESREL) and the 15th Probabilistic Safety Assessment and Management (PSAM) Conference. Venice, Italy, 2020.

2) Alkhatib, S., Sakurahara, T., Reihani, S., Kee, E., Mohaghegh, Z., Ratte, B., Kaspar, K., Billings, M.A., Hunt, S., "Methodological and Computational Developments for Fire Scenario Selection and Analysis in Fire PRA of Nuclear Power Plants," Full Paper Submitted to the 2021 ANS International Topical Meeting on Probabilistic Safety Assessment and Analysis (PSA 2021). Columbus, OH, November 2021.

3) Alkhatib, S., Sakurahara, T., Reihani, S., Kee, E., Ratte, B., Mohaghegh, Z., "I-PRA Risk- and Cost-Informed Decision-Making Algorithm for Nuclear Power Plants," Full Paper Submitted to the 2021 ANS International Topical Meeting on Probabilistic Safety Assessment and Analysis (PSA 2021). Columbus, OH, November 2021.

Presentations:

4) Mohaghegh, Z., Sakurahara, T., Pence, J., Kee, E., "Probabilistic Risk Assessment Research & Education at the University of Illinois Urbana-Champaign," an invited presentation at the U.S. Nuclear Regulatory Commission, Washington, D.C., November 2019.

5) Mohaghegh, Z., Sakurahara, T., Pence, J., Kee, E., Ratté, B., "UIUC SoTeRiA-IAP Fire PRA Research Overview," an invited presentation at the U.S. Nuclear Regulatory Commission, Washington, D.C., November 2019.

6.2 Other Products

- The beta version of the MCA computational tool (developed in Task 2) was released to Jensen-Hughes under a Software Evaluation License (January 2021).

Page intentionally left blank

REFERENCES

[1] Electric Power Research Institute (EPRI) and US Nuclear Regulatory Commission, "EPRl/NRC-RES Fire PRA Methodology for Nuclear Power Facilities (NUREG/CR-6850), Volume 2 - Detailed Methodology," 2005.

[2] T. Sakurahara, Z. Mohaghegh, S. Reihani, E. Kee, M. Brandyberry, and S. Rodgers, "An integrated methodology for spatio-temporal incorporation of underlying failure mechanisms into fire probabilistic risk assessment of nuclear power plants," *Reliability Engineering & System Safety,* vol. 169, pp. 242-257, 2018.

[3] H. Bui, T. Sakurahara, J. Pence, S. Reihani, E. Kee, and Z. Mohaghegh, "An algorithm for enhancing spatiotemporal resolution of probabilistic risk assessment to address emergent safety concerns in nuclear power plants," *Reliability Engineering & System Safety,* vol. 185, pp. 405-428, 2019.

[4] T. Sakurahara, Z. Mohaghegh, S. Reihani, and E. Kee, "Methodological and Practical Comparison of Integrated Probabilistic Risk Assessment (I-PRA) with the Existing Fire PRA of Nuclear Power Plants," (in English), *Nuclear Technology,* vol. 204, no. 3, pp. 354-377, 2018.

[5] T. Sakurahara, H. Bui, S. Reihani, E. Kee, and Z. Mohaghegh, "Enhancing Realism in Fire Probabilistic Risk Assessment of Nuclear Power Plants," presented at the 30th European Safety and Reliability Conference and the 15th Probabilistic Safety Assessment and Management Conference (ESREL 2020 & PSAM 15), Venice, Italy, 2020.

[6] T. Sakurahara, Z. Mohaghegh, and E. Kee, "Human Reliability Analysis (HRA)-Based Method for Manual Fire Suppression Analysis in an Integrated Probabilistic Risk Assessment," *ASCE-ASME J Risk and Uncert in Engrg Sys Part B Mech Engrg,* vol. 6, no. 1, p. 011010, 2020.

[7] H. Bui, T. Sakurahara, S. Reihani, E. Kee, and Z. Mohaghegh, "Spatiotemporal Integration of an Agent-Based First Responder Performance Model with a Fire Hazard Propagation Model for Probabilistic Risk Assessment of Nuclear Power Plants," *ASCE-ASME J Risk and Uncert in Engrg Sys Part B Mech Engrg,* vol. 6, no. 1, 2020.

[8] T. Sakurahara, S. Reihani, E. Kee, and Z. Mohaghegh, "Global importance measure methodology for integrated probabilistic risk assessment," *Proceedings of the Institution of Mechanical Engineers, Part O: Journal of Risk and Reliability,* vol. 234, no. 2, pp. 377-396, 2020.

[9] H. Bui, T. Sakurahara, S. Reihani, J. Biersdorf, and Z. Mohaghegh, "Integrated Probabilistic Risk Assessment (I-PRA) Importance Ranking for Fire PRA of Nuclear Power Plants," presented at the American Nuclear Society (ANS) Winter Meeting, Washington, D.C., 2019.

[10] Bui H, Sakurahara T, Reihani S, Biersdorf J, and M. Z, "I-PRA Uncertainty Importance Ranking to Enhance Fire PRA Realism for Nuclear Power Plants," presented at the American Nuclear Society (ANS) Winter Meeting and Technology Expo, Virtual Conference, 2020.

[11] F. Nmira, J. L. Consalvi, A. Kaiss, A. C. Fernandez-Pello, and B. Porterie, "A numerical study of water mist mitigation of tunnel fires," *Fire Safety Journal,* vol. 44, no. 2, pp. 198-211, 2009.

[12] E. Kee, J. Hasenbein, A. Zolan, P. Grissom, S. Reihani, Z. Mohaghegh, F. Yilmaz, B. Letellier, V. Moiseytseva, R. Vaghetto, D. Imbaratto, and T. Sakurahara, "RoverD: Use of Test Data in GSI-191 Risk Assessment," *Nuclear Technology,* vol. 196, no. 2, pp. 270-291, 2017.

[13] P. Farshadmanesh, T. Sakurahara, S. Reihani, E. Kee, and Z. Mohaghegh, "SHAKE-RoverD Framework for Nuclear Power Plants: A Streamlined Approach for Seismic Risk Assessment," *Nuclear Technology,* vol. 205, no. 3, pp. 442-463, 2018.

[14] S. Alkhatib, T. Sakurahara, S. Reihani, E. Kee, B. Ratte, and Z. Mohaghegh, "Academia-Industry Collaboration to Advance Screening Processes in Fire PRA of Nuclear Power Plants," in *30th European Safety and Reliability Conference & 15th Probabilistic Safety Assessment and Management Conference (ESREL2020 & PSAM15)*, Venice, Italy, 2020.

[15] N. Siu, K. Coyne, S. Sancaktar, and N. Melly, "Fire PRA Maturity and Realism: A Discussion and Suggestions for Improvement," in *American Nuclear Society 2015 International Topical Meeting on Probabilistic Safety Assessment and Analysis (PSA 2015)*, Sun Valley, ID, 2015.

[16] N. Siu, K. Coyne, and N. Melly, "Fire PRA Maturity and Realism: A Technical Evaluation (A Technical Opinion Paper)," 2016, Available: https://www.nrc.gov/docs/ML1602/ML16022A266.pdf.

[17] J. Chapman, "Seeking Realism in Fire PRA," in *American Nuclear Society 2013 International Topical Meeting on Probabilistic Safety Assessment and Analysis (PSA 2013)*, Columbia, SC, 2013.

[18] R. Peacock, G. Forney, P. Reneke, R. Portier, and W. Jones, "CFAST, the Consolidated Model of Fire Growth and Smoke Transport," in "NIST Technical Note (Report Number 1299)," National Institute of Standards and Technology, Gaithersburg, MD, 1993.

[19] Electric Power Research Institute, "Fire-Induced Vulnerability Evaluation (FIVE), REV 2," 2014.

[20] L. Y. Chen, W. Zhu, X. Cai, L. W. Pan, and G. X. Liao, "Experimental study of water mist fire suppression in tunnels under longitudinal ventilation," *Building and Environment,* vol. 44, no. 3, pp. 446-455, 2009.

[21] G. P. Forney, "Smokeview (Version 6)-A Tool for Visualizing Fire Dynamics Simulation Data Volume III: Verification Guide," 2013.

[22] L. M. Yuan and A. C. Smith, "Numerical modeling of water spray suppression of conveyor belt fires in a large-scale tunnel," *Process Safety and Environmental Protection,* vol. 95, pp. 93-101, May 2015.

[23] Y. M. Ferng and C. H. Liu, "Numerically investigating fire suppression mechanisms for the water mist with various droplet sizes through FDS code," *Nuclear Engineering and Design,* vol. 241, no. 8, pp. 3142-3148, 2011.

[24] US Nuclear Regulatory Commission, "FAQ 08-0043, Location of Fires within Electrical Cabinets," 2009.

[25] M. Gupta, A. Pasi, A. Ray, and S. R. Kale, "An experimental study of the effects of water mist characteristics on pool fire suppression," *Experimental Thermal and Fluid Science,* vol. 44, pp. 768-778, Jan 2013.

[26] ASME/ANS, "Standard for Level 1/large early release frequency probabilistic risk assessment for nuclear power plant applications (Addenda to ASME/ANS RA-S–2008)," *ASME/ANS RA-Sa-2009,* 2009.

[27] K. McGrattan, S. Hostikka, R. McDermott, J. Floyd, C. Weinschenk, and K. Overholt, "Fire dynamics simulator user's guide," *NIST special publication,* vol. 1019, no. 6, 2013.

[28] A. Lindeman and M. H. Salley, "Refining And Characterizing Heat Release Rates From Electrical Enclosures During Fire (RACHELLE-FIRE) Volume 1: Peak Heat Release Rates and Effect of Obstructed Plume, Final Report (NUREG-2178 Volume 1, EPRI 3002005578)," U.S. Nuclear Regulatory Commission and Electric Power Research Institute2016.

[29] U.S. Nuclear Regulatory Commission Office of Nuclear Regulatory Research (RES) and Electric Power Research Institute (EPRI), "Methodology for Modeling Transient Fires in Nuclear Power Plant Fire Probabilistic Risk Assessment (NUREG-2233/EPRI 3002018231)," 2020.

[30] R. D. Peacock, W. Jones, P. Reneke, and G. Forney, "CFAST–Consolidated Model of Fire Growth and Smoke Transport (Version 6) User's Guide," *NIST Special Publication,* vol. 1041, 2005.

[31] K. McGrattan, A. Lock, N. Marsh, M. Nyden, S. Bareham, M. Price, A. B. Morgan, M. Galaska, K. Schenck, and D. Stroup, "Cable Heat Release, Ignition, and Spread in Tray Installations During Fire (CHRISTIFIRE) Phase 1: Horizontal Trays," NUREG/CR-7010, Vol. 1, Office of Nuclear Regulatory Research, 2012.

[32] M. H. Salley and A. Lindeman, "Verification and Validation of Selected Fire Models for Nuclear Power Plant Applications: Final Report (NUREG-1824, Supplement 1)," 2016.

[33] M. H. Salley and R. Wachowiak, "Nuclear Power Plant Fire Modeling Analysis Guidelines (NPP FIRE MAG) Final Report (NUREG-1934, EPRI 1023259)," 2012.

[34] N. Melly and A. Lindeman, "Nuclear Power Plant Fire Ignition Frequency and Non-Suppression Probability Estimation Using the Updated Fire Events Database-United States Fire Event Experience Through 2009 (NUREG-2169, EPRI 3002002936)," 2015.

[35] M. Salley and A. Lindeman, "Methodology for Modeling Fire Growth and Suppression Response for Electrical Cabinet Fires in Nuclear Power Plants (NUREG-2230, EPRI 3002016051)," U.S. Nuclear Regulatory Commission, Washington, D.C., 2020.

[36] U.S. Nuclear Regulatory Commission, "FAQ-16-0011: Cable Tray Ignition," Washington, D.C., 2016.

[37] U.S. Nuclear Regulatory Commission and Electric Power Research Institute, "Refining and Characterizing Heat Release Rates from Electrical Enclosures During Fire (RACHELLE-FIRE), Volume 2: Fire modeling guidance for electrical cabinets, electric motors, indoor dry transformers, and the main control board (NUREG-2178 and EPRI 3002016052, Volume 2)," 2019.

[38] US Nuclear Regulatory Commission, "Nuclear Power Plant Fire Modeling Analysis Guidelines (NPP FIRE MAG)," *NUREG-1934,* 2012.

[39] K. McGrattan and B. Toman, "Quantifying the predictive uncertainty of complex numerical models," *Metrologia,* vol. 48, no. 3, p. 173, 2011.

[40] R. I. Hammoud, *Passive eye monitoring: Algorithms, applications and experiments*. Springer Science & Business Media, 2008.

[41] L. Cao, G. A. Davis, S. Gallagher, M. C. Schall Jr, and R. F. Sesek, "Characterizing posture and associated physiological demand during evacuation," *Safety science,* vol. 104, pp. 1-9, 2018.

[42] T. Jin, "Visibility through fire smoke-part 5, allowable smoke density for escape from fire," *Report of Fire Research Institute of Japan,* no. 42, p. 12, 1976.

[43] T. Yamada and Y. Akizuki, "Visibility and human behavior in fire smoke," in *SFPE handbook of fire protection engineering*: Springer, 2016, pp. 2181-2206.

[44] D. A. Faux and J. Godolphin, "Manual timing in physics experiments: error and uncertainty," *American Journal of Physics,* vol. 87, no. 2, pp. 110-115, 2019.

[45] Office of the Federal Register, " U.S. code of federal regulations, title 10 (Energy), Appendix R to Part 50 (fire protection program for nuclear power facilities operating prior to January 1, 1979)," 1980.

[46] IAEA. Advanced Reactors Information System (ARIS) [Online]. Available: https://aris.iaea.org/sites/overview.html

[47] K. Kim, S. Han, and K. Lee, "A Preliminary Fire PSA on PGSFR," in *Transactions of the Korean Nuclear Society Spring Meeting*, Jeju, Korea, 2017.

[48] K. Kim, S. Han, and K. Lee, "A level 1 fire PRA on PGSFR," in *14th Probabilistic Safety Assessment & Management Conference (PSAM 14)*, Los Angels, CA, 2018.

[49] K. Kim, S. h. Han, and K. L. Lee, "Sensitivity Analysis in Fire PSA on PGSFR," in *Transactions of the Korean Nuclear Society Spring Meeting*, Jeju, Korea, 2018.

[50] S. A. Eide, S. V. Chmielewski, and T. D. Swantz, "Generic, Component Failure Data Base for Light Water and Liquid Sodium Reactor PRAs (EGG-SSRE-8875)," Idaho National Laboratory, Idaho Falls, ID, 1990.

[51] W. Song, H. Yang, C. Zhang, and J. Zuo, "Discussion on the Application of Fire Probability Safety Assessment to Sodium Cooled Fast Reactor," in *21st International Conference on Nuclear Engineering (ICONE 21)*, Chengdu, China, 2013: American Society of Mechanical Engineers (ASME).

[52] W. Wang, J. Tong, and J. Zhao, "Application of NUREG/CR-6850 to the Fire Risk Quantification of a High Temperature Gas-Cooled Reactor," *Nuclear Engineering and Design,* vol. 330, pp. 332-343, 2018.

[53] J. Tong, J. Zhao, T. Liu, and D. Xue, "Development of Probabilistic Safety Assessment with respect to the first demonstration nuclear power plant of high temperature gas cooled reactor in China," *Nuclear Engineering and Design,* vol. 251, pp. 385-390, 2012.

[54] D. I. Kang and Y. H. Jin, "Applications of hybrid fire PSA approaches to the SMART," in *Transactions of the Korean Nuclear Society Autumn Meeting*, Gyeongju, Korea, 2011.

[55] D. I. Kang and S. H. Han, "Development of the IPRO-zone for Fire PSA and Its Applications," in *International Congress on Advances in Nuclear Power Plants 2012 (ICAPP 2012)*, Chicago, IL, 2012.

[56] D. I. Kang, S. H. Han, and S. Y. Yoo, "Development of the IPRO-ZONE for internal fire probabilistic safety assessment," *Nuclear Engineering and Design,* vol. 257, pp. 72-78, 2013.

[57] J. H. Park, Y. H. Jung, J. H. Cho, Y. H. Lee, and J. K. Han, "Status of SMART PPE PSA," in *Transactions of the Korean Nuclear Society Spring Meeting*, Jeju, Korea, 2019.

[58] NuScale Power LLC, "NuScale Standard Plant Design Certification Application: NuScale Final Safety Analysis Report Rev 5," 2020.

[59] D. Pyron, "Safety analysis for the licensing of molten salt reactors," *Paul Scherrer Institute,* 2016.

[60] B. Yuan, L. Song, K. M. Liew, and Y. Hu, "Mechanism for increased thermal instability and fire risk of graphite oxide containing metal salts," *Materials Letters,* vol. 167, pp. 197-200, 2016.

[61] M. R. Denman, J. Brown, A. S. Goldmann, and D. Louie, "Regulatory Cross-Cutting Topics for Fuel Cycle Facilities (SAND2013-9367)," Albuquerque, NM, 2013.

[62] P. W. Humrickhouse, "HTGR Dust Safety Issues and Needs for Research and Development (INL/EXT-11-21097)," Idaho National Laboratory, Idaho Falls, ID, 2011.

[63] Eduful.J, Bounagui.A, and Shalabi.H, "Overview of Liquid Sodium Fires: A Case of Sodium-Cooled Fast Reactors " presented at the the 25th International Conference on Structural Mechanics in Reactor Technology (SMiRT 25) – 16th International Post Conference Seminar on Fire Safety in Nuclear Power Plants and Installations, Ottawa, Canada, 2019.

[64] A. Katoh, Y. Chikazawa, T. Yamamoto, S. Ohno, S. Kubo, H. Sakaba, Y. Akiyama, and M. Iwasaki, "Evaluation of sodium combustion in the JSFR SCCV," in *International Congress on Advances in Nuclear Power Plants: Nuclear Power - A Safe and Sustainable Choice for Green Future, ICAPP 2013, Held with the 28th KAIF/KNS Annual Conference*, 2013, pp. 960-968: Korean Nuclear Society.

[65] D. F. Lisbona and G. Williams, "Fire and Explosion Hazards in Advanced Nuclear Reactor Technologies: Regulatory Insights from the United Kingdom," presented at the 25th International Conference on Structural Mechanics in Reactor Technology (SMiRT 25) – 16th International Post Conference Seminar on Fire Safety in Nuclear Power Plants and Installations, Ottawa, Canada, 2019.

[66] T. J. Olivier, R. F. Radel, S. P. Nowlen, T. K. Blanchat, and J. C. Hewson, "Metal Fire Implications for Advanced Reactors, Part 1: Literature Review (SAND2007-6332)," Sandia National Laboratories, Albuquerque, NM, 2007.

[67] G. Manzini, F. Parozzi, and F. Polidoro, "Fast Reactor Nuclear Power Plant Safety A Review of Sodium Release Fire Scenarios," in *Fire and Explosion Hazards: Proceedings of the Sixth International Seminar*, Leeds, UK, 2010, pp. 363-373.

[68] B. M. Chisholm, S. L. Krahn, and K. N. Fleming, "A Systematic Approach to Identify Initiating Events and Its Relationship to Probabilistic Risk Assessment: Demonstrated on the Molten Salt Reactor Experiment," (in English), *Progress in Nuclear Energy,* vol. 129, 2020, Art. no. 103507.

[69] Y. Chikazawa, A. Katoh, T. Yamamoto, S. Kubo, S. Ohno, M. Iwasaki, H. Hara, Y. Shimakawa, and H. Sakaba, "Secondary Sodium Fire Measures in JSFR," (in English), *Nuclear Technology,* vol. 196, no. 1, pp. 61-73, 2016.

[70] S. P. Nowlen, M. Kazarians, and F. Wyant, "Risk Methods Insights Gained from Fire Incidents (NUREG/CR-6738, SAND2001-1676P)," U.S. Nuclear Regulatory Commission, Washington, D.C., 2001.

[71] S. Miyahara, H. Seino, S. Ohno, and K. Konishi, "Development of fast reactor containment safety analysis code, CONTAIN-LMR (1) Outline of development project," in *Proceedings of the 23th international conference on nuclear engineering (ICONE-23)*, Chiba, Japan, 2015: American Society of Mechanical Engineers (ASME).

[72] A. Yamaguchi and Y. Tajima, "Validation study of computer code SPHINCS for sodium fire safety evaluation of fast reactor," *Nuclear Engineering and Design,* vol. 219, no. 1, pp. 19-34, 2003.

[73] S. Ohno, E. Hamase, and H. Kamide, "Ongoing validation of sodium fire analysis code system for SFR safety evaluation," in *International Congress on Advances in Nuclear Power Plants: Nuclear Power - A Safe and Sustainable Choice for Green Future, ICAPP 2013, Held with the 28th KAIF/KNS Annual Conference*, 2013, pp. 1021-1028: Korean Nuclear Society.

[74] T. J. Olivier, T. K. Blanchat, J. C. Hewson, S. P. Nowlen, and R. F. Radel, "Metal fires and their implications for advanced reactors," in *American Nuclear Society International Topical Meeting on Probabilistic Safety Assessment and Analysis (PSA 2008)*, Knoxville, TN, 2008.

[75] T. J. Olivier, J. C. Hewson, T. K. Blanchat, and S. P. Nowlen, "Sodium metal fires and advanced reactor safety," in *10th International Conference on Probabilistic Safety Assessment and Management (PSAM 10)*, Seattle, WA, 2010.

[76] M. Aoyagi, A. Uchibori, S. Kikuchi, T. Takata, S. Ohno, and H. Ohshima, "Identification of Important Phenomena under Sodium Fire Accidents Based on PIRT Process," in *International Conference on Fast Reactors and Related Fuel Cycles: Next Generation Nuclear Systems for Sustainable Development (FR17)* Yekaterinburg, Russia, 2017.

[77] M. Aoyagi, A. Uchibori, S. Kikuchi, T. Takata, S. Ohno, and H. Ohshima, "Identification of important phenomena through the PIRT process for development of sodium fire analysis codes," *Nuclear Engineering and Design,* vol. 353, 2019, Art. no. 110240.

[78] H. Shalabi and A. Bounagui, "Canadian Fire Protection Regulatory Requirements for Small Modular Reactors," in *25th International Conference on Structural Mechanics in Reactor*

Technology (SMiRT 25) – 16th International Post Conference Seminar on Fire Safety in Nuclear Power Plants and Installations, Ottawa, Canada, 2019.

[79] D. Grabaskas, "A Review of U.S. Sodium Fast Reactor PRA Experience," in *the 12th Probabilistic Safety Assessment & Management Conference (PSAM 12)*, Honolulu, HI, 2014.

[80] U.S. Nuclear Regulatory Commission, "Feasibility Study for a Risk-Informed and Performance-Based Regulatory Structure for Future Plant Licensing (NUREG-1860)," Washington, D.C., 2007.

[81] Y. Okano and H. Yamano, "Forest fire propagation simulations for a risk assessment methodology development for a nuclear power plant," *Case Studies in Fire Safety,* vol. 4, pp. 1-10, 2015.

[82] Y. Okano and H. Yamano, "Development of a hazard curve evaluation method for a forest fire as an external hazard," in *American Nuclear Society International Topical Meeting on Probabilistic Safety Assessment and Analysis (PSA 2015)*, Idaho Falls, ID, 2015.

[83] Y. Okano and H. Yamano, "Sensitivity study on forest fire breakout and propagation conditions for forest fire hazard curve evaluations," in *the 24th International Conference on Nuclear Engineering (ICONE 24)*, Charlotte, NC, 2016: American Society of Mechanical Engineers (ASME).

[84] Y. Okano and H. Yamano, "Hazard curve evaluation for forest fire smoke effects on air-cooling decay heat removal systems," in *American Nuclear Society 2017 International Topical Meeting on Probabilistic Safety Assessment and Analysis (PSA 2017)*, Pittsburgh, PA, 2017.

[85] Y. Okano, H. Nishino, H. Yamano, and K. Kurisaka, "A study of probabilistic risk assessment methodology of external hazard combinations - Identification of hazard combination impacts on air-cooling decay heat removal system," in *American Nuclear Society International Topical Meeting on Probabilistic Safety Assessment and Analysis (PSA 2019)*, Charleston, SC, 2019.

[86] B. Najafi, "Use of EPRI/NRC-RES fire PRA methodology (EPRI 1011989, NUREG/CR-6850) for fire PRA at nuclear power facilities other than current U.S. LWRs," in *American Nuclear Society International Topical Meeting on Probabilistic Safety Assessment and Analysis (PSA 2008)*, Knoxville, TN, 2008.

[87] U.S. Nuclear Regulatory Commission, "Presentations for May 3 & 4, 2017 Public Meeting Regulatory Improvements for Advanced Reactors," 2017, Available: https://www.nrc.gov/docs/ML1713/ML17130A782.pdf.